Doctoral Dissertation
Doctoral Program in Bioengineering and Medical-Surgical Sciences (32th Cycle)

The use of Human Liver Stem cells-Extracellular Vesicles (HLSC-EVs) as a biological treatment to recondition marginal rat livers during *ex-vivo* normothermic perfusion (NMP)

Dorotea Roggio
* * * * * *

Supervisor
Prof. Mauro Salizzoni

Doctoral Examination Committee:
Prof. Massimo Rossi, Referee, Università La Sapienza di Roma
Prof. Paolo De Simone, Referee, Università degli studi di Pisa

Politecnico di Torino
2020

Declaration

This thesis is licensed under a Creative Commons License, Attribution - Noncommercial - NoDerivative Works 4.0 International: see www.creativecommons.org. The text may be reproduced for non-commercial purposes, provided that credit is given to the original author.

I hereby declare that, the contents and organisation of this dissertation constitute my own original work and does not compromise in any way the rights of third parties, including those relating to the security of personal data.

Dorotea Roggio

2020

Acknowledgments

At the end of this journey, I would like to thank all the people that I met during these three years PhD.

Firstly, I would to kindly thank my tutors, Professor Mauro Salizzoni and Professor Renato Romagnoli, for giving me the opportunity to take part to a stimulating and interesting research project and to growth in an inspiring scientific environment.

Then, I would like to thank my research group: Victor and Chiara that helped me during the PhD to acquire values beyond the competences, as awareness and autonomy, fundamental to continue this career; Nicola, Alberto and Giada, with whom I shared the experience of this beautiful research project.

During these three years, I had the pleasure to be part also of a bigger group of scientists that welcomed me, hence I would like thank all the people of Lab 10 and 11 because the working environment is also made by sociality and collaboration.
Finally, I would like to thank the *cricca* that supported me in every moment of my PhD, helping me in the most difficult period, moving towards the most cheerful one: Linda, Sofia and Lola.

Behind each person, there is a big sphere of relatives and friends that support us remembering our motivation when we forgot it, helping us to see beyond the difficulties and clearly fill our lives of happiness.

I would like to say thank you to my parents, for all the sacrifices behind my instruction, from the beginning until this third cycle degree, for supporting me during my studies, for the patience and for believing in me.
To my brother, for the best moments of fun that raised me, for the sharing of feelings and the attempts to solve problems with simple and linear solutions.
To Danilo, who supported me with patience during all these years, who encouraged me to follow my inspirations, looking forward the obstacles.

Finally, I need to thank my friends, which I luckily knew during university: Maria and Valeria, for the best moments during our experience at Collegio Einaudi and for the friendship that continues although the distance. Valeria N, for sharing our passion for Biology during the university, thanks to which a strong friendship was born. Mario, that I met thanks to music and that I met again in Torino, having the pleasure to continue to play with him. Finally, to my musician friends of Ensemble Einaudi, with whom I continue to share with pleasure my passion for the music.

Hoping to not have forgotten anyone, I sincerely thank all people that contributed to these three years PhD, concluding that I am glad to be able to finish this last university cycle.

Abstract

Liver transplantation (LT) is the last therapy to end-stage liver diseases. However, a great number of potential recipients have not the possibility to access to liver transplant because of the lack of organ donors. To increase the pools of organs donors', marginal livers were taken in consideration for LT, such as the ones from donors after cardiac death (DCD). Nevertheless, the standard liver preservation technique, named Static Cold Storage (SCS), which consists in the slowing of hepatocellular metabolism, is imperfect in protecting marginal livers organs. In this context, the *ex-vivo* normothermic machine perfusion (NMP) could offer the possibility to recondition graft viability prior to implantation. Human Liver Stem Cells (HLSC) have been identified in the liver as a population of pluripotent resident cells expressing markers of the mesenchymal lineage together with hepatic markers, suggesting a partial hepatic commitment. The extracellular vesicles (EVs) from HLSC have been isolated and characterized, showing that they are able to mediate a regenerative effect mainly by horizontal transfer of specific mRNA and miRNA.

In this thesis, two models of marginal rat livers were reconditioned *ex-vivo* by NMP, testing the HLSC-EVs as a biological treatment to rescue injured livers, improving liver features and functionality.

The first marginal rat liver model consists of a hypoxic rat liver perfused *ex-vivo* by NMP for four hours with a low haematocrit (<10%), to obtain an ongoing and constant hypoxic injury. We compared the difference between the injured non-treated livers (control group, n=10) and the injured livers treated by HLSC-EVs (treated group, n=9). The uptake of HLSC-EVs was analysed by immunofluorescence, while tissue injury was analysed by haematoxylin-eosin (H&E) staining. Then, apoptosis was assessed by TUNEL assay. Total bile production was quantified and perfusate samples were collected hourly to measure cytolysis markers (AST, ALT, LDH). Finally, the expression of HIF-1α, and TGF-β1 was measured by RT-PCR. During the hypoxic NMP perfusion, livers were able to maintain homeostasis (pH, pO_2, pCO_2) and to produce bile. The HLSC-EVs were engrafted into the hepatic parenchyma. The HLSC-EVs treatment significantly reduced the Suzuki's score, the apoptosis index and the release of AST and LDH, already at third hour of perfusion. In addition, the HLSC-EVs treatment acted at a molecular level reducing the expression of HIF-1α and TGF-β1.

The second marginal rat liver model consists of 60 minutes warm ischemic rat liver (DCD) perfused *ex-vivo* by NMP for six hours. We tested two different doses of HLSC-EVs, EV1 and EV2, where EV2 dose is 5 times greater than EV1 one. The rat livers were divided into four experimental groups: NMP, WI+NMP, WI+NMP+EV1 and WI+NMP+EV2. The NMP livers were subjected to ≈34 minutes of SCS + 6 hours of NMP; the WI+NMP livers were subjected to 60 minutes of warm ischemia + 6 hours of NMP. The WI+NMP+EV1 and WI+NMP+EV2 livers were subjected to 60 minutes of warm ischemia + 6 hours of NMP and treated with HLSC-EVs dose 1 or 2. During NMP, metabolic (phosphates, bile, pH, HCO_3^-) and hemodynamic (pressure, flow) parameters were measured; perfusate samples were collected hourly and the release of cytolysis enzymes (AST, ALT) were measured. Then, at the end of each perfusion, tissue samples were collected to verify the engraftment of HLSC-EVs (fluorescence analysis), to do histological evaluation (H&E, TUNEL assay, PCNA immunohistochemistry) and to measure RNA expression of adhesion molecules (ICAM-1, VCAM-1, Selectin-E, Selectin-P). The HLSC-EVs were engrafted in hepatic parenchyma. The EV2 dose of HLSC-EVs was able to significantly reduce hepatocytes necrosis. Although the apoptosis level was negligible compared to necrosis, the HLSC-EVs treated livers reported an inferior apoptosis level compared to the ischemic livers. In addition, the EV2 dose of HLSC-EVs was able to increase the proliferation capability of the liver, which was ablated by ischemia. Both the two doses of HLSC-EVs were able to significantly reduce the release of the cytolysis enzymes AST and ALT at the sixth hour of perfusion and the EV2 dose decreased the AST level already at the fourth hour of perfusion. At a metabolic level, both the two doses EV1 and EV2 required a small amount of HCO^-_3 for pH regulation, and promoted the self-regulation of pH and the phosphates consumptions during perfusion. Only the EV2 dose succeeded in significant increase the amount of produced bile, compared to the control ischemic liver. The hemodynamic resistance in the perfusion circuit due to ischemia was significantly reduced by the EV2 dose. The injured ischemic hepatocytes expressed a low level of the analysed adhesion molecules, while the HLSC-EVs tended to rescue their expression in treated livers.

The HLSC-EVs treatment showed to be able to recover the hypoxic rat liver and the DCD rat liver respectively during the four and six hours *ex-vivo* NMP. Besides, between the two tested doses in DCD model, the EV2 dose could be more effective than the EV1 one. The association of HLSC-EVs to NMP in order to reduce liver injury is a promising strategy for *ex-vivo* graft reconditioning before transplant surgery although further investigations are required.

Contents

Chapter 1

The normothermic machine perfusion as a novel strategy for ex-vivo liver graft reconditioning

1.1 The needing of organ for liver transplantation and the extended criteria donors

Liver transplantation (LT) is the last therapy for end-stage liver disease, metabolic disorders, hepatocellular cancer, and other liver pathologies. As reported in the European Liver Transplant Registry (ELTR), 146.782 LTs were performed from May 1968 to December 2016, in 132.466 patients from 32 different countries. During the 50 years considered by this study, the patient survival rates were 83% at 1 year, 71% at 5 years, 61% at 10 years, 51% at 15 years and 41% at 20 years. In Figure 1.1, it is showed the total liver transplants performed in every European country compared to the number of living related liver transplantation (LRLT) (Figure 1.1)[1].

However, a great number of potential recipients have not the possibility to access to liver transplant because of the lack of organ donors. In order to expand the donor pool, the transplant community has recently acquired increased experience whit the use of so-called "extended criteria donors" (ECD)[2]. Despite a unique definition is currently lacking, the extended criteria principally refers to older age (>65 years), donation after cardiac death (DCD) or fatty infiltration or steatosis (>30% macro vesicular steatosis). Several groups already successfully transplanted liver allografts from elderly donors, demonstrating that the older age is a barrier that could be overcame[3]. DCD has been implemented to expand donor pool in several countries like USA, Spain, Belgium, UK, Netherlands and others[4]. According to the Scientific Registry of Transplant Recipients (SRTR) of the United States, referring to the adult primary liver transplants from DCD donors performed between January 2009 and December 2015, it emerged that only the liver graft with the donor warm ischemia time comprised among 30 and 40 minutes could be

included among the selected recipients to expand the donor pool[5]. However, in Italy, the use of DCD livers is limited, because, according to Italian law, the hands-off period after cardiac arrest should be of 20 minutes[6]. Finally, the use of liver with more than 30% of macro vesicular steatosis is controversial. On one hand, there is the additional risk of delayed graft function that could negatively affects the transplant outcomes, associated with a graft survival lower than one year, on the other hand there is the possibility to have a consistent pool of donors, generated by the increasing obesity and metabolic syndrome in our population[3].

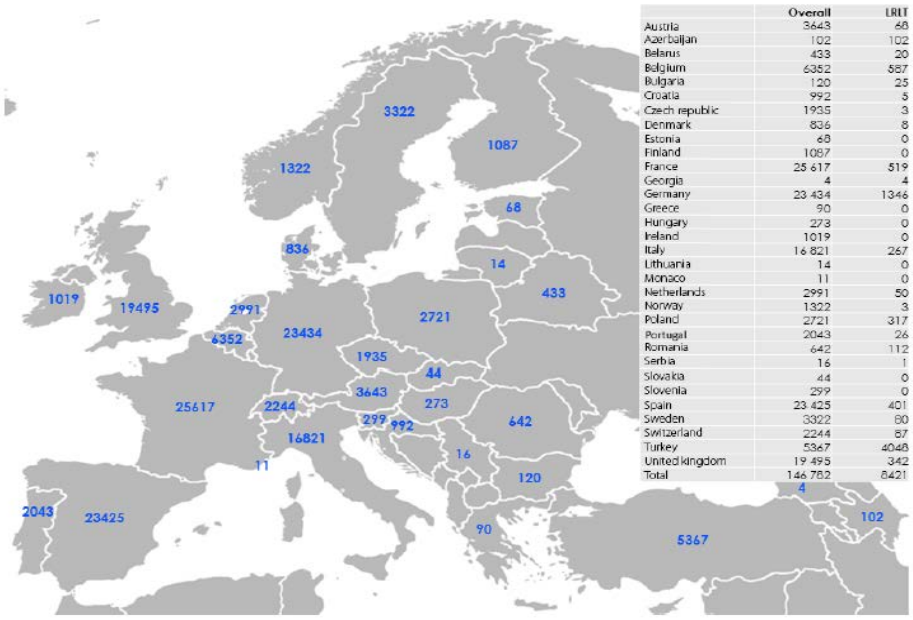

	Overall	LRLT
Austria	3643	68
Azerbaijan	102	102
Belarus	433	20
Belgium	6352	587
Bulgaria	120	25
Croatia	992	5
Czech republic	1935	3
Denmark	836	8
Estonia	68	0
Finland	1087	0
France	25 617	519
Georgia	4	4
Germany	23 434	1346
Greece	90	0
Hungary	273	0
Ireland	1019	0
Italy	16 821	267
Lithuania	14	0
Monaco	11	0
Netherlands	2991	50
Norway	1322	3
Poland	2721	317
Portugal	2043	26
Romania	642	112
Serbia	16	1
Slovakia	44	0
Slovenia	299	0
Spain	23 425	401
Sweden	3322	80
Switzerland	2244	87
Turkey	5367	4048
United kingdom	19 495	342
Total	146 782	8421

Figure 1.1: Representation of total liver transplants performed in Europe between 1968 and 2015: total number of liver transplants (Overall) and number of living related liver transplantation (LRLT) [1].

1.2 Current strategy for liver preservation: static cold storage (SCS)

SCS is the current gold standard for liver preservation. The principles of SCS are based on the rapid cooling of the organ, slowing hepatocellular metabolism by hypothermia[7].

The SCS provides the infusion of preservation solution into the organ, which then is stored statically[7]. Despite the hepatocellular metabolism is slowed down by cooling, a minimal consumption of energy results from the anaerobic metabolism[2]. Under this condition, the ATP pool is depleted, the waste products of anaerobic metabolism (intracellular calcium and lactate) accumulate, leading to acidosis, and the sinusoidal endothelial cells begin to be damaged[8]. Once SCS-liver is implanted into the recipient, the organ rewarming starts the reperfusion insult, which is characterized by the sudden exposure of the organ to oxygenated blood circulation[9,10]. In other words, the liver is subjected to the so-called ischemia-reperfusion injury (IRI), which triggers the inflammatory cascades, injuring the

hepatic parenchyma and the sinusoidal cells[2]. Regarding to DCD livers, the organ injury already started before the liver retrieval[11] and a significative ATP depletion occurs before SCS procedure begin[2]. The risk of primary nonfunction (PNF) is increased in DCD transplanted livers[12] and is manifested by hepatic cytolysis and rapidly rising of transaminases level, no bile production, hypoglycemia, acidosis and an instable hepatic hemodynamic[13]. In DCD transplanted livers, the hepatic artery thrombosis (HAT) significantly contributes to PNF development and it commonly occurs as a consequence of *in situ* blood stasis in the arterial tree during the period of donor warm ischemia[12]. According to the United Network for Organ Sharing (UNOS), the only solution to PNF is an urgent liver re-transplant during the first 10 days after the LT[14]. The Pooled United Network for Organ Sharing data together with the experiences reported by different single-institution showed that the inferior graft survival for transplanted DCD liver is related also to biliary complications, such as ischaemic cholangiopathy (IC)[15]. In fact, bile ducts are entirely dependent for oxygenation from arterial blood supply. When HAT occurred in DCD livers, a massive bile duct necrosis may result, with detrimental effects for the bile duct epithelial cells, the cholangiocytes[16].

On another hand, the composition of preservation solutions evolved during ten last years (Figure 1.2). Briefly, before 1990, the Collins solution was mainly used and then substituted almost exclusively by the University of Wisconsin (UW) solution. Thereby, after the 2000s new solutions with improved characteristics came out, such as Celsior and Institute Georges Lopez solution (IGL-1) (Figure 1.2)[1], that solved the issues observed with the use of the older preserving solutions (Collins, UW and others).

Specifically, Celsior solution has some advantages over other solutions derived from the content of antioxidant (permanently reduced glutathione) and impermeant agents (lactobionate and mannitol), that allow to extend their use for abdominal organs preservation[17]. These characteristics permit their currently and extensively use for liver transplantation[17]. More recently, the IGL-1 preservation solution, where the hydroxyethyl starch (HES) was substituted by a polyethylene glycol (PEG35), have showed to possess additional beneficial effects on organ preservation as demonstrated by clinical studies on liver and kidney transplantations[18].

Although the advantages obtained in the liver preservation, the organs subjected to SCS do not lack of hepatic complications related to DCD liver transplantations. Particularly, these complications, associated with inferior outcomes depending on PNF and biliary complications[19] lead to find newly and better organ preservation strategies.

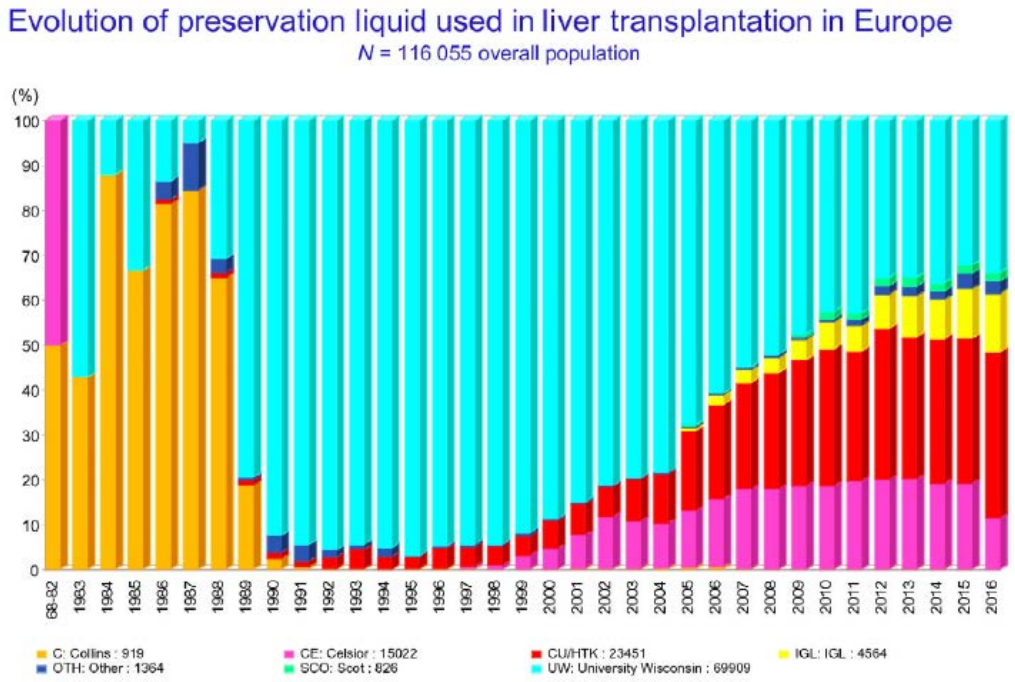

Figure 1.2: Changing of preservation solutions used between 1968 and 2015 in liver transplantation in Europe[1].

1.3 Alternative strategies for *ex-vivo* liver preservation

The attempts to preserve organs *ex-vivo* began in the 1930s, when Alexis Carrel and Charles Lindbergh first perfused various organs with an oxygenated serum at a physiological temperature, demonstrating the viability of the organs for several days[20]. Nevertheless, it was only in the 1960s when Starzl and collaborators introduced the concept of organ perfusion in transplantation field using cold fluids to perfuse canine organs through the portal vein by a heart-lung machine[21]. However, in 1970s the introduction of Collins solution for organs preservation facilitated the use of static cold preservation and moved the research away from machine perfusion. Moreover, in the last decade, the use of DCD livers for LT and their vulnerability to SCS preservation method renewed the interest in the research field of machine perfusion[2].

One of the main advantages of the machine perfusion is that maintains active liver metabolism and washout the accumulated toxic molecules. Additionally, the continuous flow during perfusion allows a better penetration of the preservation solution into the organ microcirculation and thereby, supplying nutrients to liver parenchyma[8].

Since the last years, a number of different perfusion machines were continuously tested, and the current classification is based mainly on the temperature of the preservation and on the presence or absence of the oxygen (Figure 1.3) that increase the range of temperature at which the organs could be perfused.

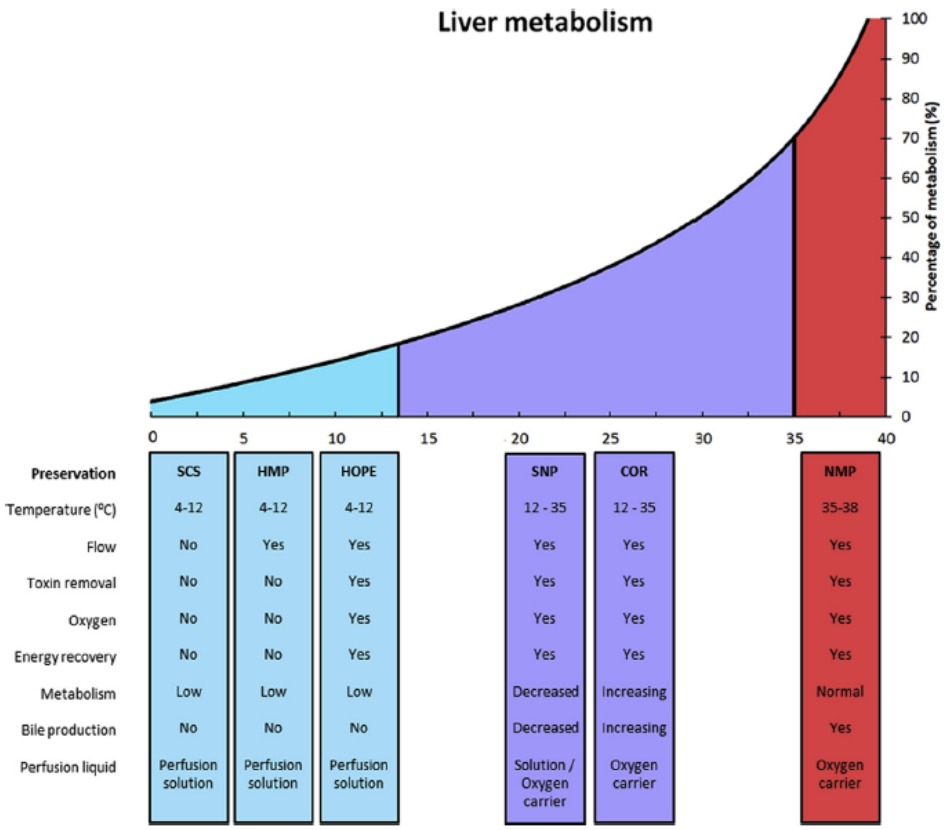

Figure 1.3: Schematic representation of different types of machine perfusion and their characteristics. The relation between the temperature of perfusion and the liver metabolism it is showed. Abbreviation: SCS: static cold storage, HMP: hypothermic machine perfusion, HOPE: hypothermic oxygenated perfusion, SNP: sub-normothermic machine perfusion, COR: controlled oxygenated rewarming, NMP: normothermic machine perfusion[8].

1.3.1 Hypothermic oxygenated perfusion (HOPE)

HOPE is based on cold perfusion of liver, in the temperature range comprised between 2 °C and 18 °C, using blood free perfusion solution in which the oxygen is physical solved. A great part of the studies on HOPE demonstrated that UW solution is considered the best solution to this aim, although the presence of HES is still a matter of discussion, because at lower temperature ranges, the liquid viscosity is increased[22].

During the last 15 years, different routes of perfusion has been also tested in experimental studies, showing that the single portal perfusion was usually preferred for rat liver models, while in pig livers the HOPE is preferred to be performed using a dual perfusion approach via hepatic artery (HA) and portal vein (PV)[22].

The protective effects of HOPE on liver preservation could be resumed in four main points[8]:

- the cold oxygenation is able to restore the levels of adenine nucleotides, usually depleted during SCS
- the improving of mitochondrial enzyme complexes functionality

- the presence of oxygen changes the cellular redox state from reduced to oxidised
- the impact of IRI after liver transplantation is reduced.

In HOPE, the combination of a low temperature together with the presence of the oxygen, allowed the reactivation of the mitochondrial respiration that occurs before organ rewarming and the blood cells influx, provided during the transplantation procedure. Hence, the activity of hepatocytes and endothelial cells are restored although the liver is below the physiological conditions. In contrast, a great disadvantage concerning the time available for perfusion is present, because during HOPE the cold perfusate increased the vascular resistance in a time-dependent way, leading to a possible further injury to sinusoidal endothelium and to endoplasmic reticulum, especially when cold perfusion is extended beyond 18 hours[23].

1.3.2 Normothermic machine perfusion (NMP)

NMP is currently an available alternative to *ex-vivo* reconditioning approach, because allows liver preservation at physiological temperature (37 °C). The NMP permits to avoid the cold ischemia and to provide oxygen and nutrients delivering to the organ during all whole perfusion procedure, thus maintaining the liver metabolism close to physiological conditions[24].
Most studies on NMP used dual perfusion routes, via the PV and HA, mimicking liver physiology[25]. The NMP machine has the peculiarity to control either flow or pressure in an interdependent manner. In general, the range of goal pressures is considered to be between 50-100 mmHg for the HA, and 3-10 mm Hg for the PV; while flow ranges are considered to be 150-700 mL/minute for HA, and 950-1750 mL/minute for the PV[25].
Usually, the oxygenation is provided by the presence of a hollow fibre membrane oxygenator, and red blood cells are required as oxygen carriers[2]. Hence, the perfusion solution should contain red blood cell concentrate, plasma, nutrients, cofactors, antibiotics, insulin, buffers and electrolytes for an adequate preservation[26].
Finally, the NMP offers the opportunity to assess the organ function prior to transplantation. Additionally, it is possible to real time monitoring the metabolic status of the liver, measuring metabolic parameters in perfusate samples, such as hepatic enzymes (ALT, AST, LDH), lactate, glucose, pH and other molecules of interest, but also to monitor the bile production, which is an important parameter of hepatocytes viability[8]. In Figure 1.4, an example of liver NMP circuit is showed. Briefly, the depicted circuit is composed by a pressure sensor placed in the PV that allows the consequent regulation of flow and a tube system connected to two roller pumps that triggers the perfusate circulation. Throughout the circuit, an oxygenator allows erythrocytes oxygenation, and a bubble trap avoid the formation of air bubbles. The liver is placed into a warmed chamber (37°C) and PV and HA are connected to the influx and efflux ways, as appropriately, while the cystic duct is connected to a third efflux way to collect the bile produced during perfusion.

Additionally, it is possible to collect perfusate samples from the HA way (Figure 1.4).

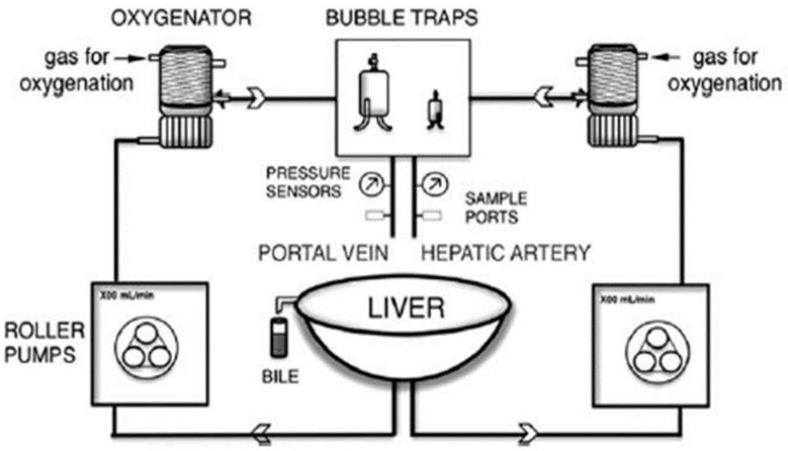

Figure 1.4: Schematic representation of a possible NMP circuit for liver perfusion[25].

In clinical application, it is important to define if benefits of NMP require the complete avoidance of cooling, before perfusion, or if they can be delivered also after a brief period of SCS. This aspect has an important and practical implication, meaning that perfusion machine has to be transportable if a continuous perfusion of the organ is required, starting in the place of organ collecting until reaching the recipient hospital[2].

Currently, two different NMP devices have been implemented in clinic of transplantation. OrganOX Metra, developed in the United Kingdom, is a transportable normothermic perfusion device that uses a single pump to deliver continuous blood directly to the HA e through a reservoir to the PV. The system is fully cannulated and almost automated, maintains the physiological temperature, analyses the blood gas parameters and regulates the arterial pressure and gas delivery (Figure 1.5)[2].

Figure 1.5: A photograph of OrganOX Metra device (OrganOx, Oxford, UK, www.organox.com).

In contrast, the second NMP device named Liver Assist (Figure 1.6), is a CE-marked device that includes a dual system of rotary pumps to transport a pulsatile flow in the HA and a continuous flow in the PV, while the inferior vena cava is left free to drain into a reservoir. A hollow fibre membrane oxygenator mediates the oxygenation and the temperature should be set manually. In this way, the Liver Assist could be used in hypothermic, sub-normothermic or normothermic modes. The main disadvantage is that it is not transportable, meaning that liver should be cold preserved before being placed into the device[2].

Figure 1.6: A photograph of the Liver Assist device (Liver Assist, Groningen The Netherlands, www.organ-assist.nl)

1.3.3 Sub-normothermic machine perfusion (SNMP) and controlled oxygenated rewarming (COR)

SNMP allows perfusing liver at 20 ºC, a temperature that is in the middle between HOPE and NMP. The advantage is the presence of the oxygen supplied in the perfusion solution, without using red blood cells and exploiting the temperature of 20 °C [27, 28] In particular, SNMP allows to gradually increase the liver rewarming until reaching 20°C, in order to gently adapt the organ to oxygenated perfusion. This technique is named controlled oxygenated rewarming (COR) [29]. On the other hand, contrary to NMP, the SNMP eliminates the dependence on oxygen carriers in perfusate. Nevertheless, limitations for analysis viability and metabolic status are present in SNMP[8].

Although the effects deriving from increasing the temperature until the physiological value of 37°C, remains to be investigated, the COR could be applied to NMP, in order to raise the restitution of cellular homeostasis, improving the functional outcomes[30].

1.4 Experimental studies of NMP conducted on DCD livers

Currently, the NMP strategy has been used to recover warmed ischemic livers aimed to amply the organ donor's pool. Toolbom et al. demonstrated that NMP improved the outcomes of 60 minutes ischemic rat livers once they were transplanted, as demonstrated by the increased animal survival[31]. Moreover, AST and ALT levels in recipient rats who received a reconditioned warm ischemic liver were comparable to those recipients who received a healthy liver preserved by SCS or NMP[31].

The beneficial effects of rat ischemic livers perfused by NMP system were also demonstrated by Schlegel and collaborators[32]. Interestingly, authors indicated that this effect was limited to organs that experienced 30 minutes of ischemia, while NMP was not able to rescue organs with an extended ischemic period of 60 minutes[32]. This last observation was correlated with the maximal levels of endothelial injury markers (ICAM-1, vWF) and inflammatory cytokines in perfusate (IL-6 and TNF-α), observed at 60 minutes of ischemia-reperfusion injury[32]. This limitation was also demonstrated by Brockman and collaborators, in a NMP model of DCD porcine livers, showing that the NMP allowed the post-transplant survival of animal who received a 40 minutes ischemic liver perfused by NMP; in contrast, as similar as reported by Schlegel, those who experienced 60 minutes of ischemia did not survive[24].

Op den Dries and collaborators performed some initial pre-clinical studies in the three main specialized transplant centers of the Netherlands,[26] perfusing DCD-derived livers for 6 hours by Liver Assist device. They demonstrated that livers preserved an active metabolic status with bile production and without acidosis. Moreover, authors demonstrated the improvement in organ morphology by the reduction in biliary injury and sinusoidal damage[26].

A more recently clinical study was performed by Mergental and colleagues where DCD donors liver were reconditioned by NMP. Once implanted, the grafts showed an immediate graft function recovery; moreover, ALT, AST, bile and creatinine were reduced during the time of follow-up (3 months) close to physiological levels[33]. Furthermore, Bral et al., confirmed the advantages of using NMP perfused DCD livers[34]. In this work, authors described that, althought AST and ALT rose progressively during NMP, the post-transplant outcomes were positive, without PNF. Nevertheless, authors remarked the fact that the host receiving the NMP reconditioned livers showed a longer intensive care and hospital stays compared with host receiving SCS reconditioned livers[34].

According to the data of these pre-clinical and clinical studies, the advantages of NMP versus SCS are still a matter of debate.

Chapter 2

The cellular and molecular mechanisms behind hepatic ischemia-reperfusion injury

2.1 The definition of IRI

As it was mentioned before, the hepatic IRI reduces the survival rate of patients requiring hepatic graft. Hence, another goal of the researchers is to deep understand the mechanisms that trigger IRI during liver transplantation, in order to find an effective therapy[35].
The IRI damage represents a complex series of events that derive from a transient deprivation of blood supply and oxygen, followed by the restoration of blood flow during reperfusion[36]. Moreover, reperfusion produces paradoxical tissue responses that promote a pro-inflammatory phenotype in ischemic tissues, amplifying tissue injury (Figure 2.1)[37].

2.2 The mechanisms of damage triggered by hepatic IRI

The magnitude of cell dysfunction, injury and death during hepatic IRI is determined by both the length and extent of the damage. The mechanisms involved are mainly dependent from[38]:

- production of reactive oxygen species (ROS) after reperfusion
- dysfunction of the endothelium
- appearance of a pro-thrombogenic phenotype
- inflammatory responses.

In the next subsections, the main mechanisms involved in overall IRI process will be more extensive described.

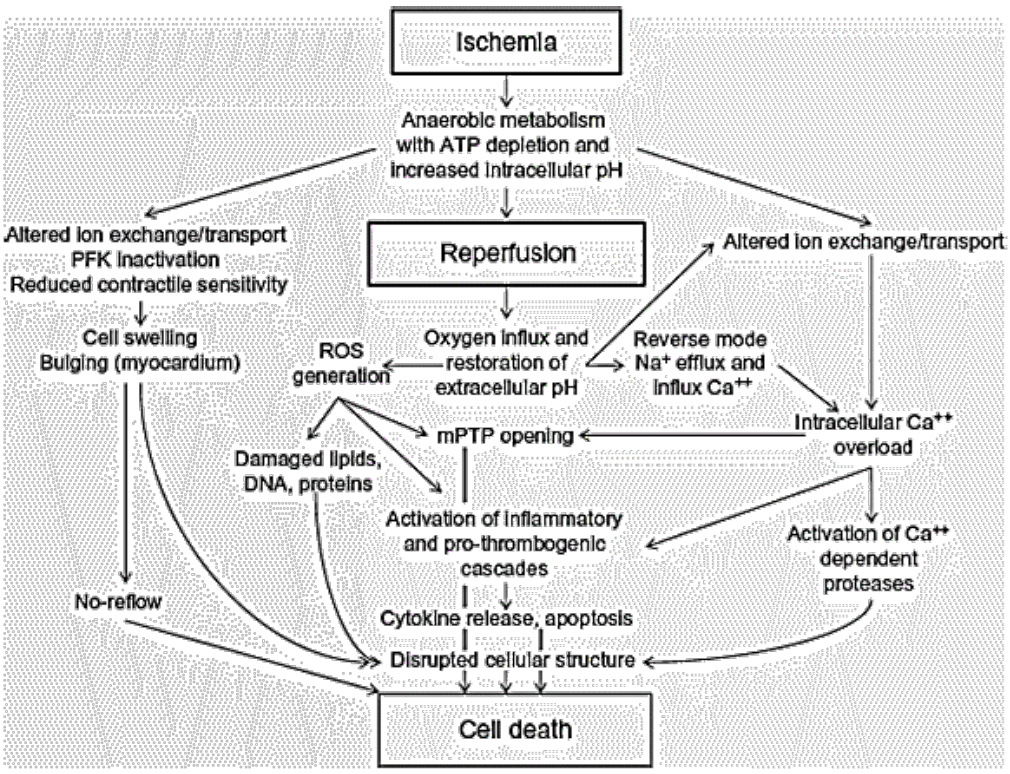

Figure 2.1: Schematic representation of the several mechanisms involved in IRI[37].

2.2.1 ROS

ROS are extremely damaging especially due to lipid peroxidation at a cell membrane level, resulting in disturbances of ion homeostasis, cell swelling and cell death. In addition, the damage is extended into the intracellular space, where all the membrane organelles are injured, including mitochondria and nucleus. In fact, within the mitochondria, ROS can cause the arrest of ATP production, through the destruction of the enzyme complexes of the respiratory chain by oxidative damage[39]. In addition, the generated ROS could stimulate the neighbouring mitochondria to produce other ROS, triggering a self-perpetuating cycle of ROS production, which leads to cellular destruction[40].

A wide variety of ROS are generated during IRI phase, such as superoxide radical (O_2^-), hydrogen peroxide (H_2O_2), hypochlorous acid (HCLO) and hydroxyl radical (OH^-). They can be generated by four main mechanisms: xanthine dehydrogenase conversion to xanthine oxidase, Nicotinamide Adenine Dinucleotide Phosphate (NADPH) oxidase activation, the activation of mitochondrial electron transport chain and of uncoupled nitric oxide synthase (Figure 2.2)[41].

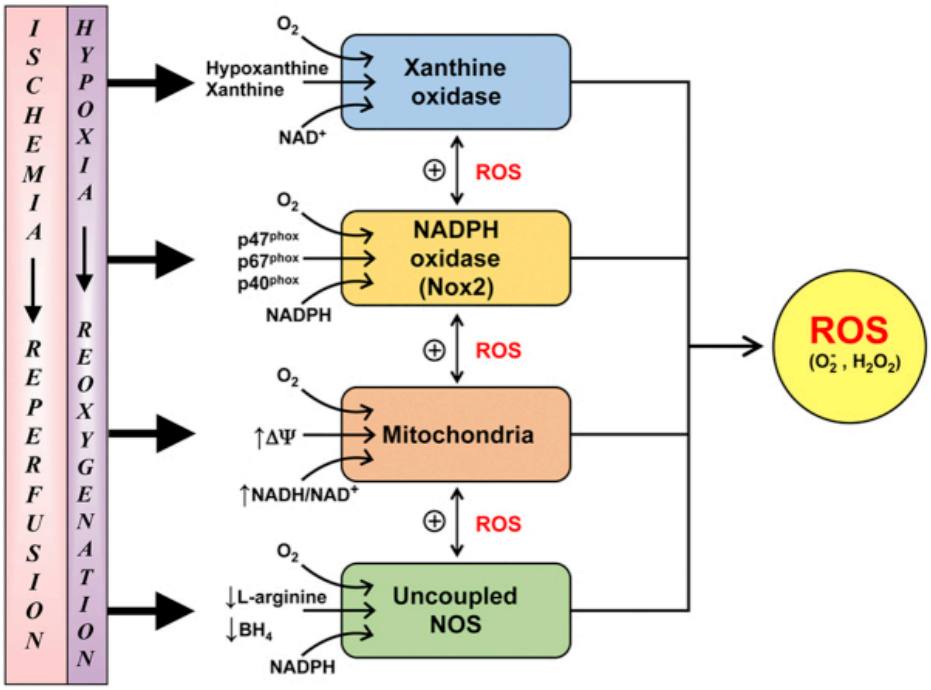

Figure 2.2: Description of the four main mechanisms of ROS generation during ischemia-reperfusion injury[41].

2.2.2 Ionic disturbances

The hepatic IRI also causes alterations in the homeostatic concentration of ions including Ca^{2+}, Na^{+}, and H^{+}. Firstly, IRI leads to the rise of cytosolic Ca^{2+} as a combination of its increased influx across the damaged plasma membrane together with its release from injured endoplasmic reticulum (ER) (Figure 2.3)[40]. Secondly, the intracellular acidosis consequent to the switch towards anaerobic metabolism (triggered by IRI), unbalances the intracellular concentration of Na^{+} and H^{+} ions. In fact, to restore intracellular pH up to physiological levels, liver cells trigger the Na^{+}/H^{+} exchanger (NHE) and the Na^{+}/HCO_3^{2-} cotransporter (NHCT) (Figure 2.3). On one hand, the NHE allows the influx of Na^{+} in the intracellular space in exchange of H^{+}, on the other hand, the NHCT transports Na^{+} and HCO_3^{2-} intracellularly, therefore leading to the accumulation of Na^{+} in the cell[41]. Both the increased concentration of intracellular Ca^{2+} and Na^{+} ions contribute to cell death[40,41].

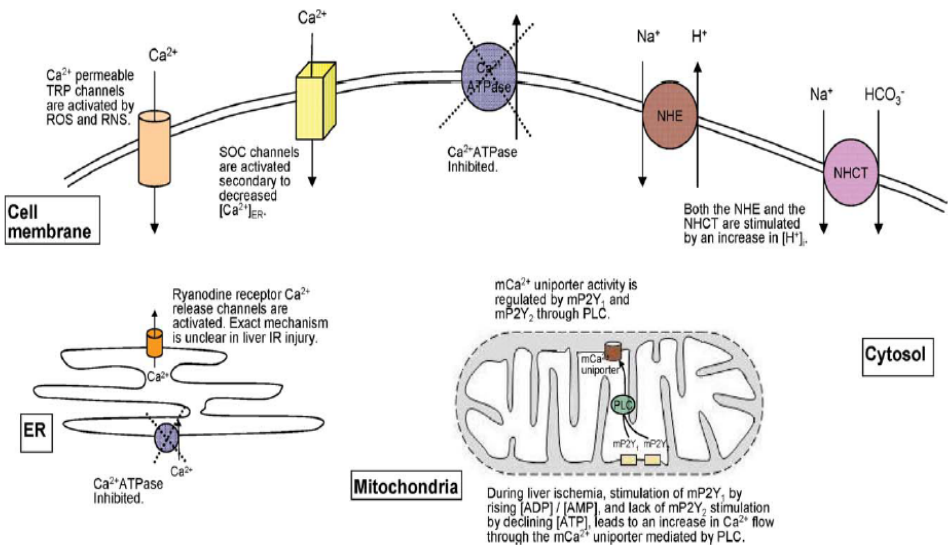

Figure 2.3: The alteration of membrane-associated ion channels, carriers and pumps elevates cytosolic Ca^{2+} and Na^{+} that promote cellular injury.[40]

2.2.3 Cytokines and chemokines

Pro-inflammatory cytokines such as Tumor Necrosis Factor α (TNF-α), Interleukin-6 (IL-6), Interferon-γ (IFN-γ) and Interferon-β (IFN-β) play a pivotal role in propagating the inflammatory response in hepatic IRI (Figure 2.4)[39].

TNF-α has been considered the most important mediator in hepatic IRI inflammation; its levels in serum raises within 30 min of reperfusion and remains up for up to 8 hours. The induction partial hepatic IRI (with 60 minutes of ischemia followed by 6 h reperfusion) in a double knockout mice model of Interferon Regulatory Factor-1 (IRF-1) showed that TNF-α is released through a cytokine cascade following IRF-1 activation[43]. Although TNF-α is released by a variety of cells in the liver, its release by Kupffer cells (KC) is the most prominent, and it is detected rapidly after reperfusion[44]. TNF-α in turn stimulates hepatocytes and KC to produce neutrophils chemoattractant, particularly chemokines[45]. Chemokines (CXCL) are small (8–10 kDa) heparin-binding proteins that are released by a variety of cell types. Specifically, chemokines are molecules able to form a local concentration gradient that guide leucocyte chemotaxis that once activated may contribute to hepatocellular damage[46]. A knockout model of CXCL-10 showed that presence of the chemokine in hepatic IRI following the first hour of reperfusion, with a consequent activation of neutrophils, KC and an increased release of TNF-α and IL-1β[45]. Gene deletion of its receptor, the Chemokines Receptor 2 (CXCR2), completely abolishes acute neutrophil accumulation after IRI. However, these studies showed that neutrophils accumulation was just delayed, suggesting that other chemoattractant, different from chemokines, are involved in the recruitment of neutrophils[47].

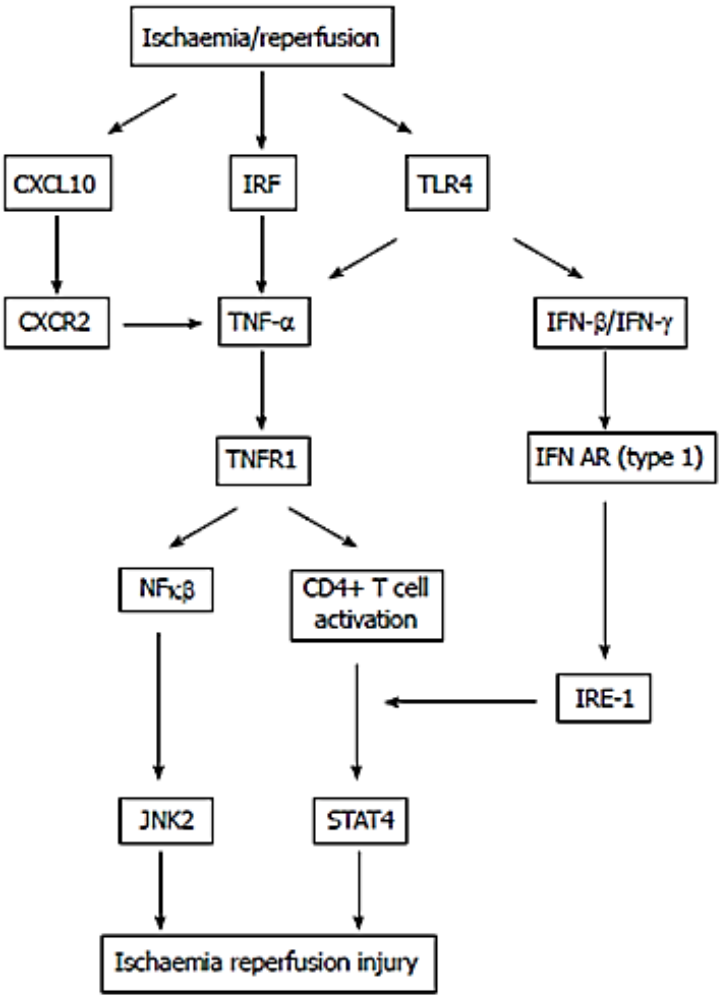

Figure 2.4: IRI damage triggers the secretion of chemokines such as CXCL10, that leads to the production of TNF-α cytokine, which in turn activate NF-kB pathway and $CD4^+$ cells. On the other hand, the activation of TLR-4 induced by IRI leads to the involvement of IFN pathway[39].

2.3 The cellular counterparts of hepatic IRI

During hepatic IRI, it is possible to distinguish between an early phase, occurring after 3-6 hours of perfusion, and a late phase, that happens at 18-24 hours after perfusion. In the early phase, the over production of ROS and the activation of T-cells and macrophages leads to hepatocytes and endothelial cells injury, while during the late phase the white blood cells, already infiltrated in hepatic sinusoids, interacts through cytokines and chemokines with surrounding micro environment, thus recruiting other neutrophils from blood circulation[48].
In the next subsections, the cellular components that participate to all the IRI process will be described.

2.3.1 Liver sinusoidal endothelial cells (SEC)

The hepatic endothelium is surrounded by liver sinusoidal endothelial cells (SEC) that are involved in maintaining the vascular tone, controlling blood flow as well as delivery of oxygen and nutrients to hepatic cells[49]. During IRI, liver SEC are predominantly injured because of ATP depletion, which leads to disruption of active transmembrane channel transporter of ions. The consequence is cell swelling and mitochondrial dysfunction. In addition, the depletion of nitric oxide (NO) stores and the lack of NO production by injured liver SEC unbalance the vascular homeostasis, causing an increment in vascular tone therefore reducing blood flow to hepatocytes[35].

2.3.2 Kupffer cells (KC)

The liver has resident macrophages known as Kupffer Cells (KC) which are a derivative of erythro-myeloid progenitor cells in the fetal liver[50]. In the healthy liver, KC are vital for the immunogenic responses when the liver is exposed to several circulating antigens. In the case of injury to the liver, KC lose their protective immunogenic profile and become pro-inflammatory[51]. Cytokines that promote inflammation are secreted by KC during IRI include IL-1β (Interleukin 1 β), TNF-α, IFN-γ and IL-12 (Interleukin-12). IL-1β and TNF-α stimulate the upregulation of adhesion molecules such as CD11b/CD18a (Mac-1) on neutrophils and of Intracellular Adhesion Molecule-1 (ICAM-1) on liver SEC, inducing the adhesion and extravasation of neutrophils into the liver parenchyma[52]. TNF-α secretion from KC during IRI induces an increased activation of Selectin-P on hepatic SEC, which leads to adhesion and activation of platelets (Figure 2.5) [35]. In addition, during the early stages of liver IRI, KC are also considered to be the lead source of ROS, followed by neutrophils in the very later stages[53].

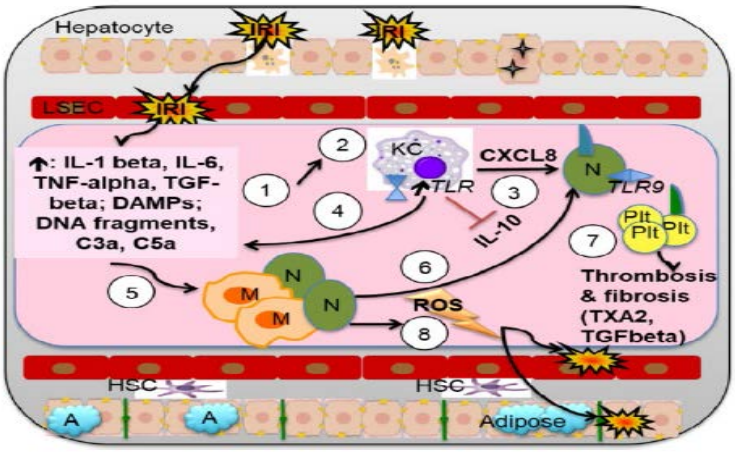

Figure 2.5: Schematic representation of IRI. Induction of the migration of neutrophils and macrophages leading to cellular destruction and ROS release[35].

2.3.3 Hepatocytes

Hepatocytes are injured directly during IRI (Figure 2.5). The lack of oxygen caused by injury interrupts the hepatic respiratory chain, leading to the depletion of remaining ATP and impairment of nutritional substrates[54]. The disruption of mitochondrial respiration chain results in generation of ROS causing tissue damage[55]. During reperfusion, the respiratory chain function is not restored up to a physiological level, therefore causing the release of Damage-Associated Molecular Patterns (DAMPs) molecules that initiates a self - propagating inflammatory cycle whereby liver SEC and KC are the main regulators[40].

2.3.4 Hepatic stellate cells (HSC)

The hepatic stellate cells (HSC) are the central regulators of fibrosis and reside in the peri-sinusoidal space[56]. During inflammation, they regulate the hepatic response towards injury by secreting antioxidants and causing apoptosis of reactive T-cells. On the other hand, severe injury could be caused by the constitutive activation of HSC, leading to the release of Matrix Metallo Proteinase (MMP), chemokines and inflammatory cytokines. This eventually leads to the destruction of Extracellular Matrix Components (ECM), intravasation of platelets and neutrophils, and further activation of HSC. Once HSC are activated, they transdifferentiate into a myofibroblast phenotype and, as a long-term consequence, giving rise to fibrosis of the liver parenchyma[57].

2.3.5 Neutrophils

Following injury in liver vasculature, the inflammatory mediators such as TNF-α, IL-1, chemokines and Platelet-Activating Factor (PAF) increase the expression of adhesion molecules of β2-integrin family and cause the recruitment of neutrophils into sinusoids[43]. The presence of DNA fragments, released by injured hepatocytes, activates the neutrophils through the Tool-Like Receptor-9 (TLR-9), enhancing ROS production and chemokines secretion. Continuation of tissue damage causes an ongoing cycle of recruitment, migration and tissue infiltration of neutrophils, therefor causing further release of damaged signals, such as DAMPs (Figure 2.5)[58].

2.3.6 T-lymphocytes

During hepatic IRI, the so-called T-helper cells, that are the T-lymphocytes $CD4^+$, undergo activation and migrated into liver sinusoids (Figure 2.6). Instead, the lymphocytes type B, the T-lymphocytes $CD8^+$ and the natural killer (NK) cells do not have a predominant role in modulating IRI[47]. A study on the role of $CD4^+$ in IRI was performed using T-cell-deficient mice and it was demonstrated that a loss of $CD4^+$ T-lymphocytes significantly decreases the injury after ischemia-reperfusion[59]. Depletion or deficiency of $CD4^+$ T-lymphocytes seems to regulate liver IRI by reducing recruitment of neutrophils; in fact, the recruited $CD4^+$ T-lymphocytes release interleukin-17 (IL-17), which attracts neutrophils into the site

of injury[39]. Then, recruited $CD4^+$ T lymphocytes are activated by ROS, IL-6, and TNF-α and begin to damage surrounding cells[60].

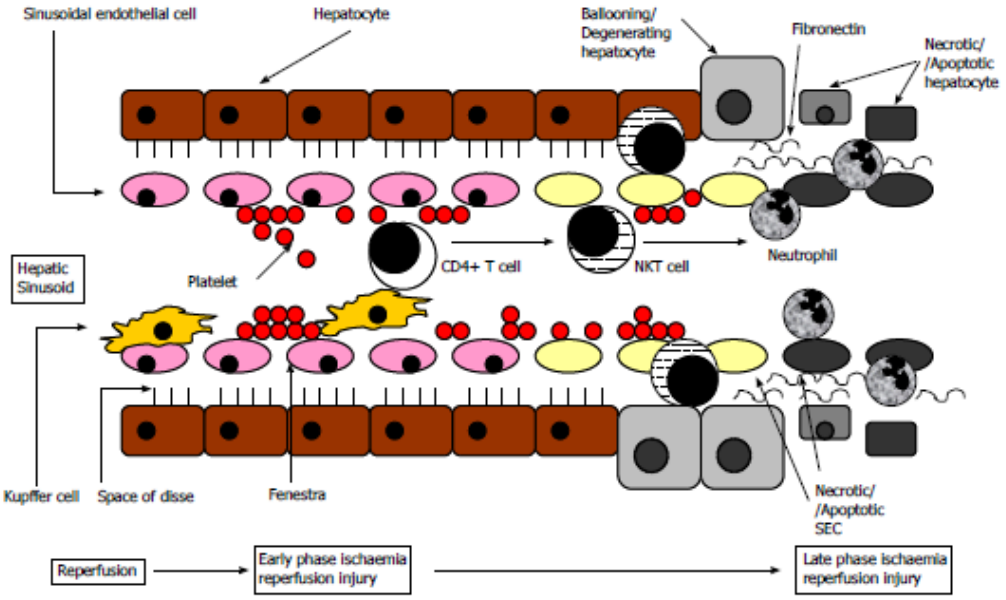

Figure 2.6: In the inner of a liver sinusoid, surrounded by hepatocytes, the immune system cells were recruited and activated, and then the cellular death occurred in liver sinusoidal endothelial cells[39].

2.4 Mechanisms of cell death during hepatic IRI

The two main cell types that are damaged in IRI are hepatocytes: which are more sensitive to warm ischemic injury (37 °C), and liver SEC: which are more sensitive to cold ischemia (4 °C) [39]. There has been controversial hypothesis on the primary mode of cell death occurring in liver IRI, which is apoptosis or necrosis.

2.4.1 Apoptosis

Apoptosis is the mechanism of controlled cell death mediated by two main pathways: the extrinsic and the intrinsic pathway.
The extrinsic pathway is activated from extracellular factors, such as TNF-family ligands or by Fas-family ligands, which are able to recognize and bind the deaths receptors exposed on cell surface, leading to the caspase activation cascade[61]. In particular, pro-caspase-8 and/or pro-caspase-10 which promotes the formation of the death-inducing signalling complex (DISC), further increases the local concentration of pro-caspases, promoting their auto-activation. The activation of pro-caspase continues until reaching the activation of the effector caspases- 3/6/7, which once activated, induce cell death (Figure 2.7, left) [61].
On the other hand, the intrinsic pathway is activated during: inadequate presence of nutrients, lack of survival stimuli, hypoxia, oxidative stress and DNA damage. This activation depends on the balance between pro- and anti-apoptotic proteins of the B-cell lymphoma 2 (BCL-2) family. During an insult, the pro-apoptotic BCL-2

associated X proteins (Bax) and the BCL-2 antagonist/killer (Bak) proteins neutralizes the anti-apoptotic proteins BCL-2, BCL-2 like (Bcl-xL) and Myeloid cell leukemia-1 (Mcl-1). Consequently, the mitochondrial outer membrane is disrupted, and the intracellular proteins, such as cytochrome-c, are released into the cytoplasm. Cytochrome-c binds to the cytosolic apoptosis protease activating factor-1 (Apaf-1), leading to the formation of apoptosome, which in turn activates the initiator pro-caspase-9, giving start to the caspase activation cascade, until cell death occurs (Figure 2.7, right) [62].

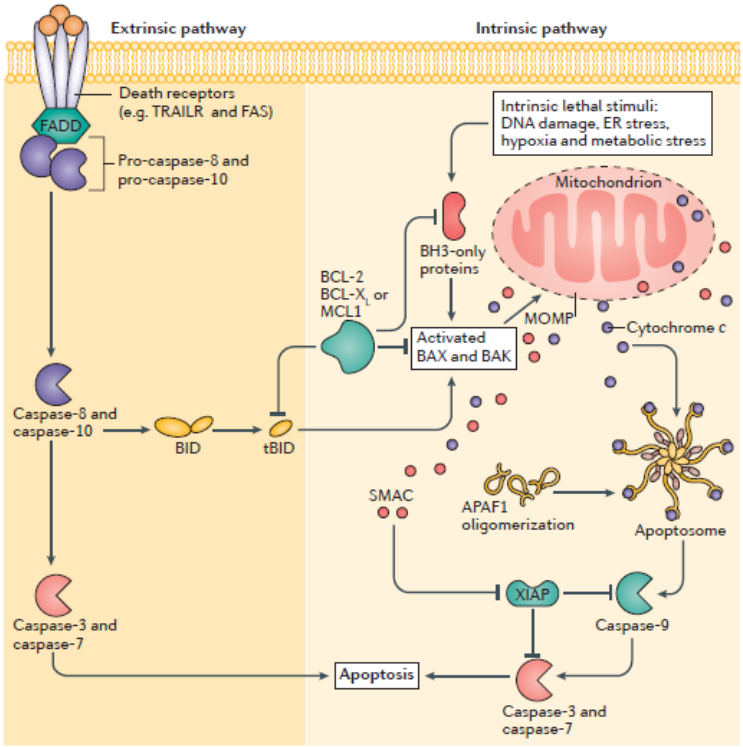

Figure 2.7: The figure describes the extrinsic and intrinsic pathway of apoptosis, which are respectively mediated by the Fas-ligand interaction and by the mitochondrial activation[62].

2.4.2 Necrosis and necroptosis

Necrosis is mainly characterized by an increase in cell volume, swelling of organelles, mitochondrial dysfunction and lack of nuclear fragmentation, plasma membrane rupture and subsequent release of intracellular contents[63]. The mechanism of necrosis is not dependent from caspase cascade activation and it is able to trigger an inflammatory reaction, by the release of factors such as HMGB1 (Hight Mobility Group Box 1) and HDGF (Hepatoma-derived growth factor) that in turn lead to the release of pro-inflammatory interleukins[64].
Recently, a new form of cell death called necroptosis has been identified and it is believed to play a role in several pathologies, such as sepsis, colitis, pancreatitis, stroke[65], but also hypoxic/ischemic injury, including IRI[66]. The discovery of necroptosis showed that cells can execute necrosis through a regulated pathway and therefore, apoptosis is not always the preferred form of cell death[66].

Chapter 3

An overview on the regenerative potential of stem cells

3.1 Human mesenchymal stem cells and their interest in regenerative medicine

Many definitions exist to describe what regenerative medicine is, but, in each definition, some aspects of this large field are not underlined. Hence, the scientists Daar and Greenwood have tried to unify them in a unique explanation: "Regenerative medicine is an interdisciplinary field of research and clinical applications focused on the repair, replacement or regeneration of cells, tissues or organs to restore impaired function resulting from any cause, including congenital defects, disease, trauma and ageing. It uses a combination of several converging technological approaches, both existing and newly emerging, that moves it beyond traditional transplantation and replacement therapies. The approaches often stimulate and support the body's own self-healing capacity. These approaches may include, but are not limited to, the use of soluble molecules, gene therapy, stem and progenitor cell therapy, tissue engineering and the reprogramming of cell and tissue types"[67].

3.1.1 The identity of mesenchymal stem cells

The Mesenchymal and Tissue Stem Cell Committee of the ISCT (International Society for Cellular Therapy) proposed, in 2006, the three minimal criteria to define mesenchymal stem cells (MSCs) [68]:

- adherence to plastic
- specific surface antigen (Ag) expression
- multipotent differentiation potential

Firstly, MSCs must be able to adhere on plastic during standard culture conditions using tissue culture flasks. Secondly, more than 95% of the MSCs population must express a set of markers that should be demonstrated by flow cytometry analysis: CD105, CD73 and CD90. In the same manner, almost all the MSCs population must negatively express (≤ 2% positive) CD11b, CD79a or CD45, CD34, CD14 or CD19 markers as well as HLA class II. Thirdly, MSCs must be multipotent, demonstrating to be able to differentiate *in-vitro* into adipocytes, osteoblasts, and chondroblasts, under standard differentiating conditions. Differentiation to osteoblasts can be identified through Alizarin Red or von Kossa staining, specific for calcium deposits; adipocyte differentiation is most readily demonstrated by Oil-Red-O staining, which detects fat drop deposition; and chondroblast differentiation is evaluated by staining with Alcian blue, a specific marker of glycosaminoglycans, or by immunohistochemical staining for collagen type II[68].

MSCs were first found in the 1960s by McCulloch and Till in the bone marrow (BM) [69]. In the 1970s, Friedenstein et al. observed the clonogenic potential of BM stromal cells through an *in-vitro* assay, referring to them as colony forming-unit fibroblast (CFU-F) [70]. Further experiments revealed the multi-potency of BM cells and how their fate was determined by environmental influences[71].

In 1978, Raymond Schofield proposed the hypothesis of the stem cell niche, which consists in the presence of fixed compartments that promote and maintain the stem cells characteristics, controlling the balance between the self-renewal and the differentiation state. Both the composition of the microenvironment surrounding the cells and the site where it is located defined the niche and its interaction with the stem cells. Some well-defined stem cell niches are located in tissues characterized by sustained cell turnover, such as bone marrow, the bulge of hair follicles and crypts of the small intestine[72].

MSCs found in BM are considered to be a rare population since they exist at an estimate of about 1 in 100.000 BM cells[73].Therefore, researchers focused on other alternative sources of MSC-like cells, including adipose tissue, umbilical cord, placenta, synovial membrane, dental pulp, peripheral blood, periodontal ligament, endometrium[74]. The existence of mesenchymal stem cells was demonstrated also in human liver, as reported by Herrera and colleagues[75].

3.1.2 Therapeutic properties of human mesenchymal stem cells

For many years, the preclinical investigation focused on the potential therapeutic benefit of both autologous and allogenic human MSCs (hMSCs) from multiple sources, since they demonstrated interesting capability that could be involved in regenerative medicine. The three main properties of hMSCs that had been associated with their therapeutic effects includes: tissue replacement by multipotent differentiation[76], immunomodulatory and anti-inflammatory effects[77] and paracrine activity that either initiates or supports tissue repairing[78].

Although early studies focused primarily on the potential transdifferention of hMSCs, it is currently well known that is a rare event *in-vivo*. Engraftment studies

in animal models confirmed that hMSCs are relatively short-lived post injection, only being detectable in various organs for a period of 48 h to 3 months, regardless of the disease type or mode of administration[79].
In recent years, the beneficial effects of hMSCs has been related to their immunoactivity, which can be mediated by both cell-cell contact and secreted bioactive molecules. In fact, the hMSCs are able to induce a suppressive local microenvironment by the secretion of prostaglandin E2, IL-10, stem cell factor (SCF) and macrophage colony-stimulating factor (M-CSF). Nevertheless, hMSCs are also able to suppress natural killer cells through cell-cell contact or by modulation of dendritic cells[80].

3.2 The proliferative potential of the liver

It is well known that the liver has a great proliferative potential, which is quiescent under physiological condition. On the other hand, liver regeneration could be stimulated after an insult, such as chemical injury, partial hepatectomy or hepatotropic virus infection, Hence, in the last decade, the researchers began to search an explanation to this phenomena, investigating the possible presence of undifferentiated cells in liver[81].

3.2.1 The "*oval cells*" population in adult rodent liver

In 1956, Farber identified non-parenchymal liver cells and described it as "small oval cells with scant lightly basophilic cytoplasm and pale blue-staining nuclei", meaning that the oval cells had oval nuclei with a high nuclear-to-cytoplasmatic ratio[82]. Their morphological appearance came out post-treatment of rats with cancer causing agents such as ethionine, 2-acetylaminofluorine and 3-methyl-4-dimethyl aminobenzene[82]. Other rodent models demonstrated that the oval cells could be also induced by: administration of a choline-deficient diet supplemented with ethionine[83]; treatment with DNA alkylating agents[84]; phenobarbital and cocaine[85]; acute allyl alcohol toxicity[86] or D-galactosamine administration, which temporarily blocks hepatocytes proliferation[87].
In all these experimental models, the oval cells showed to possess these features[88]:

1) Expression of biliary epithelial cells markers, such as cytokeratin-7 (CK-7), CK-8, CK-18, CK-19, rat oval cell marker OV-6, glutathione -*S*-transferase, connexin-43; expression of immature fetal hepatoblasts markers, such as gamma- glutamyltranspeptidase, muscle pyruvate kinase and alpha-fetoprotein (AFP); finally some of these cells express markers of hematopoietic stem cells, such as c-kit, CD34, and Sca-1 and CD90.
2) Proliferation induced by a hepatic injury, followed by the formation of duct-like structures in the peri-portal region. After several days, their appearance is changed to clusters of small basophilic hepatocytes and mature bile ducts, which diffuse in the liver acinus.

3) Close contact with HSCs, which secrete growth factors necessary for oval cells proliferation, such as transforming growth factor-α (TGF-α), fibroblast growth factor (FGF), hepatocyte growth factor (HGF) and TNF.

In this way, it was hypothesized that oval cells, probably raised from the bone marrow, could be bipotent progenitor cells capable of regenerating into both hepatocytes and bile duct cells[89].

The precursor-product relationship between oval cells and hepatocytes was confirmed in several experimental animal models. One of the most known models that showed the ability of oval cells to repopulate the liver is the transplantation of oval cells into fumarylacetoacetate hydrolase (FAH) deficient mice. The oval cells were isolated from adult mouse liver after 3,5-diethoxycarbonyl-1,4-dihydrocollidine (DDC) treatment. The experimental results highlighted that the oval cells were able to repopulate the liver, also when they were transplanted with hepatocytes. To determine the source of oval cells, bone marrow transplanted wild-type mice were subjected to DDC for 8 months and then the isolated oval cells were transplanted into FAH deficient mice. These cells were able to repopulate the liver and they showed lack of genetic markers from the original bone marrow donor. Altogether, these findings allowed the researchers concluding that hepatic oval cells possessed liver regenerative properties, but they do not originate in bone marrow[90].

3.2.2 The "*hepatic progenitor cells*" in adult human liver

During the so-called "ductural reaction" [91, 92], which occurs in a variety of human liver disease, the human counterpart of the rodent oval cells was identified. The ductural reaction consists of an increased formation of ductules, the finest ramifications of the biliary tree, followed by peri-portal fibrosis, and leads to the differentiation of a population of human liver cells into the biliary or the hepatocytes lineage, as described for the oval cells found in rodents[93]. During the 2001 and 2002, the national meetings of the "American Association for the Study of Liver Diseases" made of a group of liver pathologists and hepatologists, aimed to arrive at a consensus on a nomenclature for this liver cells population[94]. They proposed to name it as "intermediate hepatobiliary cells", referring to their dual characteristics of both hepatocytes and cholangiocytes. Specifically, their diameter is comprised between 6 and 40 microns, where 6 microns represents the smallest cholangiocyte and 40 microns is the typical size of a hepatocyte; they express OV-6 as rodent oval cells and, simultaneously, biliary markers such as CK-7 and 19 together with hepatocyte markers such as albumin (ALB), alpha-1-antitrypsin, biliary glycoprotein-1 and, rarely, AFP. In addition, they observed the basement membrane formation, typical of cholangiocytes, and canalicular membranes formation, typical of hepatocytes[94].

Recently, it was proposed to name them by the general definition of "hepatic progenitor cells" (HPCs) referring to their ability of rapidly dividing and their identity as stem cells progeny, because they do not possess the capability to self-renew[95].

Table 1 shows a summary on oval cells and hepatic progenitor cellular markers revealed in several studies (Table 1).

Marker name	Sources	Species
Cytokeratin (K)7	Adult biliary marker	Human
Cytokeratin (K)19	Adult biliary marker	Human
Cytokeratin (K)14	Adult biliary marker	Human
Epithelial cell adhesion molecule (EPCAM)	Fetal hepatoblast and adult biliary marker	Mouse Human Rat
Sry-like HMG box protein 9 (Sox9)	Fetal hepatoblast and adult biliary marker	Mouse
Cytokeratin (K) 8	Adult hepatocyte marker	Human
Cytokeratin (K) 18	Adult hepatocyte marker	Human
c-Met	Adult hepatocyte marker	Human
α-fetoprotein protein	Fetal hepatoblast marker	Mouse Rat Human
Albumin	Adult hepatocyte marker	Mouse Rat Human
c-Kit	Fetal hepatoblast and adult hematopoietic marker	Mouse
Sca-1	Fetal hepatoblast and adult hematopoietic marker	Mouse
Thy-1 (CD90)	Adult hematopoietic marker	Rat
Prominin/CD133	Adult hematopoietic marker	Mouse
C-X-C chemokine receptor type 4 (CXCR4)	Adult hematopoietic marker	Mouse
Neural cell adhesion molecule (NCAM)	Adult neural cell marker	Human

Table 1: Summary of oval cells (rat, mouse) and hepatic progenitor cells (human) markers and their cellular lineage[96].

Although various experiments have shown that HPCs are involved in liver regeneration after acute or chronic hepatic damage, few researchers have successfully isolated HPCs from adult human liver. For example, Li and colleagues isolated the HPCs from adult human liver and demonstrated that they possessed the bipotential differentiation ability by culturing them in conditioned media. Even though bioinformatics gene analysis showed a high similarity to primary hepatocytes (67.8%), they demonstrated that the cultured HPCs were also positive for eights markers previously reported as HPCs markers (ALB, AFP, CK-8, 18 and 19, CD90, CD117 and OV-6) and for two hematopoietic cell markers (CD45 and CD109)[97].

Lu and his colleagues confirmed the existence of HPCs population activated in their mouse model with mouse double minute 2 homolog (Mdm2) gene deletion in over 98% of hepatocytes, which leads to apoptosis, necrosis and senescence of hepatocytes. The activated HPCs were able to reconstitute completely and functionally the injured liver. In addition, they isolated HPCs from healthy mice using a stringent selection of cell surface markers and showed that the HPCs were phenotypically stable *in-vitro* and expandable. Furthermore, the HPCs were not able to consistently repopulate a healthy liver, therefore suggesting that they do not contribute towards homeostatic repair and are probably activated after an injury or in pathological liver condition[98].

3.2.3 The "human liver stem cells" isolated from adult human liver

In 2006, Herrera and her colleagues isolated a stem cell line from normal adult human liver, thus demonstrating the presence of a population of resident progenitor cells in adult human liver[75].

The human liver stem cells (HLSCs) were isolated by culturing under stringent conditions the hepatocytes obtained from eight different normal human liver preparations. After two weeks of culture, the hepatocytes dead and the surviving cells were cultured in stem cells medium for other three weeks. After that, single clones were isolated and sub-cultured; twenty-four different cell clones were cultured in undifferentiating medium for six months, without undergoing in senescence, indicating the capability of these cells to self-renew[75].

The subsequent analysis by fluorescence-activated cell sorting (FACS) or by immunofluorescence on HLSCs demonstrated that clones were positive for the mesenchymal stem cell markers CD73, CD90, CD29 and CD44, and negative for the hematopoietic stem cell markers CD54, CD34, CD117 and CD133. In addition, the HLSCs were positive for the liver tissue-specific protein such as AFP, ALB, CK-8 and CK-18. In contrast, the HLSCs were negative for the oval cell's marker CK19, as well as cytochrome P450, a marker of mature hepatocytes (Table 2). All these results indicated that HLSCs represent a population of progenitor cells different from oval cells, possessing a partial commitment towards hepatic lineage[75].

The HLSCs were able to differentiate into hepatocytes when cultured in microgravity conditions and with the supplying of HGF and FGF-4 in culture media, expressing markers typical of mature hepatocytes such as cytochrome P450, CK-8 and CK-18[75].

Furthermore, the capability of HLSCs to differentiate into osteogenic, adipogenic and endothelial lineage was analysed. The HLSCs cultured in osteogenic medium are able to produce calcium deposits and to express osteocalcin and osteopontin, as well as under vascular endothelial growth factor (VEGF) stimulation, HLSCs expressed endothelial markers CD31, CD34, VEGF receptor, CD44 and von Willebrand factor. Moreover, in both cases, the expression of ALB, AFP and CK18 were lost. In contrast, HLSCs did not differentiate into adipocytes, also after three weeks of culturing in adipogenic medium[75].

Finally, a model of severe combined immunodeficiency (SCID) mice with acute liver injury was established by *N*-acetyl-*p*-aminophen treatment and the HLSCs were injected. After thirty days of HLSCs treatment, the damaged parenchyma was regenerated, showing clusters of cells positive for HLA class I antigen and for human chromosome 17, and negative for mouse β_2-microglobulin. These observations demonstrated that the HLSCs contributed to liver regeneration, they are able to extent the self-renew capability *in-vivo* and they possess the ability of multipotent differentiation[75].

Markers	FACS analysis (% of positive cells: mean ± SD)
Isotypic control	0
CD34	0
CD45	0
CD14	0
CD73	100
CD29	100
CD44	100
CD117	0
CD90	80 ± 10
CD146	18 ± 11
CD133	0
CD105	20 ± 12
	Immunofluorescence analysis (% of positive cells: mean ± SD)
Albumin	100
AFP	100
CK8	11 ± 7
CK18	15 ± 8
CK19	0
Vimentin	100
Nestin	100
α-SMA	0
NCAM	0
STRO-1	0

Table 2: Characterization of HLSCs immunophenotype. Abbreviations: α-SMA: α-smooth muscle actin; NCAM: neural cell adhesion molecule[75].

Chapter 4

The new frontiers of regenerative medicine: extracellular vesicles derived from human liver stem cells

4.1 The definition and characterization of extracellular vesicles

Communication cell-to-cell and cells-to-environment covers an essential role in all organisms and, recently, the attention of scientist has focused on the intercellular communication mediated through extracellular vesicles (EVs). The name EVs in general is used to indicate the category of secreted membrane-enclosed vesicles, comprising exosomes, ectosomes and microvesicles, ranging from 30 up to 500, which contain growth factors, hormones, chemokines, cytokines and neurotransmitters[99, 100].

According to the International Society of Extracellular Vesicles (ISEV), the EVs is the generic term to indicate particles physiologically released by cells that are delimited by a lipid bilayer and that are not able to replicate, i.e. they do not contain a functional nucleus[101].

The exact process of the formation of EVs is currently discussed, it has been suggested that EVs can be formed by the direct budding of plasma membrane into the extracellular space in a calcium-dependent way. In this process, the cytoskeleton reorganization and the redistribution of membrane components occur, while the plasma-mediated attractive forces between membranes lead to the creation of nanodomains[102].

On the other hand, it has been proposed that the exosomes are formed by the invagination of endosomal membrane cell compartment and released into a structure known as multivesicular bodies, which in turn fuses with the plasma membrane and, therefore discharging its cargo of exosome into the extracellular space. This process is dependent by cytoskeleton activation, but independent from cell calcium concentration[103].

Although their molecular composition is highly heterogeneous, the shedding vesicles are enriched in cholesterol and phosphatydilserine; conversely, the exosomes expressed molecules on their surface, such as CD81, CD63 and CD9[104]. However, the EVs extracted from cells supernatant or present in extracellular fluids are inexorably a heterogeneous population of both shedding vesicles and exosomes, and it is currently very difficult to accurately distinguish between the two types[100].

4.1.1 The role of EVs in cellular communication exploited by several mechanism

The EVs can interact to a recipient cell through different manner, such as the internalization following a receptor-ligand recognition. In this way, the EVs may act in intercellular communication as carrier of proteins, bioactive lipids and nucleic acids to the cytoplasm of recipient cells[100]. For example, the EVs derived from monocytes stimulated by lipopolysaccharides can convey a cell death message transporting the caspase-1 enzyme[105].

Interestingly, the EVs are also involved in the transfer of genetic information since they can contain nucleic acids such as miRNA and mRNA. The horizontal transfer of miRNAs has been demonstrated in EVs deriving from cancer stem cells that were able to induce a pre-metastatic niche in the lungs through the pro-angiogenic RNAs they contain, whereas the EVs from cancer cells that have been differentiated did not possess this capability[106].

Recently, it has been suggested that EVs could deliver miRNA implicated in immune system regulation, as observed in the immune synapses of a model of communication between T-cells and antigen-presenting cells (APCs) during antigen recognition. The $CD63^+$ exosomes, delivered from the T-cells during immune synapse formation, were able to modulate gene expression in recipient cells by transferring the miR-355 to APCs[107].

Moreover, the EVs has been demonstrated to be involved in stem cell biology. For example, the EVs deriving from embryonic stem cells could be involved in maintenance of pluripotency of stem cells[108]. On the other hand, also the EVs produced by adult stem cells may convey genetic information, such as the endothelial progenitor cells, that were able to transfer a subset of mRNA specifically associated with angiogenic signalling cascade, which could initiate angiogenesis in quiescent endothelial cells[109].

4.1.2 Biological effects of MSC-EVs on injured liver

A number of studies were conducted on EVs derived from MSCs and showed to find a widespread application in improving the condition of injured livers.

In this context, it has been showed that the MSC-EVs have anti-apoptotic[110, 111,112] and anti-oxidant effects[110, 111]; the MSC-EVs have the ability to down-regulate the inflammation[110, 111,113] and they are able to protect liver from fibrosis[113, 114,115]. In addition, MSC-EVs are able to induce and sustain liver proliferation[116].

Therefore, as described, the MSC-EVs have a number of biological properties with

important effects on tissue regeneration and/or in the prevention of tissue damage. Considering that, cell-derived biological products deriving from stem cells such as EVs succeeded in ameliorate liver injury and that, HLSC are mesenchymal stem cells directly derivate from the liver tissue with protective and regenerative properties, we decided to evaluate the biological effects of HLSC-EVs in the hepatic damage induced by the ischemia-reperfusion injury.

4.2 The extracellular vesicles from HLSC and their role in regenerative medicine

In 2010, Herrera and colleagues isolated and characterized the EVs deriving from HLSCs, the human liver stem cells lineage described in the third chapter. Starting from cultured HLSCs, EVs were extracted by ultracentrifugation and showed to have a size ranging between 80 nm and 1 μm[117]. Several markers were identified on the surface of HLSC-EVs, such as CD44, CD29 and α-4 integrin, which are also present on HLSCs plasma membrane. In addition, HLSC-EVs are negative for α5- and α6-integrins and HLA-class I molecules[117]. The HLSC-EVs labelled with the red fluorescent chromophore PKH26 showed the ability to be internalized into human hepatocytes (Figure 4.1). Moreover, the trypsin treatment of HLSC-EVs abrogated their incorporation in human hepatocytes, because of the removal of surface molecules involved in HLSC-EVs uptake[117]. The HLSC-EVs content was analysed by gene array analysis providing information that more than 60 different transcripts were present inside them and these genes were especially involved in cell proliferation, such as MATK, VASP, MRE11A, MYH11, CHECK and CDK2. CDK2 gene has been shown to be involved the regeneration of the liver (Table 3)[117]. Moreover, the HLSC-EVs were able to increase the proliferative potential of human hepatocytes and this effect is suppressed by RNase treatment of HLSC-EVs, because the genetic material shuttled inside the EVs is totally degraded[117]. Finally, the biological effects of HLSC-EVs were tested on a 70% hepatectomy rat model, showing that they were able to recover the injured tissue, decreasing the hepatic lesions and cellular apoptosis[117].

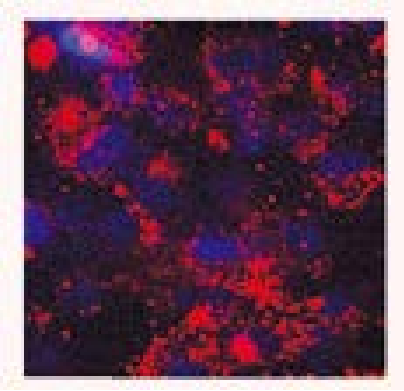

Figure 4.1: Representative confocal microscopy micrograph showing HLSC-EVs internalized by human hepatocytes (Modified image[117]).

Functional category	mRNA	Description
Transcription regulators	CASP8AP2	CASP8 associated protein 2
	DMRT2	Doublesex and mab-3 related transcription factor 2
	HOXC12	Homeobox C12
	NFIX	Nuclear factor I/X (CCAAT-binding transcription factor)
	HOXA3	Homeobox C3
	MIB2	Mindbomb homolog 2
	NFIX	Nuclear factor I/X
	NR2E3	Nuclear receptor subfamily 2
	SIM2	Single-minded homolog 2
Translation regulator	EIF2C2 (AGO2)	Eukaryotic translation initiation factor 2C, 2
Enzymes/metabolism	CREG2	Cellular repressor of E1A-stimulated genes 2
	FKBP9	FK506 binding protein 9, 63 kD
	IMPDH1	IMP (inosine monophosphate) dehydrogenase 1
	MRE11A	MRE11 meiotic recombination 11 homolog A (S. cerevisiae)
	ST3GAL4	ST3 β-galactoside α-2,3-sialyltransferase 4
	STK40	Serine/threonine kinase 40
	ACPP	Acid phosphatase, prostate
	PGC	Progastricsin (pepsinogen C)
	B3GAT1	β-1,3-glucuronyl-transferase 1
	CDK2	Cyclin-dependent kinase 2
	CHEK2	Cell cycle checkpoint regulator
	LTK	Leucocyte receptor tyrosine kinase
	MATK	Megakaryocyte-associated tyrosine kinase
	PTEN	Phosphatase and tensin homolog
	PTPN2	Protein tyrosine phosphatase
Transporter	AP3M2	Adaptor-related protein complex 3, mu 2 subunit
	ATP1A2	ATPase, Na^+/K^+ transporting, $\alpha 2^+$ polypeptide
	PODXL	ATP binding
	SLC22A16	Organic cation/carnitine transporter
Ion channel	CACNG1	Calcium channel, voltage-dependent, γ subunit 1
G-protein coupled receptor	MC3R	Melanocortin 3 receptor
Other	TMEM179	Transmembrane protein 179
	TOR1AIP2	Torsin A interacting protein 2
	TSPAN7	Tetraspanin 7
	VASP	Vasodilator-stimulated phosphoprotein

Table 3: Description of mRNA content in HLSC-EVs and their involving in the main cellular processes[117].

4.2.1 HLSC-EVs and their regenerative potential in *in-vivo* injury models

Different studies have been demonstrated the biological effects of HLSC-EVs in several animal models. Herrera and colleagues evaluated the protective effects of HLSC-EVs in a mouse model of acute kidney injury (AKI), induced by intra-muscle glycerol injection. The authors showed that the EVs were able to ameliorate the tubular injury, decreasing the plasma levels of creatinine and blood urea nitrogen after 5 days from glycerol injection[118].
In another study, Herrera and colleagues reported that the HLSC-EVs could extent their regenerative effects also in a model of liver disease citrullinemia type I, a rare disorder that lead to early neonatal death, in which a mutation of arginosuccinate synthase 1 (ASS1) enzyme occurs. In this study, the enzymatic activity of ASS1

was restored by HLSC-EVs treatment, such as the urea production, thanks to the transfer of ASS1 enzyme and its mRNA from HLSC-EVs to diseased cells[119].
The HLSC-EVs were able to prevent *in-vivo* kidney fibrosis, as demonstrated in the study of Kholia and collaborators, in which the authors treated a mouse model of kidney fibrosis, induced by the aristolochic acid, with the HLSC-EVs. They showed that the HLSC-EVs treatment reduced infiltration of fibroblast, interstitial fibrosis and tubular necrosis. Moreover, the HLSC-EVs were able to inhibit the up-regulation of pro-fibrotic genes, such as α-SMA, TGF-β1 and COL1A1, induced by the disease both *in-vitro* and *in-vivo*[120].
The HLSC-EVs exhibited also anti-tumor properties, as demonstrated in these two studies. As reported by Fonsato and colleagues, the HLSC-EVs combined with tyrosine kinase inhibitors (TKIs) increased apoptosis on cancer stem cells (CSCs), known to be cells responsible for the maintenance and the recurrence of tumors. In this case, the HLSC-EVs acted on the axis of intracellular pathway that promoted tumor growth and survival, such as cAMP response element binding protein (Creb) and extracellular signal-regulated kinases (ERK) [121].
Moreover, as demonstrated by Lopatina and collaborators, the HLSC-EVs were able to inhibit, both *in-vitro* and *in-vivo,* angiogenesis of tumor-derived endothelial cells (TEC). Specifically, they exerted this effect by down-regulating the predicted target genes directly involved in angiogenesis, such as FGF1 and plasminogen activator urokinase (PLAU), through the miRNA that they carried out to the tumor cells, namely miR-181b, miR-15a, miR-874 and miR-320c[122].

Chapter 5

Evaluation of HLSC-EVs effects in an *ex-vivo* hypoxic rat liver model during four hours of normothermic perfusion (NMP).

5.1 Introduction on hypoxic model

As already described in the previous chapters, to satisfy the increasing donor's request for LT, the scientific interest moved towards the ECD organs, with a particular attention for DCD livers[2]. The standard technique for liver preservation before transplant, the SCS, is imperfect in protecting DCD livers[14], because livers from DCD may have suffered from a period of hypoxia before the cardiac arrest occurred[123]. The hypoxia experienced by hepatocytes switched the cellular metabolism from aerobic to anaerobic, with the consequent production of lactate, which are responsible of lactic acidosis. The only chance to recover liver metabolism is by restoring of oxygen supply[123]. Hence, an alternative strategy for liver preservation before transplantation is the NMP, which excelled in preserving liver at physiological conditions and offers also the possibility to provide a pharmacological or biological treatment during the *ex-vivo* reconditioning[2]. According with that explained before, in this first project we set up an *ex-vivo* model of hypoxic rat liver during normothermic perfusion (NMP), in order to evaluate the beneficial effects of HLSC-EVs administration in ameliorating the hypoxic-induced liver injury. Briefly, the hypoxic *ex-vivo* NMP model consisted in an NMP of 4 hours with a low haematocrit (<10%) to obtain a hypoxic injury. Our first objective was to understand if HLSC-EVs could be rapidly internalized in the treated livers during the 4 hours perfusion; the second objective was to evaluate in all experimental groups the degree of hypoxic injury, comparing the HLSC-EVs

treated livers with the non-treated one, in order to investigate a potential beneficial effects deriving from HLSC-EVs in ameliorating the injured livers.

5.2 Material and methods

5.2.1 HLSC culture

HLSC were isolated from human cryopreserved adult hepatocytes purchased from Lonza Bioscience (Lonza, Basel, Switzerland) and cultured as described by Herrera et al., 2006[75]. Briefly, HLSC were cultured in a medium containing α-miminum essential medium (α-MEM) and Endothelial Cell Growth Basal Medium (EBM) in a 3:1 proportion, supplemented with L-glutamine (2 mM), penicillin (100 U/mL), streptomycin (100 µg/mL) and 10% fetal calf serum (FCS) (all by Sigma, St. Louis, MO). HLSC were maintained in a humidified incubator with 5% CO_2 at 37°C. For all experiments, HLSC between passages 5 to 11 were used.

5.2.2 Isolation of fluorescent HLSC-EVs

The cultured HLSC were detached and suspended in Dulbecco Phosphate Buffered Saline (DPBS) (Sigma, St. Louis, MO), then 1 µM of DIL (1,1'-Dioctadecyl-3,3,3',3'-Tetramethylindocarbocyanine Perchlorate; Molecular Probes Life Technology, USA) was added to stain of $1x10^6$ cells/ml. After an incubation of 15 minutes at 37 °C, the staining was blocked adding 15 ml of Roswell Park Memorial Institute (RPMI) medium supplemented with L-glutamine (2 mM), penicillin (100 U/mL), streptomycin (100 µg/mL) and with 10% FCS (Sigma, St. Louis, MO). The HLSC were then centrifuged and plated. Once at 80% confluence, HLSC were starved overnight (O/N) in RPMI medium deprived of FCS at 37°C in a humidified incubator with 5% CO_2. Supernatants were collected, centrifuged at 3,500 rpm for 15 minutes to remove cell debris, and then submitted to ultracentrifugation at 100.000 g for 2 hours at 4°C (Beckman Coulter Optima L-90 K, Fullerton, CA, USA). After that, the DIL-labelled EVs were collected and suspended in RPMI-serum free medium plus 1% of the total volume of DMSO and stored at −80°C. Quantification and size distribution of EVs were performed using NanoSight LM10 (NanoSight Ltd, Minton Park, UK). For quantification, EVs preparations were diluted (1:200) in sterile saline solution.

5.2.3 Surgical procedures

All the experiments were approved by the local Ethic Committee for Experimental Animal Research and conducted in accordance with the National Institutes of Health *Guide for the Care and Use of Laboratory Animals*. Male Wistar rats from 8 to 12 weeks aged, with the weight between 200 and 250g, were obtained from Charles Rivers (Italy) and maintained on standard conditions, providing food and water *ad libitum*. After intraperitoneal heparin administration, (1250 U) a midline laparotomy was performed. The bowel was retracted to expose the liver and the hepatic pedicle. The common bile duct (CBD) was cannulated with a 22-G cannula,

the hepatic artery (HA) was ligated and the portal vein (PV) was cannulated with an 18-G cannula. After sternotomy, the heart was opened to exsanguinate the animal. The liver was flushed with 40 mL of cold Celsior solution through PV cannula. Then, the liver was freed from its ligaments, weighed and placed into a Petri dish filled with ice-cold Celsior solution and transported into perfusion room. Animals were euthanized by hearth exsanguination and cervical dislocation.

5.2.4 Normothermic Machine Perfusion (NMP)

The NMP circuit was constituted of a warmed perfusion chamber, connected to a peristaltic pump, an oxygenator (Hollow Fiber Oxygenator D150, Hugo Sachs Elektronik), which gassed the perfusion solution with a 99% O_2 mixture and a bubble trap, to avoid air embolism in circulating perfusate. A thermostatic circulator maintained the physiological temperature of 37 °C. A Transducer Amplifier Module (TAM-D, Hugo Sachs Elektronik, Harvard Apparatus) and a Servo Controller (SCP Type 704, Hugo Sachs Elektronik, Harvard Apparatus) allowed constant pressure perfusion (8-10 mmHg) and continuous monitoring of perfusate flow (1.1-1.3 mL/min/g liver). The perfusion solution consisted of phenol red-free Williams E Medium, supplemented with 2 mM L-glutamine, 100 U/mL penicillin, 100 µg/mL streptomycin, 11.6 mM glucose, (all from Sigma), 1 U/ml insulin (Lilly, Italy), 1 U/mL heparin (PharmaTex, Italy), named complete Williams Medium. The hypoxic injury was established through an isovolemic hemodiluition of the perfusate, performed by adding 20 mL of fresh rat blood to 50 mL of complete Williams Medium. The obtained haematocrit had a mean value of 9.67±0.66%. This low haemoglobin content induced a limited but progressive hypoxic injury to hepatic tissue[124]. Before to connect to NMP circuit, the livers were flushed with 10 mL of complete Williams Medium to wash the Celsior solution. Once connected, the NMP circuit allowed continuous perfusion at 37 °C through the PV cannula for four hours in controlled conditions of flow and pressure. Heparin (500 U) was added hourly during perfusion and 2 mEq/2 ml of sodium bicarbonate (Na^+HCO_3) were used to prevent pH fluctuations. A tube was inserted into the CBD cannula to collect bile. The experimental groups were divided in NMP group (n=10), in which the hypoxic livers were subjected to NMP, and the NMP+HLSC-EVs group (n=9), in which the hypoxic livers received the HLSC-EVs treatment at the beginning of NMP. Specifically, the HLSC-EVs were added to the circuit within 15 minutes from perfusion start, in a single dose of $5x10^8$ HLSC-EVs/g of liver, while in the control liver, an equivalent quantity of HLSC-EVs suspension medium was added.

5.2.5 Immunofluorescence analysis

At the end of each experiment, some liver biopsies were snap frozen and stored at -80°C, then serial slides were cut (3‑5 µm) by a cryostat and fixed in acetone. After rinsing in phosphate buffered saline (PBS), the non-specific signal of the slices was blocked by an incubation with a solution of PBS with 3% bovine serum albumin and 0.1% Tween-20, for 1 hour at room temperature (RT). After that, they were

incubated overnight at 4 °C with a primary antibody directed against rat cytochrome P450-4A (Invitrogen) at the dilution of 1:50. The day after, the slices were washed in PBS and then incubated with the secondary antibody Alexa Fluor 488 (Invitrogen) for 1 hour at RT. Finally, nuclei were stained with 4',6-diamidino-2-phenylindole (DAPI) and, after washing in PBS, slides were mounted with the aqueous mountant Fluoromount (Sigma). The uptake of HLSC-EVs was observed using a Cell Observer SD-ApoTome laser scanning system (Carl Zeiss).

5.2.6 Histopathological analysis

At the end of each experiment, liver biopsies were formalin fixed and paraffin embedded, then haematoxylin-eosin (H&E) staining was performed to evaluate tissue morphology, while cell apoptosis was analysed by TUNEL assay.
After deparaffinization, liver slices were immersed in hematoxylin staining for three minutes, then washed under tap water for five minutes. After that, slices were immersed in eosin staining for five minutes and then washed again under tap water. Finally, the slices were dehydrated and mounted using an anhydrous mounting medium (Neo-Mount®, Merck). An experienced liver pathologist blindly scored the severity of histological damage according to modified Suzuki criteria[125]: sinusoidal congestion, hepatocyte necrosis and vacuolization, graded from 0 to 4. Specifically, absence of necrosis, congestion or vacuolization is grade=0; minimal congestion, vacuolization or necrosis is grade=1; mild congestion, vacuolization or necrosis <30% is grade=2; moderate congestion, vacuolization or necrosis 30-60% is grade=3; severe congestion, vacuolization or necrosis >60% is grade=4. Each animal final score was determined by the summation of the grades for the three items.
To investigate apoptosis, the terminal deoxynucleotidyl transferase dUTP nick-end labelling (TUNEL) assay was performed. After deparaffinization, slices were digested by proteinase-K (1 mg/ml) (Invitrogen) for 15 minutes at RT and the ApopTag® Peroxidase In Situ Apoptosis Detection Kit was used according to the manufacturer's protocol (Millipore, Burlington, Massachusetts). To detect the positive cells for the apoptosis staining, the 3,3'-Diaminobenzidine (DAB) (Dako, Agilent) was used as peroxidase substrate. To counterstain, the slices were immersed in haematoxylin for 30 seconds. At the end, slides were mounted using an anhydrous mounting medium (Neo-Mount®, Merck). Positive and negative TUNEL cells were blindly counted on 20 microscopic fields acquired at 200× magnification using Olympus Microscope (Olympus Life Science, Massachusetts), then the apoptosis index was calculated as the ratio between the number of positive cells and the number of total cells.

5.2.7 Perfusate and bile analysis

The inflow and outflow perfusate samples were collected hourly and analysed by a blood gas analyser (ABL 705L Radiometer, Copenhagen), testing pO_2, pCO_2 and pH. In addition, outflow samples were collected at the end of each hour of

perfusion, centrifuged at 3,500 rpm for 10 minutes at 4 °C and then the supernatants stored at -80 °C. The levels of cytolytic hepatic enzymes were measured by the Biochemistry Laboratory of Molinette Hospital (Turin, Italy): aspartate aminotransferase (AST), alanine aminotransferase (ALT) and lactate dehydrogenase (LDH). Then, all the results were normalized towards the animal liver weight (U/L/g of liver).
At the end of each perfusion experiment, the total bile produced by liver was collected and the total volume was quantified (µl). Then, all volumes were normalized towards the animal liver weight (µl/g of liver).

5.2.8 RNA extraction and retro-transcription

RNA was extracted from paraffin embedded liver samples using the RecoverAll™ Total Nucleic Acid Isolation Kit (Invitrogen) according to the manufacturer's protocol. Briefly, 5 µm slices were cut for each samples and paraffin was removed by xylene. After several washes in ethanol, the recovered tissue was digested by protease. Then, the RNA was isolated using the filter cartridge and the appropriate isolation buffer. The eventual presence of DNA was removed using a DNase enzyme, and then the RNA was washed several times in ethanol using the filter cartridge and finally eluted in nuclease free water. The RNA was quantified using Thermo Scientific™ NanoDrop 2000/2000c (Thermo Fisher, Waltham, Massachusetts) and a total amount of 400 ng of RNA was retro-transcribed in a 20 µl of total volume reaction using High Capacity cDNA Reverse Transcription Kit (Applied Biosystems, Thermo Fisher, Massachusetts).

5.2.9 Quantitative Reverse Transcription Polymerase Chain Reaction

To perform the real time polymerase chain reaction (RT-PCR), a mix containing 1x SYBR GREEN PCR Master Mix (Applied Biosystems, Thermo Fisher, Massachusetts), 200 nM of each couple of primers (Table 4) and 10 ng of cDNA was assembled in a 96-well plate and ran by StepOne Real Time System (Applied Biosystems, Thermo Fisher, Massachusetts). The ΔΔCt method was used to quantify the relative expression of HIF-1α (hypoxia induced factor-1) and TGF-β1 normalized towards the β-actin (housekeeping gene), while one liver explant from a healthy rat, named sham, was used as reference sample.

Gene	Forward sequence (5'→3')	Reverse sequence (5'→3')
ACTβ	ACCGTGAAAAGATGACCCAGAT	CACAGCCTGGATGGCTACGT
HIF-1α	TGTGTGTGAATTATGTTGTAAGTGGTATT	GTGAACAGCTGGGTCATTTTCAT
TGF-β1	TTGCCCTCTACACCAACACAA	GGCTTGCGACCCACGTAGTA

Table 4: Sequences of forward and reverse primers used for RT-PCR.

5.2.10 Statistical analysis

Data are expressed as mean ± SEM. Statistical analysis was performed by Student's t-test or analysis of variance with Sidak's multi-comparison test where appropriate

(GraphPad Prism, version 6.00, USA). A p-value < 0.05 was considered to be statistically significant.

5.3 Results

5.3.1 Monitoring of normothermic perfusion parameters

As showed by the similarity between all the experimental groups concerning the liver weight, the pre-perfusion temperature and the ischemia time, our experiments were reproducible (Table 5). During the four hours of perfusion, the flow rates and the venous resistances were stable and all the livers were able to self-regulate pH, pO_2 and pCO_2 (Table 5).

	NMP (n=10) Mean (SEM)	**NMP+HLSC-EV (n=9)** Mean (SEM)	**p-value**
Liver weight [g]	10.35 (0.41)	10.16 (0.22)	0.69
Pre-perfusion temperature [°C]	13.80 (1.78)	9.89 (0.89)	0.08
Pre-perfusion ischemia time [min]			
- Warm ischemia	3.10 (0.35)	3.56 (0.24)	0.31
- Total ischemia	29.30 (1.51)	34.78 (2.39)	0.06
Flow [ml/min/g liver]			
- t = 60 min	1.23 (0.06)	1.14 (0.06)	0.33
- t = 120 min	1.30 (0.05)	1.24 (0.07)	0.49
- t = 180 min	1.30 (0.04)	1.23 (0.07)	0.41
- t = 240 min	1.19 (0.07)	1.21 (0.07)	0.80
Venous resistance [mmHg/(ml/min/g liver)]			
- t = 60 min	7.22 (0.45)	8.14 (0.47)	0.18
- t = 120 min	6.84 (0.38)	7.53 (0.47)	0.27
- t = 180 min	6.69 (0.25)	7.52 (0.43)	0.11
- t = 240 min	7.65 (0.59)	7.65 (0.45)	0.99
pH (Inflow)			
- t = 60 min	7.52 (0.09)	7.41 (0.03)	0.35
- t = 120 min	7.53 (0.09)	7.44 (0.02)	0.42
- t = 180 min	7.43 (0.06)	7.48 (0.05)	0.51
- t = 240 min	7.37 (0.08)	7.44 (0.08)	0.61
pH (Outflow)			
- t = 60 min	7.43 (0.08)	7.39 (0.06)	0.70
- t = 120 min	7,41 (0.09)	7.39 (0.03)	0.84
- t = 180 min	7.33 (0.06)	7.42 (0.04)	0.24
- t = 240 min	7.26 (0.08)	7.37 (0.05)	0.30

Table 5 (continue)			
pO_2 (Inflow) [mmHg]			
- t = 60 min	273 (122)	240 (102)	0.84
- t = 120 min	343 (108)	273 (105)	0.66
- t = 180 min	241 (71)	290 (106)	0.75
- t = 240 min	230 (61)	239 (81)	0.93
pO_2 (Outflow) [mmHg]			
- t = 60 min	26.38 (3.67)	29.93 (3.99)	0.57
- t = 120 min	33.05 (5.06)	42.87 (7.15)	0.37
- t = 180 min	33.18 (4.78)	42.07 (6.51)	0.37
- t = 240 min	25.28 (7.40)	35.69 (4.16)	0.21
pCO_2 ((Inflow) [mmHg]			
- t = 60 min	39.98 (7.67)	36.83 (4.32)	0.71
- t = 120 min	31.30 (5.34)	29.13 (3.01)	0.71
- t = 180 min	37.53 (4.86)	29.20 (1.13)	0.10
- t = 240 min	34.03 (4.40)	27.35 (3.78)	0.29
pCO_2 (Outflow) [mmHg]			
- t = 60 min	49.43 (9.12)	44.63 (4.24)	0.60
- t = 120 min	38.98 (7.96)	36.10 (2.63)	0.68
- t = 180 min	46.03 (8.46)	34.83 (1.78)	0.11
- t = 240 min	47.60 (7.17)	34.88 (3.39)	0.11

Table 5: Description of the operating parameters measured during each NMP.

5.3.2 The HLSC-EVs are engrafted in hepatic parenchyma and improved the morphology of hepatic injured tissue

Firstly, we ascertained that HLSC-EVs were engrafted in hepatic parenchyma by immunofluorescence analysis. As showed in Figure 5.1-D, the red HLSC-EVs, stained by DIL, co-localized with the green hepatocytes, stained by the hepatic marker cytochrome P450-4A (Figure 5.1, A-D).

Then, we analysed the morphology of hepatic tissue through H&E staining, and we found out that while the control livers showed evident area of necrosis, the treated livers had a well-conserved hepatocytes structure (Figure 5.1-E). This observation was confirmed by the Suzuki's score damage quantification, which allowed calculating the total grade of damage on the base of sinusoidal congestion, hepatocyte necrosis and vacuolization. The NMP+HLSC-EVs livers had a significant lower value of Suzuki's score compared to the NMP control group ($p<0.05$) (Figure 5.1-F), suggesting that the HLSC-EVs treatment could reduce tissue damage due to hypoxic injury. Moreover, the NMP+HLSC-EVs livers had a reduced level of apoptosis compared to the control ones, as showed in Figure 5.1-G. Effectively, the quantification of apoptosis index demonstrated that the HLSC-

EVs treatment significant reduced the relative number of apoptotic cells compared to the non-treated livers ($p<0.05$) (Figure 5.1-H), suggesting that the treatment could protect the damaged livers from cellular death.

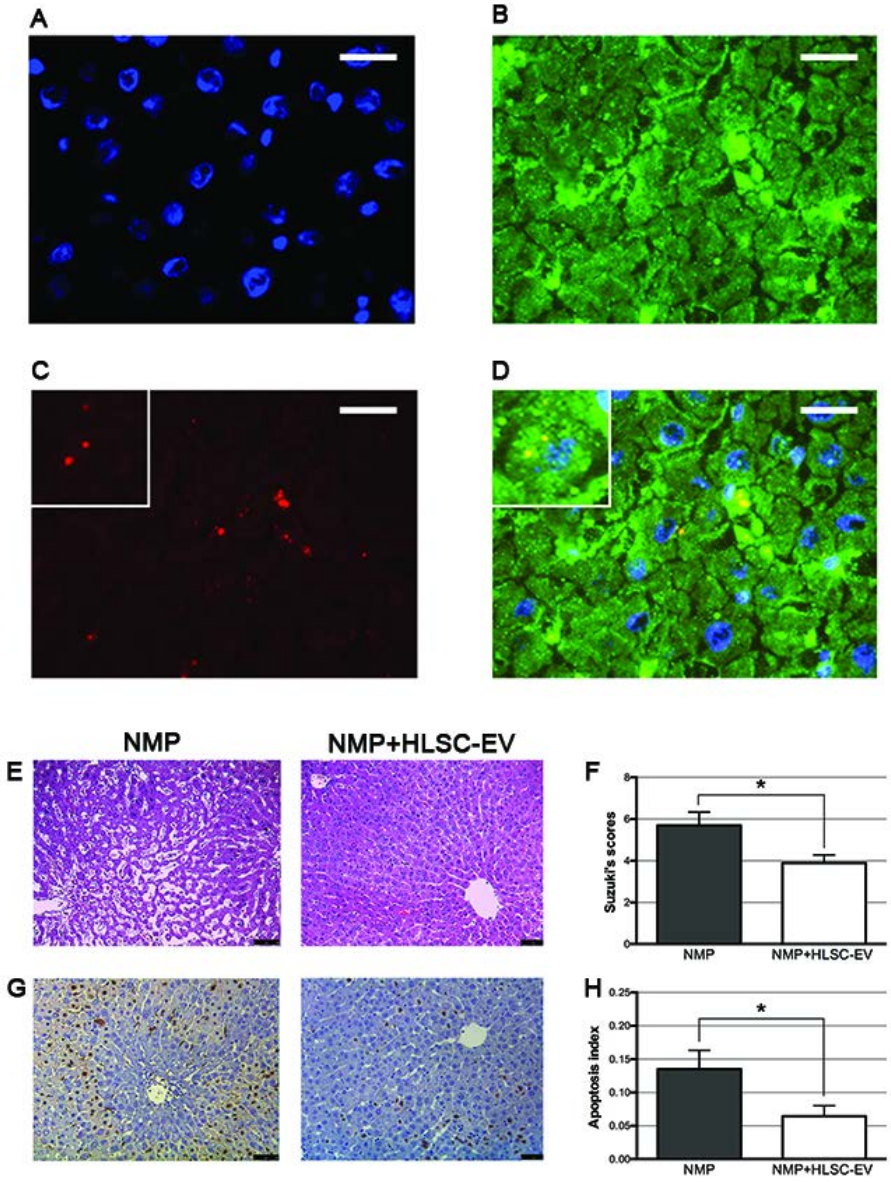

Figure 5.1: Immunofluorescence and histology in HLSC-EVs-treated (NMP+ HLSC-EV) (panels A, B, C, D, E, F, G, and H) and in control (NMP) (panels E, F, G, and H) rat livers after 4 hours of *ex-vivo* normothermic perfusion. Representative micrographs of fluorescence microscopy showing cell nuclei (A), rat P450-4A immunofluorescence (B), DIL-stained HLSC-EVs (C) and the merged colours (D) (original magnification, 630x; magnification of the insert representing the center of the image, 2520x; scale bar, 20 µm). (E) Representative micrographs of haematoxylin-eosin staining showing the grade of tissue injury (original magnification, 200x; scale bar, 50 µm). (F) Quantitative analysis for tissue damage (Suzuki score; *p = 0.030). (G) Representative micrographs of TUNEL assay showing apoptotic cells in brown and health cells in violet (original magnification, 200x; scale bar, 50 µm). (H) Quantitative analysis for apoptosis grade (apoptosis index; *p = 0.049). Data are represented as mean ± SEM.

5.3.3 The HLSC-EVs treatment decreased the release of hepatic cytolysis enzyme

The biochemical analysis of NMP perfusate samples showed a progressive increment in the levels of AST, ALT and LDH cytolysis enzymes, reaching the maximum level at the fourth hour of perfusion (Figure 5.2 A-C). Compared with the NMP group, the levels of AST, ALT and LDH were reduced in the NMP livers treated with HLSC-EVs, specifically, the levels of this markers were significantly decreased at the third hour of perfusion ($p<0.05$); in addition, the reduced levels of AST were maintained until the last hour of perfusion ($p<0.01$) (Figure 5.2 A-C). These data suggested that the HLSC-EVs treatment could be able to protect hepatocytes from cytolysis, which translated in a reduced release of the three enzymes analysed.
The livers were able to continuously produce a small quantity of bile during the four hours of perfusion. Nevertheless, the HLSC-EVs treatment had no effect in influencing the quantity of produced bile (Figure 5.2-D).

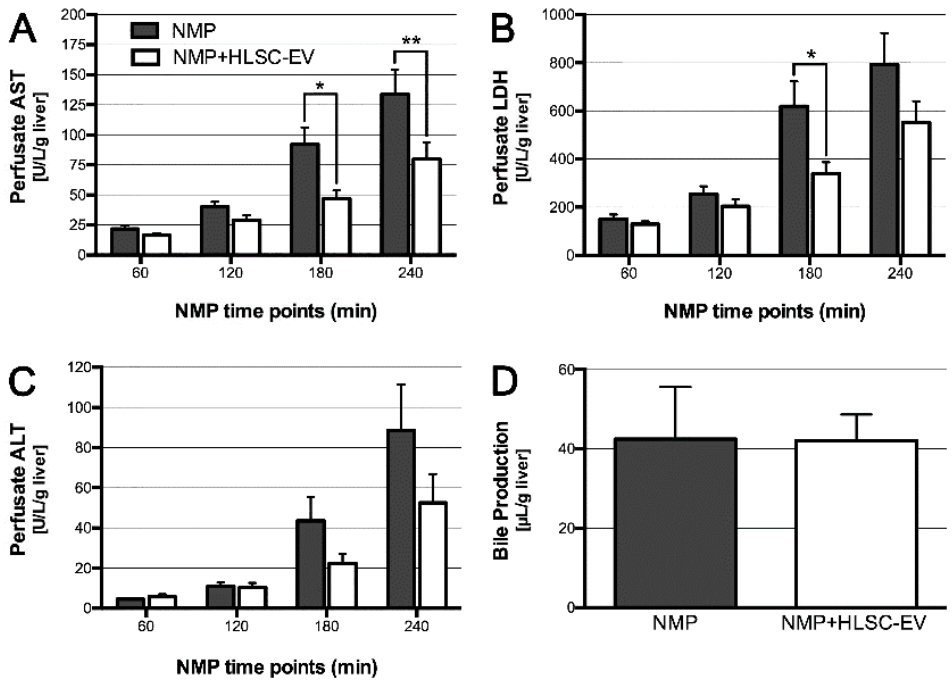

Figure 5.2: Biochemical profile of hepatic cytolysis markers in HLSC-EVs treated (NMP + HLSC-EV) and control (NMP) rat livers assessed at different time points during *ex-vivo* normothermic perfusion. (A) AST (*p = 0.018; **p = 0.003), (B) LDH (*p = 0.032), (C) ALT, and (D) Bile production. All values are normalized to the animal liver weight in grams. Data are represented as mean ± SEM.

5.3.4 The HLSC-EVs treatment influenced the hypoxic damage at a molecular level

To investigate how the HLSC-EVs could decreased the damage deriving from hypoxic injury, two factors involved in the hypoxia regulation were analysed: HIF-1α and TGF-β1. The quantification of RNA expression through RT-PCR demonstrated that hypoxia induced the overexpression of HIF-1α and TGF-β1 in the control liver (NMP group), as showed by the comparison with the physiological level of SHAM sample (Figure 5.3 A-B). On the other hand, the HLSC-EVs treatment (NMP+HLSC-EV group) restored the expression of HIF-1α ($p<0.0001$) and TGF-β1 ($p<0.05$) at the levels of the SHAM liver, suggesting that these factors are possible targets of HLSC-EVs in our model.

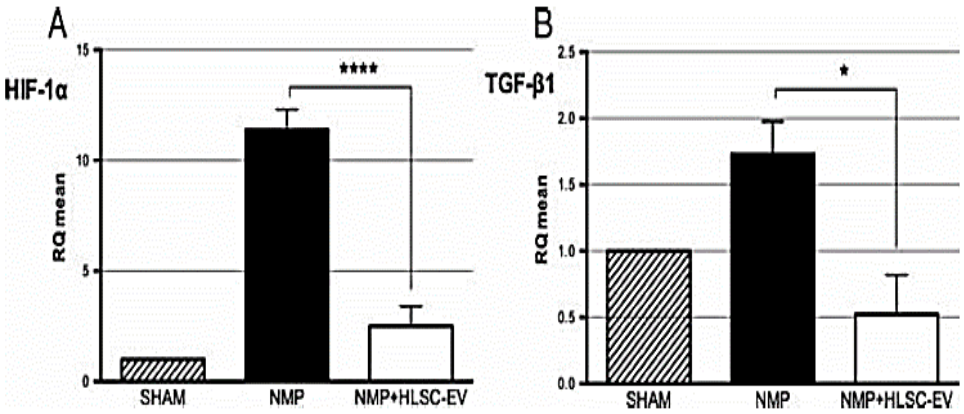

Figure 5.3: RT-PCR mean relative quantification (RQ mean) of RNA expression of hypoxia-induced markers in a sample of rat livers after 4 hours of *ex-vivo* normothermic perfusion. Gene level expression in sham (n = 1), control (NMP, n = 6), and HLSC-EVs-treated (NMP + HLSC-EV, n = 5) rat livers of (A) HIF-1α (****P < 0.0001) and (B) TGF β1 (*P = 0.014). One liver explant from a sham rat was used as health reference sample for comparison. All values are normalized to actin-β. Data are represented as mean ± SEM.

Chapter 6

Evaluation of HLSC-EVs effects in an *ex-vivo* DCD rat liver model during six hours of NMP.

6.1 Introduction on rat DCD model

In this second project, we used an *ex-vivo* 60 minutes warm ischemic rat liver as a DCD model and we aimed to investigate two main points: to evaluate if HLSC-EVs treatment was able to recover the ischemic rat liver during 6 hours *ex-vivo* NMP and to test two different doses of HLSC-EVs, in order to understand if it could be possible to establish a dose-effect correlation.

6.2 Material and methods

6.2.1 HLSC culture

HLSC were isolated from human cryopreserved adult hepatocytes purchased from Lonza Bioscience (Lonza, Basel, Switzerland) and cultured as described by Herrera et al., 2006[75]. Briefly, HLSC were cultured in a medium containing α-miminum essential medium (α-MEM) and Endothelial Cell Growth Basal Medium (EBM) in a 3:1 proportion, supplemented with L-glutamine (2 mM), penicillin (100 U/mL), streptomycin (100 µg/mL) and 10% fetal calf serum (FCS) (all by Sigma, St. Louis, MO). HLSC were maintained in a humidified incubator with 5% CO_2 at 37°C. For all experiments, HLSC between passages 5 to 11 were used.

6.2.2 Isolation and staining of HLSC-EVs

Once at 80% confluence, HLSC were starved overnight O/N in RPMI medium (Sigma, St. Louis, MO) supplemented with L-glutamine (2 mM), penicillin (100 U/mL), streptomycin (100 µg/mL) and deprived of FCS at 37°C in a humidified incubator with 5% CO_2. Supernatants were collected, centrifuged at 3,500 rpm for

15 minutes to remove cell debris, and then submitted to ultracentrifugation at 100,000 g for 2 hours at 4°C (Beckman Coulter Optima L-90 K, Fullerton, CA, USA). After that, EVs were collected and labelled with DIL fluorescent dye (Molecular Probes Life Technology, USA). The staining was performed by suspending the collected EVs in DPBS (Sigma, St. Louis, MO) until reaching 1 ml of volume; 1 µM of DIL dye was added to the solution for an incubation of 15 minutes at 37º C. Then, DPBS was added to wash the stained EVs by ultracentrifugation at 100,000 g for 1 hour at 4° C. The EVs-DIL stained were resuspended in RPMI-serum free plus 1% of the total volume of DMSO and stored at -80 °C. Quantification and size distribution of EVs were performed using NanoSight LM10 (NanoSight Ltd, Minton Park, UK). For quantification, EVs preparations were diluted (1:200) in sterile saline solution.

6.2.3 Experimental groups

The rat livers were divided into four groups, each comprising 6 livers: NMP, WI+NMP, WI+NMP+EV1 and WI+NMP+EV2. The experimental conditions are described in Table 6.

Group	Pre-perfusion condition	Duration of perfusion	Treatment
NMP	≈ 34 minutes of SCS	6 hours	No
NMP+WI	60 minutes of warm ischemia (WI)	6 hours	No
NMP+WI+EV1	60 minutes of warm ischemia (WI)	6 hours	Yes, dose 1: $5x10^8$ EVs/g of liver (EV1)
NMP+WI+EV2	60 minutes of warm ischemia (WI)	6 hours	Yes, dose 2: $25x10^8$ EVs/g of liver (EV2)

Table 6: Description of the four experimental groups

6.2.4 Surgical procedures and DCD model

All the experiments were approved by the local Ethic Committee for Experimental Animal Research and conducted in accordance with the National Institutes of Health *Guide for the Care and Use of Laboratory Animals*. At the end of the surgical procedure, animals were euthanized by cervical dislocation.
Male Wistar rats from 8 to 12 weeks aged, with the weight between 200 and 250g, were obtained from Charles Rivers (Italy) and maintained on standard conditions, providing food and water *ad libitum*. After intraperitoneal heparin (1250 U) administration, a midline laparotomy was performed. The bowel was retracted to expose the liver and the hepatic pedicle. The CBD was cannulated with a 22-G cannula, the hepatic artery HA was ligated and the portal vein PV was cannulated with an 18-G cannula. From this point, the warm ischemia began to be timed. After sternotomy, the heart was opened to exsanguinate the animal.
For the livers belonging to NMP group, the organ was flushed with 30 ml of cold Celsior, resulting in the interruption of the warm ischemia. Then, the liver was freed from its ligaments, weighed and placed into a Petri dish, filled of cold Celsior. The Petri dish was put on ice to simulate SCS and transported to the perfusion room, in order to connect the liver to NMP circuit. Before to be connected, the liver was flushed with 10-15 ml of Williams-E-Medium, removing the residual Celsior and thus blocking the SCS.

On the other hand, for the livers belonging to WI+NMP, WI+NMP+EV1 and WI+NMP+EV2 groups, the organ was flushed with 30 ml of warmed saline solution, in order to continue the ischemic period. Then, the liver was freed from its ligaments, weighed and placed into a Petri dish, filled of warmed saline solution and transported to the perfusion room. The liver was maintained at the controlled temperature of 34°C until completing the 60 minutes of warm ischemia[31,126,127] and, after that, it was flushed with 10-15 ml of Williams-E-Medium and connected to the perfusion circuit.

6.2.5 Normothermic Machine Perfusion (NMP)

The liver was placed in a warmed perfusion chamber (Moist Chamber-Harvard Apparatus, Hugo Sachs Elektronik) and connected through PV to the perfusion circuit by a metallic cannula, supplied by the chamber, while a tube was inserted into the CBD cannula to collect bile. The liver received the perfusate from a reservoir, in which the eventual circulation of clots was prevented thanks to a 40 μm Nylon filter (Falcon). The oxygenation to perfusate was provided by a fibers oxygenator, which gassed the perfusion solution with a 99% O_2 mixture, while the air embolism was avoided though two different bubble traps: the first one, placed immediately after the oxygenator, and the second one, placed upstream to the hepatic PV and supplied by the warmed chamber. A Transducer Amplifier Module (TAM-D, Hugo Sachs Elektronik, Harvard Apparatus) and a Servo Controller (SCP Type 704, Hugo Sachs Elektronik, Harvard Apparatus) allowed constant pressure perfusion (10-16 mmHg) and continuous monitoring of perfusate flow (1-2 ml/min). This system managed the perfusate circulation through two peristaltic pumps, one involved in inflow perfusate through hepatic PV and the other one involved in the reuptake of the outflow perfusate, which freely came out from hepatic vena cava. Although the perfusion chamber was already warmed thanks to an internal heating system, a second heating circuit was connected to perfusion chamber, to maintain stable the perfusate temperature at 37 °C, using a water bath thermocirculator (LAUDA Heating Thermocirculator).
The perfusion solution, with a final volume of 150 ml, was made of 100 ml of Williams E Medium and 50 ml of concentrated human red blood cells, in order to obtain a final haematocrit of 16-20%, a value already described in literature as a compromise between a good level of oxygen carriers and perfusate viscosity[128]. During perfusion, 10 ml of concentrated red blood cells were added to perfusate if haematocrit decreased under 16%. The Williams E Medium was supplemented with 0,292 g/L L-glutamine, 100 U/ml penicillin, 100 μg/ml streptomycin (all from Sigma), 1 U/ml insulin (Lilly, Italy) and 1 U/ml heparin (PharmaTex, Italy). The red blood human cells derived from expired blood bags not suitable for clinic procedures and they were donated to our group by “S.C. Banca del Sangue e Immunoematologia - A.O.U. Città della Salute e della Scienza di Torino”. During perfusion, two constant infusion pumps contributed to NMP circuit: the first pump (5 ml/h) allowed the refill of nutrients with 30 ml of fresh Williams E Medium, complemented as described before, except for heparin which had a concentration

of 4U/ml; the second pump (1 ml/h) supported the biliary salts production, providing 6 ml of taurocholic acid (Sigma) dissolved in sterile water (10 mg/ml).
Before liver connection, the perfusate was primed in the circuit until the pO_2 reached a value >400 mmHg and 3-4 mEq of sodium bicarbonate were added to obtain a pH comprised between 7.30 and 7.50. During perfusion, an appropriate amount of sodium bicarbonate was provided if the pH decreased under 7.30, to avoid liver acidosis and to complete the six hours perfusion. The total mEq of sodium bicarbonate supplied for each perfusion were quantified. The constant monitoring of pressure and flow allowed us to calculate the resistance in the NMP circuit, expressed as the ratio between Pressure and Flow (mmHg/ml/min).

6.2.6 Immunofluorescence analysis

To analyse HLSC-EVs uptake, serial slices were cut (3-5 μm) from snap frozen liver samples by a cryostat and fixed in acetone. After the re-hydration step in PBS (Sigma, St. Louis, MO), the nuclear staining Hoechst was used at 1:5000 dilution in PBS, then the slides were washed three times in PBS and were mounted using the aqueous mountant Fluoromount (Sigma, St. Louis, MO). Fluorescence microscopy analysis was performed using a Cell Observer SD ApoTome laser scanning system (Carl Zeiss).

6.2.7 Histological analysis

At the end of each experiment, liver biopsies were formalin fixed and paraffin embedded, then haematoxylin-eosin (H&E) staining was performed to evaluate tissue morphology, the apoptosis level was analysed by TUNEL assay and the percentage of cell proliferation was analysed by PCNA immunohistochemistry
The H&E staining was performed as described below (paragraph 5.2.6). An experienced liver pathologist blindly scored the severity of histological damage according to modified Suzuki criteria[125]: sinusoidal congestion, hepatocyte necrosis and vacuolization were graded from 0 to 4 as described previously, then the mean value for each parameter was calculated.
The level of apoptosis was identified by TUNEL assay, as described below (paragraph 5.2.6). Then, 10 microscopic fields at 200× magnification were acquired for each experiment using Olympus Microscope and the positive apoptotic cells were blindly counted.
The cell proliferation was evaluated performing an immunohistochemistry against the anti-Proliferating Cell Nuclear Antigen (PCNA). Briefly, after quenching of internal peroxidase with 6% of H_2O_2 for 6 minutes at RT, the slices were washed by H_2O and the antigen sites were unmasked by incubation with citrate tampon solution at pH 6, for 20 minutes at 102.5 °C. Then, the slices were incubated with the primary antibody anti-PCNA (Santa Cruz Biotechnology, Dallas, Texas) in a 1:300 dilution in PBS-BSA 0,1% solution for 1 hour at RT. After three washing in PBS-Tween-0,1%, the incubation with the secondary antibody Horseradish Peroxidase (HRP) (Invitrogen) was performed in a 1:300 in PBS-BSA 0,1%

solution and the slices were incubated for 1 hour at RT. Slices were washed again by PBS-Tween-0,1% solution. To label the cells positive for the PCNA antigen, DAB was used as a peroxidase substrate. To counterstain the negative PCNA cells, the slices were immersed in hematoxylin for 30 seconds. At the end, slides were mounted using an anhydrous mounting medium (Neo-Mount®, Merck). Positive and negative PCNA cells were blindly counted on 10 microscopic fields at 200× magnification acquired by Olympus Microscope, then the proliferation index, expressed in percentage, was calculated as the ratio between the number of positive cells and the number of total cells (negative + positive cells).

6.2.8 Perfusate and bile analysis

The inflow and outflow perfusate samples were collected hourly and analysed by a blood gas analyser (ABL 705L Radiometer, Copenhagen), testing pO_2, pH and haematocrit. In addition, outflow samples were collected at the end of each hour of perfusion, centrifuged at 3,500 rpm for 10 minutes at 4 °C and then the supernatants stored at -80 °C. The levels of AST, ALT and phosphates were measured by the Biochemistry Laboratory of Molinette Hospital (Turin, Italy). Then, all the results were normalized towards the animal liver weight (AST and ALT: U/L/g; Phosphates: mg/dL/g of liver).
The bile samples were collected hourly for each perfusion experiment and weighted.

6.2.9 RNA extraction and retro-transcription

RNA extraction was performed on liver sample snap frozen at -80° C in RNAlater® solution (Invitrogen, Thermo Fisher, Massachusetts) to preserve RNA from degradation. An equal amount of each sample of about 200 mg was put in a tube containing 0.5 mm zirconium oxide beads (Next Advanced, NY); then 600 ul of TRIzol solution (Thermo Fisher, Massachusetts) were added. The homogenization of tissue was performed using the Bullet Blender instrument (Next Advanced, NY) and, after that, the samples homogenized in TRIzol solution were recovered and centrifugated at 12,000 g for ten minutes at 4°C, finally the supernatants were collected. The RNA was extracted from the collected supernatants in TRIzol solution according to the manufacturer's protocol. Briefly, 200 µl of chloroform were added to each sample and after three minutes recovery at RT, samples were centrifuged at 12,000 g for 15 minutes at 4° C. After that, chloroform-RNA phase was collected, and an appropriate quantity of isopropanol was added. After ten minutes recovery at RT, samples were centrifuged at 12,000 g for ten minutes 4°C. Then, the supernatant was removed, and the pelleted RNA was washed with absolute ethanol and centrifuged at 12,000 g for five minutes 4°C. After supernatant removal, isolated RNA was left to dry at RT and, according to the RNA pellet size, an adequate quantity of RNAse free water (Sigma) was added to each sample to suspend it. The RNA was quantified using Thermo Scientific™ NanoDrop 2000/2000c (Thermo Fisher, Waltham, Massachusetts) and then, a total amount of

200 ng of RNA was retro-transcribed in a 20 µl of total volume reaction using High Capacity cDNA Reverse Transcription Kit (Applied Biosystems, Thermo Fisher, Massachusetts).

6.2.10 Real Time Polymerase Chain Reaction

To perform the real time polymerase chain reaction (RT-PCR) a mix containing 1x SYBR GREEN PCR Master Mix (Applied Biosystems, Thermo Fisher, Massachusetts), 100 nM of each couple of primers (Table 7) and 5 ng of cDNA was assembled in a 96-well plate and ran by StepOne Real Time System (Applied Biosystems, Thermo Fisher, Massachusetts). The ΔΔCt method was used to quantify the expression of the adhesion molecules: intercellular adhesion molecule (ICAM-1), vascular cell adhesion protein (VCAM-1), Selectin-E and Selectin-P. All the values were normalized towards the Actin-β (housekeeping gene) while liver explants from four healthy rats, named sham group, were used as reference samples.

Gene	Forward sequence (5'→3')	Reverse sequence (5'→3')
ACTβ	ACCGTGAAAAGATGACCCAGAT	CACAGCCTGGATGGCTACGT
ICAM-1	ATCACTGTGTATTCGTTCCCAGAG	CACGGAGCAGCACTACTGAGAG
SELECTIN E	ACACAGCTTCCTGTACCAACACAT	CCTGTTCTTGGCAGGTCACA
SELECTIN P	AACCTGCAAAGGTGTAACATCACTT	GTTCGGACCAAAGCTTTCCA
VCAM-1	TGTCAACGTTGCTCCGAAAG	CTTTAGCTGTCTGCTCCACAGGA

Table 7: Sequences of forward and reverse primers used for RT-PCR.

6.2.11 Statistical analysis

Data are expressed as mean ± SEM. Statistical analyses were performed using one-way or two-way ANOVA, or Kruskal Wallis test, depending on data normality; post-hoc tests were performed with Tukey's multiple comparison test or Dunn's multiple comparison test as appropriate (GraphPad Prism, version 6.00). A p-value <0.05 were considered as statistically significant.

6.3 Results

6.3.1 Operating parameters of perfusion experiment

Liver weight and ischemia time were comparable between the four experimental groups (Table 8). During the six hours of perfusion, the pressure measured in the PV was stable between in all the experimental groups. The haematocrit was comprised in the established range previously described (Table 8).

Parameter	NMP Mean±SEM	WI+NMP Mean±SEM	WI+NMP+EV1 Mean±SEM	WI+NMP+EV2 Mean±SEM	p-value
Ischemia time [min] **- cold** **- warm** **- total**	 33,8 (7,34) 3,00 (1,00) 36,8 (8,24)	 - 60,0 (0) 60,0 (0)	 - 60,0 (0) 60,0 (0)	 - 60,0 (0) 60,0 (0)	-
Liver weight [g]	17,10 (1,93)	15,17 (0,83)	14,17 (1,28)	13,67 (1,17)	**0,40**
pO_2 [mmHg]	500,9 (32,1)	448 (39,6)	484,6 (38,3)	517,9 (25,6)	**0,61**
Haematocrit [%]	19,02 (0,47)	17,97 (0,50)	18,56 (0,60)	18,47 (0,62)	**0,47**
PV pressure [mmHg]	15,69 (0,02)	15,19 (0,13)	14,83 (0,14)	14,98 (0,26)	**0,36**

Table 8: Description of operating parameters monitored for each perfusion experiment. Data are expressed as mean ± SEM.

6.3.2 Engraftment of HLSC-EVs in hepatic tissue

The HLSC-EVs engraftment in the hepatic parenchyma was demonstrated by the fluorescence analysis. We confirmed that the HLSC-EVs were able to be internalized in the liver, demonstrating that after 6 hours of normothermic perfusion the HLSC-EVs were still present in hepatic tissue (Figure 6.1 D).

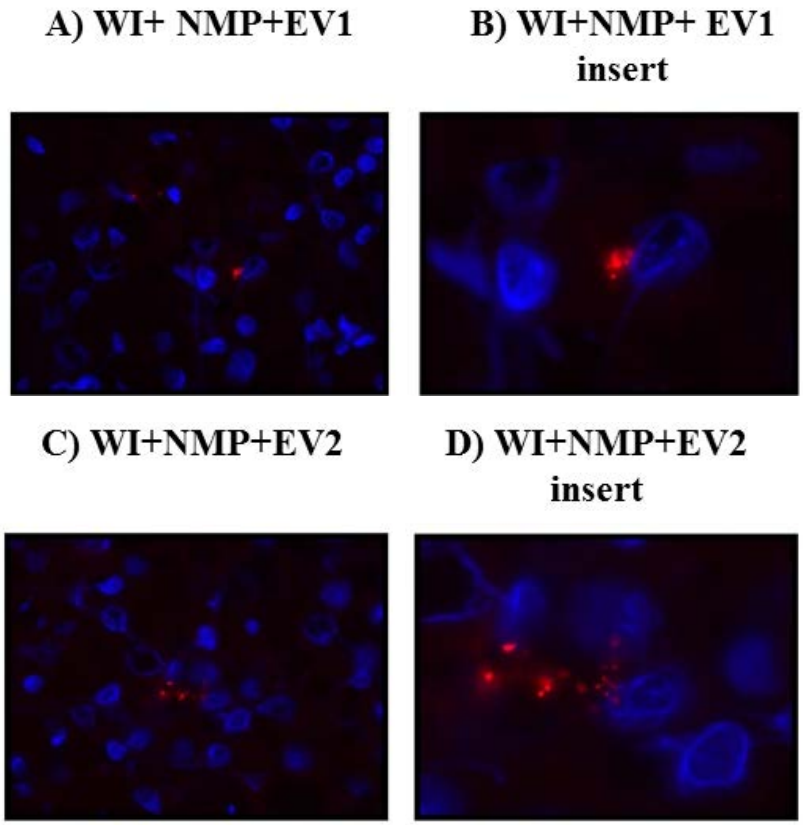

Figure 6.1: Representative micrographs of fluorescence microscopy showing HLSC-EVs engraftment in hepatic rat tissue. Blue nuclei, stained by Hoechst and red HLSC-EVs, stained by DIL. (A) WI+NMP+EV1 (B) Insert of WI+NMP+EV1 (C) WI+NMP+EV2 (D) Insert of WI+NMP+EV2. Original magnification, 630x. Magnification of the insert 2520x.

6.3.3 Evaluation of ischemic damage pattern on hepatic tissue

Next, we aimed to investigate the grade of hepatic tissue injury due to the ischemic insult. Analysing the H&E images from the four experimental groups, it is possible to observe that the ischemic insult impaired on hepatocytes structures, provoking congestion and necrosis (Figure 6.2 B), while a diffused vacuolization was observed in all experimental groups (Figure 6.2 A-D).

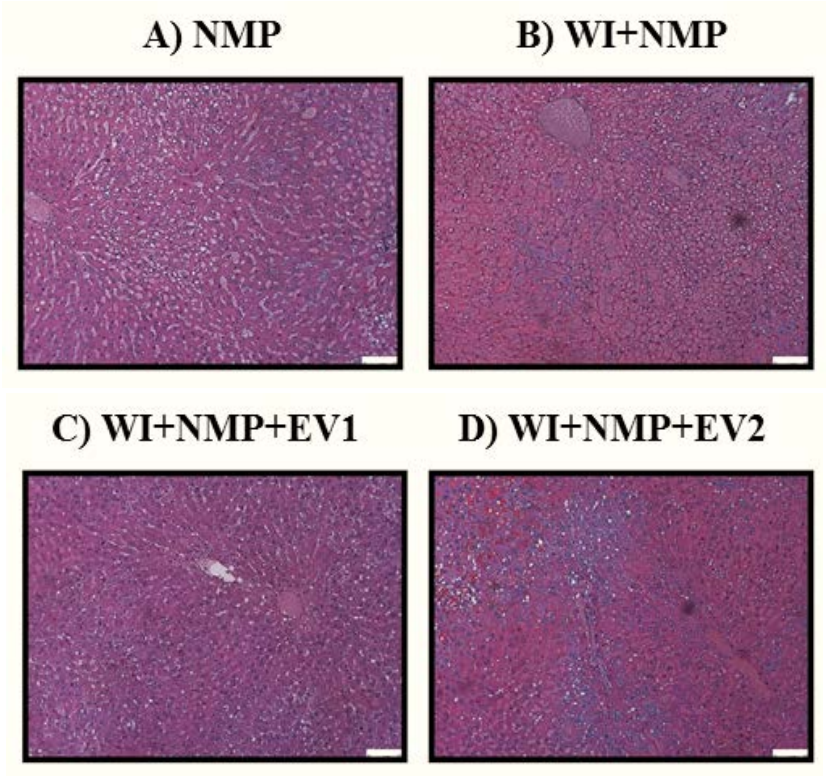

Figure 6.2: Representative micrographs of H&E staining performed on liver tissue from the four experimental groups. (A) NMP (B) WI+NMP (C) WI+NMP+EV1 (D) WI+NMP+EV2. Original magnification 200x; scale bar, 50 μm.

The quantification of hepatic injury according to Suzuki's criteria confirmed that ischemic non-treated livers had a moderate congestion, compared with NMP control livers. Moreover, livers from WI+NMP+EV1 group showed mild level of congestion as the health livers; on the other hand, those from WI+NMP+EV2 groups showed a moderate level of congestion (Figure 6.3 A). All the experimental groups showed a comparable level of vacuolization and in this case, either ischemia or HLSC-EVs treatment had no influence (Figure 6.3 B). The analysis of necrosis revealed that the ischemic damage caused significative hepatocytes' death in WI+NMP livers, compared to the health livers ($p<0.05$) (Figure 6.3 C). Although both the two doses of HLSC-EVs showed a lower level of necrosis, compared to the WI+NMP group, only the EV2 dose of HLSC-EVs was able to significantly decrease the level of necrosis ($p<0.05$) (Figure 6.3 C).

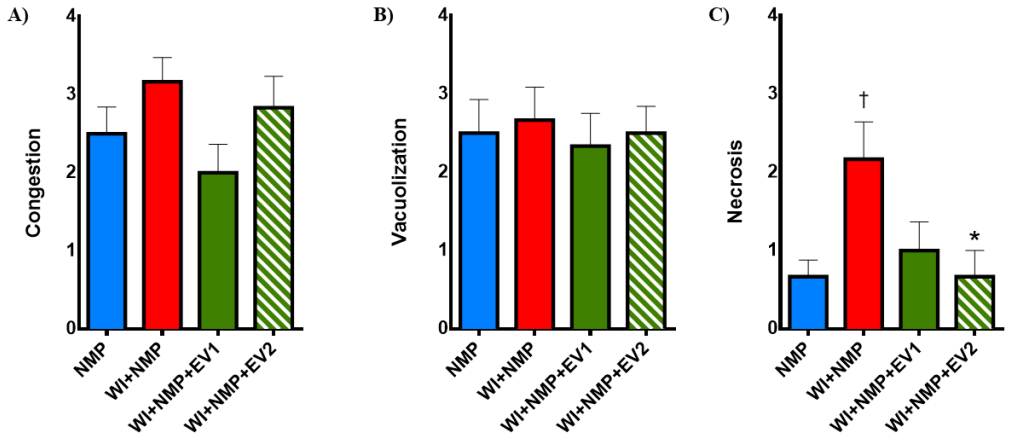

Figure 6.3: Quantification of congestion (A), vacuolization (B) and necrosis (C) in hepatic tissue according to Suzuki's criteria in all experimental groups. †: NMP vs WI+NMP $p<0.05$. *: NMP+WI vs NMP+WI+EV2 $p<0.05$. Data are expressed as mean ± SEM.

We investigated if apoptosis could be also involved in the hepatic injury triggered by ischemia. Analysing the images from TUNEL assay, we observed that the ischemic perfused liver (WI+NMP) had the double of apoptotic cells, compared to the other three experimental groups (Figure 6.4 A-D). This trend was confirmed by the quantitative analysis of apoptotic cells (Figure 6.4 E). Interestingly, the number of apoptotic cells found in the ischemic treated livers (WI+NMP+EV1 and WI+NMP+EV2) was very similar to the one find in the health perfused liver (NMP), while the maximum number of apoptotic cells was found in the ischemic non-treated livers (WI+NMP) (Figure 6.4 E).
This observation corroborates with the finding on necrosis grade showed by Suzuki's quantification, suggesting that the ischemia provoked hepatocytes' death mainly by necrosis; besides, only the EV2 dose of HLSC-EVs treatment was able to preserve hepatocytes from the ischemic induced death.

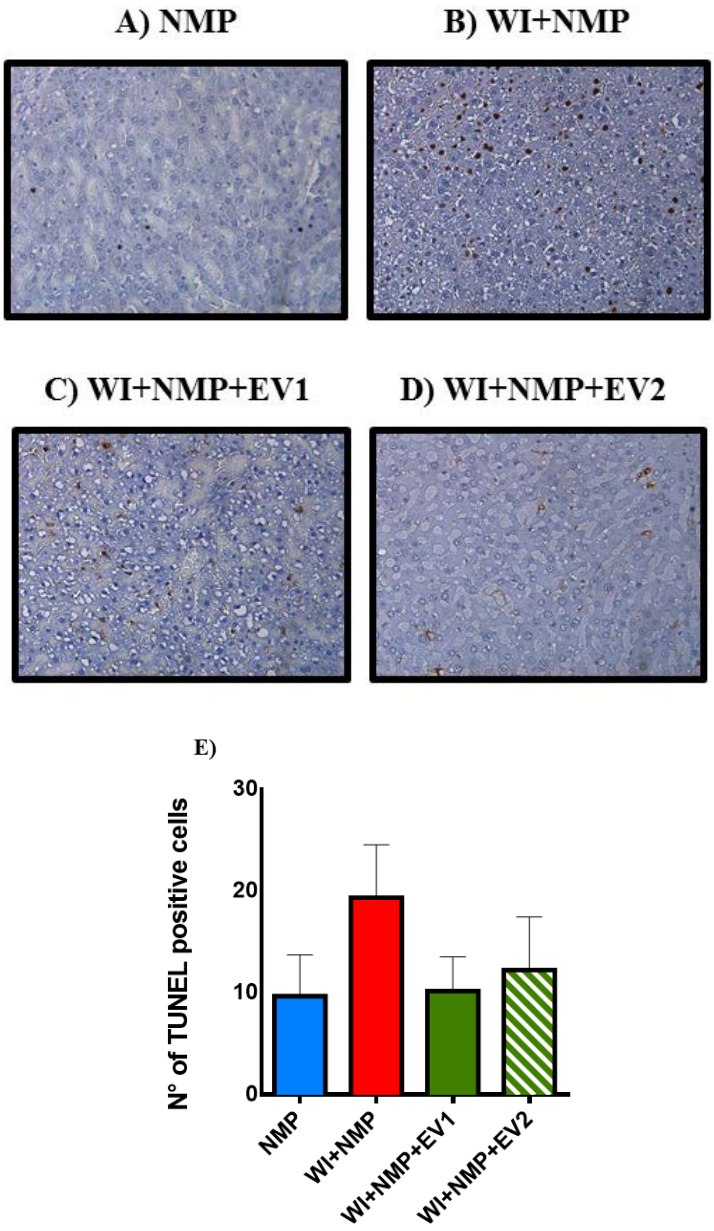

Figure 6.4: Representative micrographs of TUNEL assay on (A) NMP, (B) WI+NMP, (C) WI+NMP+EV1, (D) WI+NMP+EV2 livers, showing apoptotic cells in brown. Original magnification 200x; scale bar, 50 µm. (E): Quantification of the number of cells positive to apoptosis in the four experimental groups. Data are expressed as mean ± SEM.

6.3.4 Evaluation of cell proliferation in NMP livers and the effect of HLSC-EVs thereof

We next evaluated the proliferation capability of hepatic tissue induced by ischemia and investigated the possible modifications triggered by HLSC-EVs. Compared to the NMP livers, cell proliferation was reduced in the WI+NMP (Figure 6.5 A-D). Interestingly, cell proliferation was restored in the NMP livers treated with EV1 or EV2 (WI+NMP+EV1/EV2) (Figure 6.5 A-D). This observation was confirmed by proliferation index, calculated on the blindly counted cells positive or negative to

PCNA antigen. The PCNA index significantly decreased in the non-treated ischemic liver, compared to the health perfused liver ($p<0.05$). In addition, both the two doses of HLSC-EVs treatment were able to recover the liver proliferation capability, but only the EV2 dose was able to significantly highlight this different, when compared to the ischemic non-treated liver ($p<0.05$) (Figure 6.5 E).
This data suggested that the EV2 dose of HLSC-EVs treatment was able to significantly recover the proliferation capability of the liver, which was ablated by the ischemic insult.

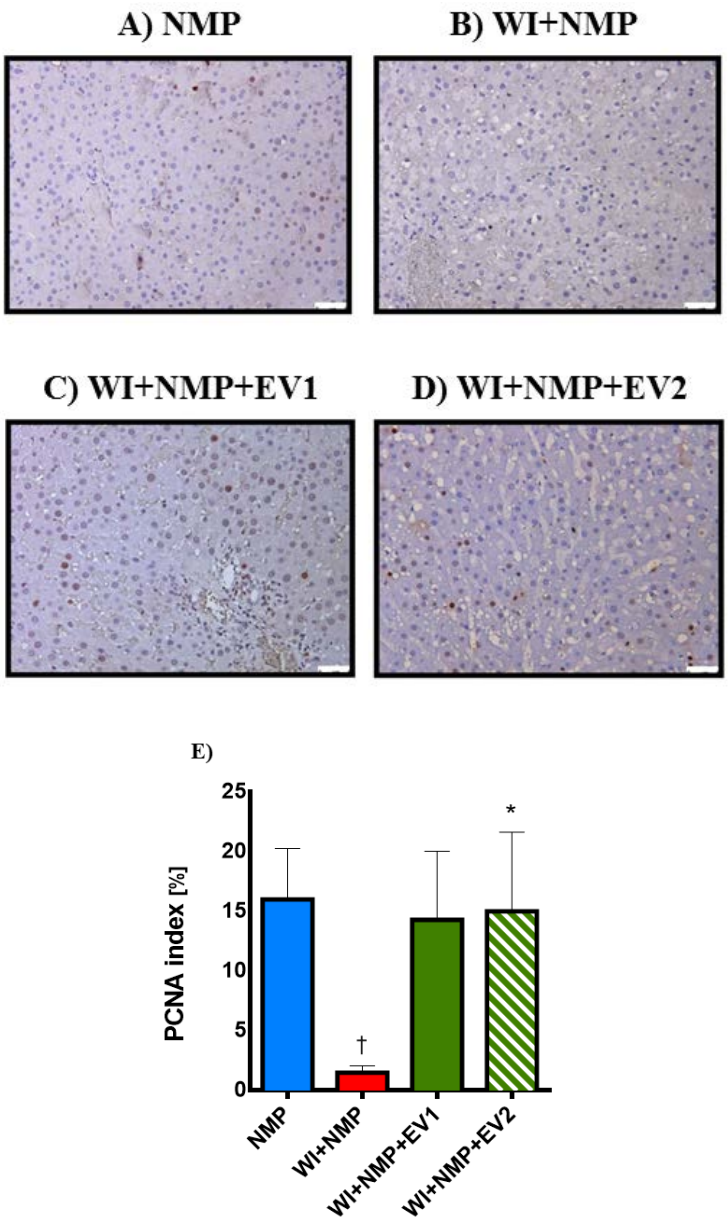

Figure 6.5: Representative micrographs of PCNA immunohistochemistry on (A) NMP, (B) WI+NMP, (C) WI+NMP+EV1, (D) WI+NMP+EV2 livers, showing PCNA positive cells in brown and PCNA negative cells in violet. Original magnification 200x; scale bar, 50 µm. (E): Quantification of the proliferation index (%) calculated for the four experimental groups. †: NMP vs WI+NMP, $p<0.05$; *: WI+NMP vs WI+NMP+EV2, $p<0.05$. Data are expressed as mean ± SEM.

6.3.5 Analysis of the release of liver cytolysis enzymes

In presence of liver damage, the transaminases (AST and ALT) are massively released by injured hepatocytes[126]. According with this, we decided to measure by biochemical analysis the levels of cytolysis hepatic enzymes (AST, ALT) on the perfusate hourly collected.
We observed that compared to the NMP livers, ischemic livers (WI+NMP) showed higher levels of AST and ALT (Figure 6.6 A-B). In particular, significant differences were observed from the third to the six hour of perfusion for ALT, while this increase was significant from the fourth hour until sixth hour of perfusion for AST (Figure 6.6 A-B). Both the two doses of HLSC-EVs were able to gradually reduce the levels of ALT and AST during all the perfusion. The reduction reached a significative difference only at sixth hour of perfusion (AST: WI+NMP vs WI+NMP+EV1 $p<0.05$; WI+NMP vs WI+NMP+EV2 $p<0.05$. ALT: WI+NMP vs WI+NMP+EV1 $p<0.001$; WI+NMP vs WI+NMP+EV2 $p<0.01$) (Figure 6.6 A-B). In addition, the EV2 dose was able to significantly reduce the AST level already at the fourth hour of perfusion (WI+NMP vs WI+NMP+EV2 $p<0.05$) (Figure 6.6 A). This data allowed us to demonstrate that both the two doses of HLSC-EVs treatment were able to protect hepatocytes, limiting the release of cytolytic enzymes induced by ischemia, with particular attention for EV2 dose, which was able to significantly reduce the release of AST already at the fourth hour of perfusion.

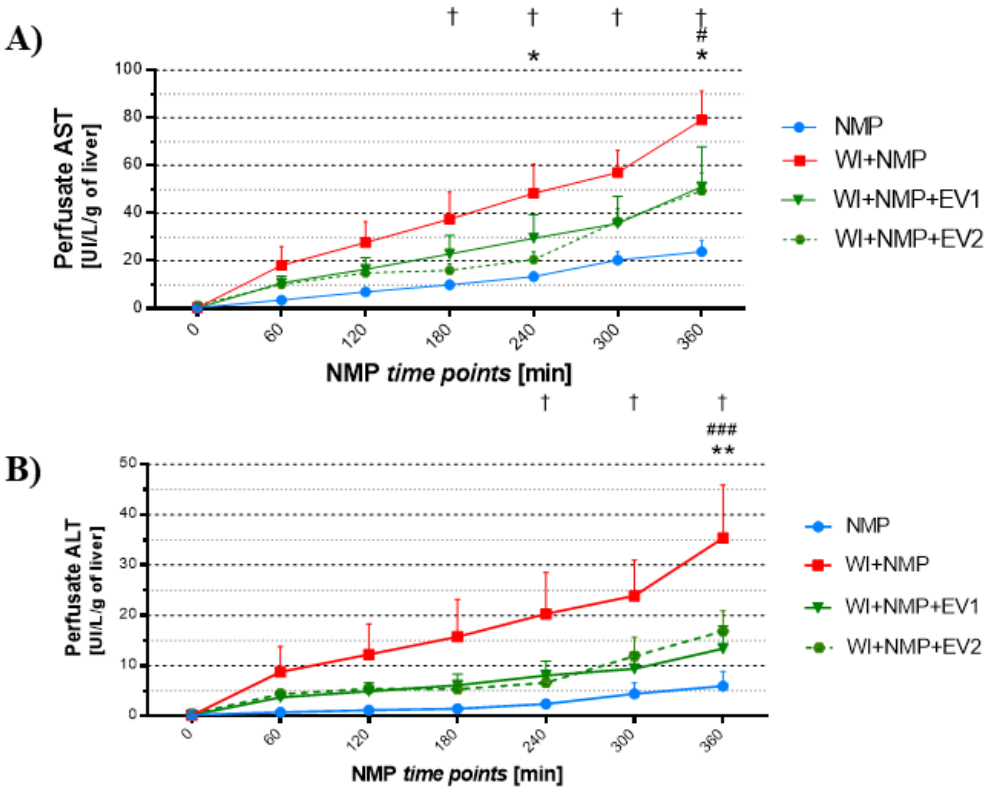

Figure 6.6: Biochemical profile of hepatic cytolysis enzymes in the four experimental groups measured for each hour of perfusion. (A) AST enzyme release: † NMP vs WI+NMP at 180 min ($p<0.05$), 240 min ($p<0.01$), 300 min ($p<0.01$), 360 min ($p<0.0001$); # WI+NMP vs WI+NMP+EV1 at 360 min ($p<0.05$); * WI+NMP vs WI+NMP+EV2 at 240 min ($p<0.05$), at 360 min ($p<0.05$). (B) ALT enzyme release: † NMP vs WI+NMP at 240 min ($p<0.01$), 300 min ($p<0.01$), 360 min ($p<0.0001$); ### WI+NMP vs WI+NMP+EV1 at 360 min ($p<0.001$); ** WI+NMP vs WI+NMP+EV2 ($p<0.01$). All values are normalized to the animal liver weight in grams. Data are represented as mean ± SEM.

6.3.6 Evaluation of liver metabolism

In order to better understand the biological effects of HLSC-EVs on liver metabolism, we analysed three markers for evaluating liver metabolism, the phosphates consumption, the bile production and the consumption of bicarbonate to self-regulate pH.

Phosphates are a fundamental substrate for ATP production and an increased concentration of phosphates could indicate a decreased level of their consumption to produce ATP[129]. The phosphates consumption charged by livers from all experimental groups demonstrated that the ischemic damage had a great impact on this metabolic parameter, already at the first hour of perfusion until the end. In fact, there was a significative difference of phosphates consumption between the NMP liver and the ischemic non-treated perfused livers for each time point analysed, meaning that the ischemic hepatocytes were not able to use the phosphates ions to

produce ATP (Figure 6.8 A). On the other hand, the ischemic livers treated with HLSC-EVs were able to use phosphates for hepatic metabolism from the fourth hour of perfusion (WI+NMP vs WI+NMP+EV1: $p<0.05$; WI+NMP vs WI+NMP+EV2: $p<0.01$) and the EV2 dose anticipated this effect from the third hour of perfusion (WI+NMP vs WI+NMP+EV2: $p<0.05$).

Because the bile production is a marker of liver viability, since it indicates the secretory status of hepatocytes and cholangiocytes[130], we proceeded to measure the quantity of bile produced by livers from all experimental groups. It is evident that the ischemia affected the capability of hepatocytes to produce bile, in fact from the third hour of perfusion the ischemic non-treated livers (WI+NMP) were able to maintain a small amount of bile production, which was significantly decreased compared to the amount of bile produced by the health perfused liver (Figure 6.8 B). Compared to the ischemic non-treated livers, both doses of HLSC-EVs showed the tendency to increase in time the bile production, reaching the maximum value at the sixth hour of perfusion, which was significantly higher for the ischemic livers treated by EV2 dose (WI+NMP vs WI+NMP+EV1 : $p<0.05$) (Figure 6.8 B). Nevertheless, the bile produced by treated livers did not reach the quantity of that produced by the NMP livers, suggesting that the HLSC-EVs partially recovered the ability of damaged hepatocytes to produce bile.

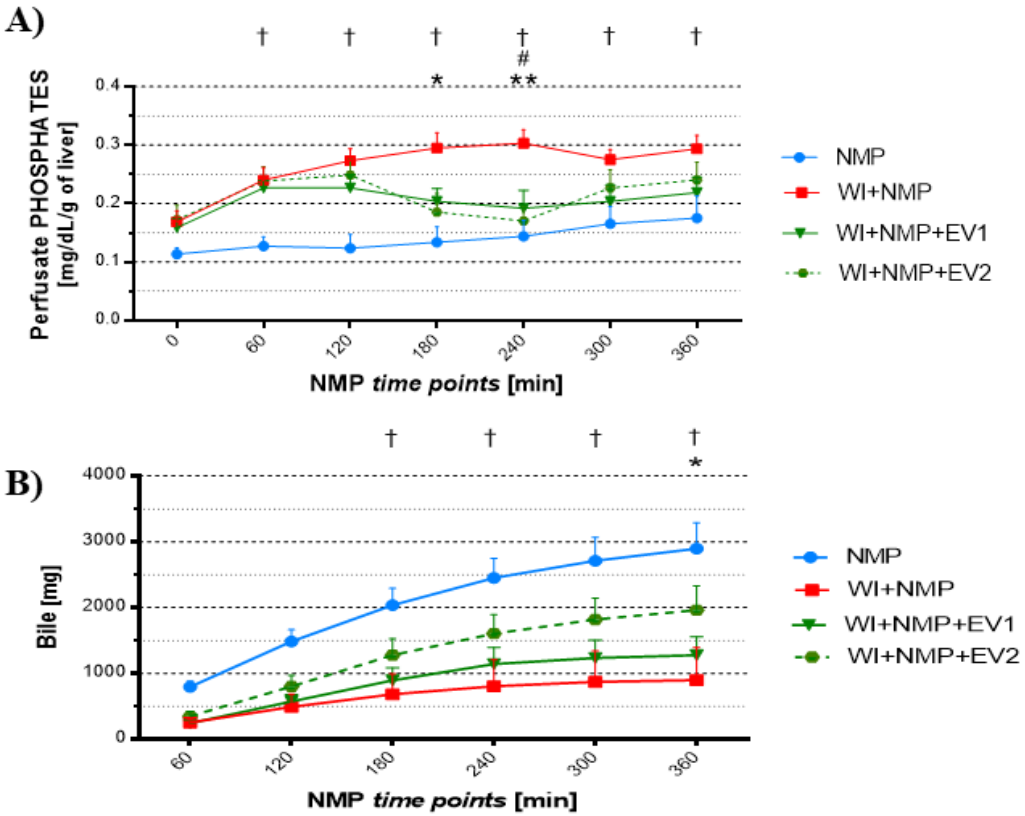

Figure 6.8: (A): Phosphates consumptions measured in perfusate samples for each hour of perfusion in the four experimental groups. †: NMP vs WI+NMP at 60 min ($p<0.01$), 120 min ($p<0.001$), 180 min ($p<0.0001$), 240 min ($p<0.0001$), 300 min ($p<0.05$), 360 min ($p<0.01$); #: WI+NMP vs WI+NMP+EV1 ($p<0.05$); *: WI+NMP vs WI+NMP+EV2 at 180 min ($p<0.05$); **: WI+NMP vs WI+NMP+EV2 at 240 min ($p<0.01$). All values are normalized to the animal liver weight in grams. Data are represented as mean ± SEM. (B): Bile quantification (mg) of collected bile produced during each hour of perfusion in the four experimental groups. †: NMP vs WI+NMP at 180 min ($p<0.01$), NMP vs WI+NMP at 240 min ($p<0.001$), NMP vs WI+NMP at 300 min ($p<0.0001$), NMP vs WI+NMP at 360 min ($p<0.0001$). *NMP+WI vs NMP+WI+EV2 at 360 min ($p<0.05$). Data are represented as mean ± SEM.

During perfusion, we aimed to maintain the perfusate pH in a range comprised between 7.30 and 7.50, as explained previously in paragraph 6.2.5. In Table 9, the mean of measured pH for each perfusion was reported (Table 9). Not all livers were able to self-regulate pH, for this reason, to avoid liver acidosis, an appropriate amount of bicarbonate was provided during perfusion if pH decreased under 7.30. In this context, we quantified the total amount of bicarbonate eventually supplied during perfusion, considered as an indirect indicator of liver metabolic status. Interestingly, the major amount of bicarbonate was provided to the ischemic non-treated livers (NMP+WI), with a significantly difference towards all the experimental groups (NMP vs WI+NMP: $p<0.01$; WI+NMP vs WI+NMP+EV1: $p<0.001$; WI+NMP vs WI+NMP+EV2: $p<0.001$) (Figure 6.7). On the other hand,

a comparable amount of bicarbonate was provided to the treated ischemic liver and to the NMP livers, allowing us to demonstrate that the ischemic insult inflicted the ability of liver to self-regulate the pH of perfusate, while the HLSC-EVs treatment at both doses recovered this ability.
All these data suggested that the HLSC-EVs treatment had beneficial effects on liver metabolism, promoting phosphates consumption, sustaining bile production and allowing the pH self-regulation.

Parameter	NMP Mean±SEM	WI+NMP Mean±SEM	WI+NMP+EV1 Mean±SEM	WI+NMP+EV2 Mean±SEM	p-value
pH					
- t = 0 min	7,35 (0,05)	7,44 (0,08)	7,50 (0,05)	7,41 (0,03)	
- t = 60 min	7,24 (0,05)	7,26 (0,08)	7,28 (0,02)	7,32 (0,05)	
- t = 120 min	7,30 (0,05)	7,24 (0,06)	7,37 (0,09)	7,30 (0,04)	**0,23**
- t = 180 min	7,33 (0,05)	7,24 (0,06)	7,39 (0,05)	7,36 (0,03)	
- t = 240 min	7,30 (0,07)	7,24 (0,05)	7,44 (0,07)	7,34 (0,05)	
- t = 300 min	7,28 (0,05)	7,23 (0,06)	7,38 (0,04)	7,35 (0,06)	
- t = 360 min	7,23 (0,06)	7,32 (0,09)	7,27 (0,06)	7,26 (0,04)	

Table 9: Mean value of measured pH for each perfusion experiment. Data are expressed as mean ± SEM.

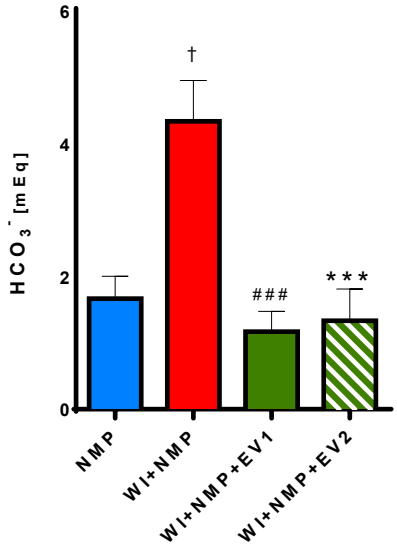

Figure 6.7: Quantification of HCO_3^- (mEq) supplied during perfusion for all the four experimental groups. †: NMP vs WI+NMP, $p<0.01$; ###: WI+NMP vs WI+NMP+EV1, $p<0.001$; ***: WI+NMP vs WI+NMP+EV2, $p<0.001$. Data are represented as mean ± SEM.

6.3.7 Hemodynamic resistance in perfusion circuit

Another criteria proposed to assess liver viability during NMP is the hemodynamic resistance[33]. Thereby, the circuit resistance was assessed. As showed in Figure 6.9, the WI+NMP livers showed an increasing resistance that reach the maximum level at the last hour of perfusion (NMP vs WI+NMP $p<0.0001$) (Figure 6.9). The NMP livers showed the lower value of resistance when compared to the other experimental groups and, interestingly, the livers treated by the EV2 dose of HLSC-EVs had a decreased level of resistance, which was significative at the last hour of

perfusion (WI+NMP vs WI+NMP+EV2: $p<0.05$) (Figure 6.9). The livers treated by EV1 dose of HLSC-EVs showed the same trend, although the difference with the ischemic non-treated livers was not still significant (Figure 6.9). These data allowed us to hypothesize a possible collapse in certain point of the hepatic microcirculation, which caused the reduction of the perfusate flow and, as a consequence, an increase of the circuit resistance. In this context, the HLSC-EVs treatment could have a protective effect on sinusoidal microcirculation. Nevertheless, this needs to be demonstrated.

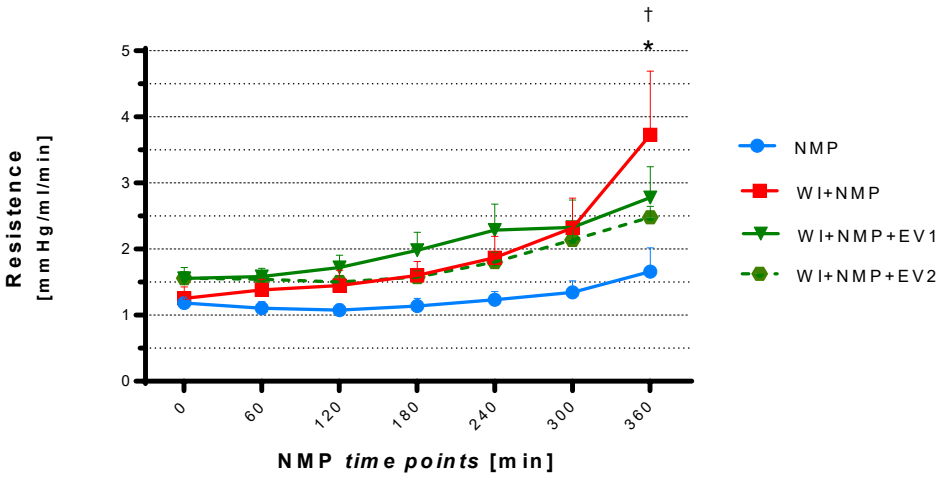

Figure 6.9: Resistance on NMP circuit calculated on measured parameters of pressure and flow during all time points for all experimental groups. †: NMP vs WI+NMP $p<0.0001$; *: WI+NMP vs WI+NMP+EV2 $p<0.05$

6.3.8 Molecular profiles of adhesion molecules expression

Lastly, considering the impact of ischemia on liver microcirculation, we aimed to investigate the expression of some adhesion molecules: ICAM-1 and VCAM-1, typically expressed by liver sinusoidal endothelial cells (LSEC) [131] and Selectin-E and -P, expressed by vascular endothelial cells[132]. The RT-PCR analysis showed that the NMP triggered the expression of the adhesion molecules ICAM-1, VCAM-1, Selectin-E, Selectin-P, compared to the sham livers (Figure 6.10 A-D). The ischemic insult inflicted on the expression of the adhesion molecules, as showed by the halved values of RQ from WI+NMP livers compared to ones from NMP livers (Figure 6.10 A-D). On the other hand, the HLSC-EVs treated livers showed a similar expression of ICAM-1, Selectin-E and Selectin-P than NMP livers. In contrast, VCAM-1 expression tended to be reduced in the WI+NMP, compared to NMP control liver (Figure 6.10 B). Additionally, the HLSC-EVs treatment did not modify the VCAM-1 levels (Figure 6.10 D).
These data demonstrated a tendency in reducing levels of these analysed markers in the WI+NMP livers; however, this reduction was not statistically significant. Moreover, the HLSC-EVs treatment have not effects.

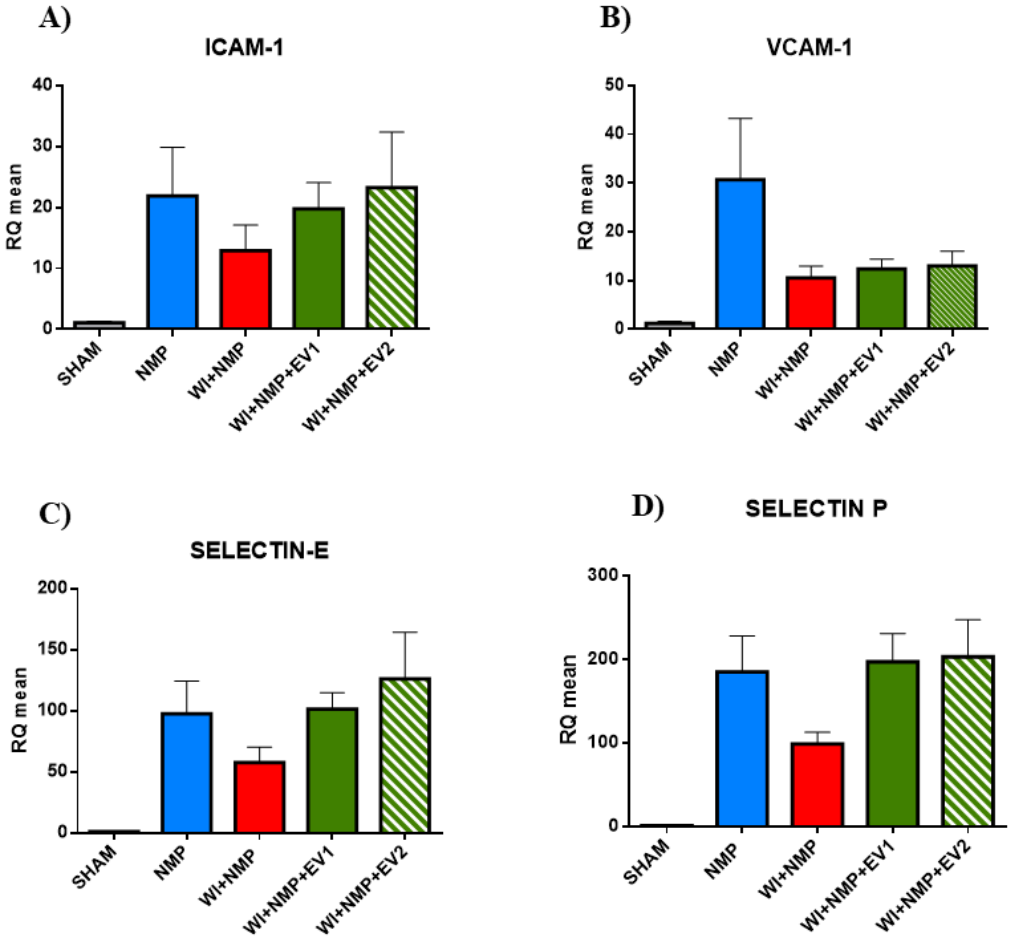

Figure 6.10: RT-PCR mean relative quantification (RQ mean) of RNA expression of adhesion molecules after 6 hours of *ex-vivo* normothermic perfusion in Sham, NMP, NMP+WI, WI+NMP+EV1 and WI+NMP+EV2. A) ICAM-1, B) VCAM-1, C) SELECTIN-E, D) SELECTIN-P. Liver explants from four healthy rats (SHAM group) were used as reference samples. All values are normalized to Actin-β. Data are represented as mean ± SEM.

6.4 Discussion

The needing to amply the number of transplantable organs moved the clinics to use marginal livers for liver transplantation, such as DCD livers[2]. Unlikely, the DCD livers graft are associated with inferior outcomes because of PNF and biliary complications[19]. In this context, new approaches to rescue DCD livers are required, in order to improve the outcomes of graft transplantation[2]. Promising results were obtained on DCD livers perfused by normothermic machine, thanks to its ability to provide a superior preservation of the organ[2].

The literature has provided evidences that HLSC-EVs hold different therapeutics features, including their abilities to repair liver after 70% hepatectomy[117], to recover liver functionality in hepatic citrullinemia[119], to be effective in improving tubular injury in AKI[118] and in kidney fibrosis[120] and even to have anti-tumoral

properties[121,122].
Despite all these indications of their biological effects, a possible use of HLSC-EVs to recondition marginal liver graft was yet to be determined.
Hence, in our studies, we aimed to evaluate the possibility to recondition livers in two different *ex-vivo* rat marginal liver models. The first model was characterized by hypoxia-induced ischemia, while the second by a warm ischemia. In both models, the HLSC-EVs were added during the *ex-vivo* normothermic perfusion (NMP). In the first model, we used one single dose of HLSC-EVs ($5x10^8$/g of liver), while in second model, we compared two different doses: $25x10^8$/g of liver (EV1) and $25x10^8$/g of liver (EV2).

Firstly, we ascertained the engraftment of HLSC-EVs in hepatic parenchyma, showing that the HLSC-EVs were able to engraft in liver parenchyma injured by hypoxia after four hours of perfusion. Previously, it has been demonstrated that MSC-EVs were able to localize in injured organs after five hours from their *in-vivo* injection in AKI mice[133]. Our results showed that it is possible to detect internalized HLSC-EVs after four hours in hepatic parenchyma, allowing us to hypothesize that the NMP system permitted a faster bio-distribution of HLSC-EVs in an *ex-vivo* organ isolated system.
We showed that HLSC-EVs were engrafted also in our *ex-vivo* DCD perfused model, demonstrating that HLSC-EVs were successfully internalized also in hepatocytes after six hours of *ex-vivo* perfusion.

We analysed the hepatic tissue morphology, scoring the sinusoidal congestion, hepatocytes necrosis and vacuolization according to Suzuki's criteria[125]. In both our models of marginal liver, the HLSC-EVs treatment was able to significantly improve hepatocytes morphology. Specifically, in the hypoxic *ex-vivo* rat liver model, the total Suzuki's score was significantly decreased in the hypoxic treated liver, compared to the hypoxic non-treated liver. On the other hand, in the warm ischemic *ex-vivo* rat liver model, we decided to analyse the three parameters of Suzuki's score separately, in order to identify in what extent the HLSC-EVs could influence tissue morphology. We found out that the HLSC-EVs treatment acted above all on preserving hepatocytes from necrosis, as showed by the reduced level of necrosis detected on treated livers. Although both the two doses of HLSC-EVs showed this trend, only the EV2 dose was able to significantly decrease hepatocytes necrosis, when compared to the ischemic non-treated livers.
Despite the preservation of hepatocytes structure is one of the advantages deriving from the use of normothermic perfusion[134], the literature showed that NMP alone is not always sufficient to recover hepatocytes damaged by ischemia. In the study of Schlegel and collaborators, the NMP performed on 60 minutes warm ischemic rat livers was not sufficient to preserve hepatic tissue from parenchymal and non-parenchymal injury[32]. In according to the suboptimal liver preservation, the recipient rat who received the reconditioned ischemic livers did not survive[32]. In another study, Matton and colleagues showed that the NMP succeeded in preserve hepatocytes structure of perfused human DCD livers, although without significative difference in the Suzuki's score calculated on liver tissue before and after NMP[135].

These observations, taken together with our data, allow us to hypothesise that the improvement in hepatocytes morphology obtained in our HLSC-EVs treated livers could be strictly associated to the specificity of the biological treatment and, in this way, the HLSC-EVs treatment could ameliorate the power of NMP liver reconditioning.

Another analysis we used to evaluate the liver tissue condition was the quantification of apoptosis. We showed that the hypoxic damage was able to trigger hepatocytes apoptosis, which was significantly limited in the HLSC-EVs hypoxic liver treated. On the other hand, the warm ischemia was able to stimulate apoptosis, as showed by ischemic perfused liver, although no significative differences were detected if compared to the NMP livers. Besides, the number of apoptotic cells found in HLSC-EVs treated livers at both doses were close to the one found in NMP livers. The different duration of damage could explain the different extent of apoptosis that we found between the two models, considering that apoptosis was more accentuated in the hypoxic ones. In fact, in the hypoxic model, the damage was obtained using a low haematocrit, that did not permit a good hepatocytes oxygenation for all the four hours of perfusion, instead, in the ischemic model, the damage was limited to one hour of warm ischemia, followed by six hours of normothermic perfusion. In addition, some studies indicated that the apoptosis detected in DCD perfused livers was very limited[31] or that the apoptosis detected in both DCD perfused livers and in NMP livers was similar[136].
These findings corroborate with our results on necrosis for DCD livers, suggesting that after a warm ischemic injury, hepatocytes died mainly by necrosis and in a limited way by apoptosis. On the other hand, in front of an ongoing and continuous hypoxic damage, a great part of hepatocytes died by apoptosis. In this context, the HLSC-EVs treatment were able to preserve hepatocytes from both the two types of cell deaths, necrosis and apoptosis.

We also analysed the hepatocytes proliferation ability on ischemic perfused livers to investigate the effects of the two tested doses of HLSC-EVs. Firstly, we showed that the NMP livers were able to actively proliferate and secondly, we showed that the one hour of ischemia ablated this capability. Both the two doses of HLSC-EVs treatment were able to recover liver proliferation capability and the EV2 dose was the most effective, because it significantly increased the proliferation index of the ischemic treated livers (WI+NMP+EV2), when compared to the ischemic non-treated livers (WI+NMP). Our results are in according to what demonstrated in the study of Herrera and colleagues, in which they showed the ability of HLSC-EVs to improve the hepatocytes proliferation in a model of 70% hepatectomized rats[117].

Next, we analysed the levels of cytolytic enzymes in perfusate, in both the two models of marginal livers. In fact, the transaminases (AST and ALT) are widely considered as surrogate markers of liver damage, because they are massively released by injured hepatocytes[126].
In the *ex-vivo* perfused hypoxic livers, the release of AST and ALT increased during perfusion time, reaching the maximum levels at the fourth hour of perfusion.

Although an increasing release during time was observed also in the treated livers, the HLSC-EVs were able to significantly reduce the AST levels already at the third hour of perfusion, until the perfusion end. The same trend was observed for ALT release; nevertheless, the difference between the NMP and the NMP+HLSC-EV was not still significant.
In the DCD *ex-vivo* perfused rat livers, both the release of AST and ALT was significantly increased by the ischemic insult with a significative difference for almost all the timepoints of NMP, in comparison with the NMP livers. Both the two doses of HLSC-EVs treatment were able to reduce the release of the cytolytic enzymes for each time-point of NMP, reaching the significance at the sixth hour of perfusion. Moreover, the two doses decreased the levels of these enzymes close to the ones measured for the healthy perfused liver and, in addition, the EV2 dose reduced significantly the AST levels already at the fourth hour of perfusion. Considering that the perfusate ALT levels are a direct indicators of organ viability in the NMP settings[126] while the AST represents one of the main predictors of graft survival when measured after liver transplantation (post-LT AST peak) [137], our results are very encouraging, because we showed that the HLSC-EVs treatment were able to reduce the levels of both these two enzymes in two different model of liver injury. We could speculate that HLSC-EVs treatment was most effective in recovering the warm ischemic rat liver rather than the hypoxic rat liver, because the reducing of ALT release was not still significant in the hypoxic treated livers. Nevertheless, the post-LT AST peak is also commonly used as a major outcome in clinical trials involving NMP[137] and in our results we showed that the HLSC-EVs treatment were able to significantly reduce the release of AST in both the two model of marginal rat livers.

Then, we investigated liver metabolism examining several markers, according to the liver injury model analyzed.

The LDH enzyme is present ubiquitously in all cell types and it is responsible for the production of lactic acid from pyruvate, taking advantage of the oxidation of NADH to NAD^+, which in turn takes part in glycolysis. Therefore, an increased activity of LDH triggers the production of ATP by anaerobic metabolism[138]. Moreover, it has been showed that the LDH production is increased under hypoxic condition, such as during acute liver failure[139]. In our hypoxic *ex-vivo* rat liver model, the LDH released by hepatocytes increased during time perfusion, reaching the maximum level at the fourth hour of perfusion, while the HLSC-EVs treatment succeeded to significantly reduce the LDH level at the third hour of perfusion. Usually, the elevated LDH serum levels of patients with liver morbidity has been considered as a result of the release of the enzyme by damaged hepatocytes[139]. Actually, we could combine this aspect of LDH with its role in anaerobic metabolism as well as its expression under hypoxic condition, allowing us to might hypothesize that the HLSC-EVs protected hepatocytes from hypoxic injury improving aerobic liver metabolism, as showed by the lower level of released LDH.

The production of bile is a marker of liver viability since it indicates that the secretory function of hepatocytes and cholangiocytes are preserved[130]. Although the bile was produced constantly during all the four hours of perfusion, we collected only a small amount of bile at the end of the hypoxic liver's perfusion. However, in this first model, the quantity of collected bile was similar between the control and the HLSC-EVs treated livers. These observations suggests that HLSC-EVs treatment had no effect in influencing the quantity of produced bile in this model. In contrast, in our second model (DCD), we demonstrated that the ischemia injury negatively impaired livers, compared to the NMP livers. In particular, a significant decrease of bile production was observed in the ischemic livers during all the perfusion. Interestingly, in this model the HLSC-EVs treatment restored the bile production in a dose-dependent manner. Nevertheless, the bile produced by treated livers did not reach the quantity produced by NMP perfused livers.
These data allow us to hypothesize that our higher dose of HLSC-EVs treatment may partially preserved the hepatocytes and cholangiocytes ability to secrete bile in the setting of a warm ischemic damage.

The reaction of ATP production, which consists in the addition of a molecule of phosphate to ADP substrate, demonstrates how phosphate is fundamental for mitochondrial ATP synthesis. Hence, an increase in phosphates concentration may indicate a decreased level of oxidative phosphorylation[129].
In our *ex-vivo* ischemic rat liver model, we showed that in the perfusate of ischemic non-treated livers (WI+NMP) the levels of phosphates rose during perfusion, reaching a concentration which was almost three times higher than the one detected on perfusate from healthy livers (NMP). The two doses of HLSC-EVs significantly reduced the concentration of phosphates in the perfusate of treated livers at the fourth hour of perfusion and, in addition, the EV2 dose anticipated this effect at the third hour of perfusion. The peak of phosphates consumptions was already observed after hepatic surgery and, although the mechanism has not been still clarified, it has been suggested that it is caused by the rapidly uptake of phosphates by hepatocytes, which began to regenerate[140]. These observations corroborate with our data, suggesting that the ischemic livers were not able to sustain the ATP production, as showed by the release of phosphates in perfusate, while the HLSC-EVs treatment recovered hepatocytes metabolism, promoting cellular ATP synthesis.

The pH self-regulation is another important indicator of liver metabolic activity during and after NMP[141]. During NMP, bicarbonate was added where necessary to maintain perfusate pH above the value of 7.30. The administration of bicarbonate during perfusion was significantly higher in the ischemic group (NMP+WI) compared to all the other three experimental groups, suggesting that the ischemia compromised the acid-base homeostasis of bicarbonate. On the other hand, the HLSC-EVs treated livers required the same amount of bicarbonate of the healthy livers, indicating that the treatment protected the livers from the unbalanced homeostasis due to ischemia. These observations reflected on the liver ability of pH self-regulation during perfusion, meaning that the ischemic livers needed a supply of bicarbonate to overcome acidosis because they were not able to self-regulate pH,

while the HLSC-EVs helped the treated livers in pH self-regulation, as showed by the small needed amount of bicarbonate provided.

Hemodynamic parameters are among the criteria proposed to assess liver viability during NMP[33]. In all the experimental groups of DCD model, a progressive increase in resistance over time was observed, particularly evident in the groups subjected to the ischemic damage. The EV2 dose of HLSC-EVs was able to significantly reduce the intrahepatic resistance compared to the ischemic perfused livers. Although the ability of NMP to improve graft hemodynamics performance has already been described[127], in our DCD model we showed that the perfusion was not sufficient to maintain a stable intrahepatic resistance, while the HLSC-EVs treatment at the highest dose maintain the resistance close to the one showed by the NMP control livers. It is possible that, in certain point of the hepatic microcirculation, the injured endothelial cells collapse happened, causing the reduction of the perfusate flow and, therefore, an increase of the resistance in the circuit.
In this context, we aimed to analyse the ability of liver cells to express, after the ischemic injury, the adhesion molecules ICAM-1, VCAM-1, Selectin-E and -P which were known to be expressed mainly by liver sinusoidal endothelial cells and by vascular endothelial cells[131, 132]. Our results indicated that the ischemia tended to decrease the expression of ICAM-1, VCAM-1, Selectin-P and Selectin-E, compared to the NMP livers, on the other hand the HLSC-EVs treatment promoted the recovery of the expression of ICAM-1, Selectin-E and Selectin-P, while no effect was found for VCAM-1 expression. Although the role and behaviour of LSEC during the NMP have to been still elucidated, some studies began to search potential biomarkers to assess the status of LSEC during perfusion[142]. For example, it has been showed that the expression of the adhesion molecule PECAM1 (Platelet endothelial cell adhesion molecule), which play a key role in modulating vascular integrity, is associated with a decreased LSEC injury in a model of hepatic IRI[143]. Taken together, our data showed that the ischemia impacted on the liver sinusoidal milieu and allowed us to might hypothesized that the endothelial hepatic cells of WI+NMP livers were not able to express the adhesion molecules markers, probably due to the impact of ischemic damage on endothelium. The HLSC-EVs showed to have a protective effect on sinusoidal milieu, which could be also reflected by an improvement on hepatic microcirculation.

Finally, for the hypoxic rat liver model, we were able to draft a hypothesis on the molecular action of HLSC-EVs. We found out that the hypoxia induced an over-expression of HIF-1α, in according to what described in a study on normothermic perfused liver with an oxygen carrier deficiency[144]. Our HLSC-EVs significantly reduced the HIF-1α expression on treated livers and, besides, the HLSC-EVs significantly decreased also the expression of TGF-β1, which is known to be involved in a cross talk with HIF-1α, in a pathway recently described in hypoxic hepatocytes[145]. Although a deeper investigation on the factors involved in the pathway are required, these data allows us to might hypothesize a modulation on hypoxia activation pathway. This hypothesis is supported by our recently

experiments where the modulation of HIF1-alpha and TGFb1 by HLSC-EVs was demonstrated[146].

6.5 Conclusions and final considerations

In these two studies, we showed that the HLSC-EVs, efficiently delivered by NMP, were able to recover almost completely two marginal rat liver models. Our analysis demonstrated that the HLSC-EVs improved liver morphology, decreased hepatocytes death, reduced the release of cytolytic enzyme and improved liver metabolism. Moreover, between the two doses analysed in the DCD model, we obtained superior results with the highest dose.

As regard the mechanism of action of HLSC-EVs, we demonstrated that they possibly act modulating the hypoxia pathway, while the molecular mechanism behind the HLSC-EVs preservation of hepatocytes from ischemia it has to be still elucidated.

We are aware that the weakness of these studies is lack of transplantation of the reconditioned *ex-vivo* livers. However, beyond the limitations, we demonstrated for the first time the use of HLSC-EVs during *ex-vivo* NMP, testing them in two different models of damage and showing that the HLSC-EVs could represent a promising approach to increase the reconditioning power of NMP.
Since now we acquired the knowledge of HLSC-EVs effects during liver perfusion, in the next steps of the research we will perform an *ex-vivo* model of liver transplant, adding a final hour of perfusion with full rat blood, in order to simulate the interactions of the perfused liver with the immune system of a recipient rat. Once investigated these aspects, we will able to actually reproduce the liver transplant model using *ex-vivo* reconditioned livers treated by HLSC-EVs.

References

1. Adam, R., Karam, V., Cailliez, V., O Grady, J. G., Mirza, D., Cherqui, D., […] and Christophe Duvoux and all the other 126 contributing centers (www.eltr.org). (2018). 2018 Annual Report of the European Liver Transplant Registry (ELTR)–50-year evolution of liver transplantation. *Transplant International*, *31*(12), 1293-1317.

2. Ravikumar R, Leuvenink H, Friend PJ (2015). Normothermic liver preservation: a new paradigm? *Transpl Int*; 28:690-699.

3. DeLemos, A. S., Vagefi, P. A. (2013). Expanding the donor pool in liver transplantation: Extended criteria donors. *Clinical liver disease, 2(4), 156-159.*

4. Manara, A. R., Murphy, P. G., O'Callaghan, G. (2012). Donation after circulatory death. *British journal of anaesthesia,* 108(suppl_1), i108-i121.

5. Paterno, F., Guarrera, J. V., Wima, K., Diwan, T., Cuffy, M. C., Anwar, N., Woodle, E.S., Shah, S. (2019). Clinical Implications of Donor Warm and Cold Ischemia Time in Donor after Circulatory Death (DCD) Liver Transplantation. *Liver Transplantation*.

6. Geraci, P. M., Sepe, V. (2011). Non-heart-beating organ donation in Italy. *Minerva Anestesiol, 77(6), 613-623.*

7. Bejaoui, M., Pantazi, E., Folch-Puy, E., Baptista, P. M., García-Gil, A., Adam, R., Roselló-Catafau, J. (2015). Emerging concepts in liver graft preservation. *World journal of gastroenterology: WJG*, *21*(2), 396.

8. Selten, J., Schlegel, A., de Jonge, J., Dutkowski, P. (2017). Hypo-and normothermic perfusion of the liver: Which way to go? *Best practice & research Clinical gastroenterology*, *31*(2), 171-179.

9. Saidi RF, Kenari SK. (2014). Liver ischemia/reperfusion injury: an overview. J *Investig Surg*; 27:366e79.

10. Sokharev AS, Krasnov KA, Budaev AV, Krasnov OA, Plotnikova EY. (2015) Ischemic reperfusion injury of hepatocytes in the preservation of the liver transplant. Eksp Klin *Gastroenterol*:66e73.

11. Guan LY, Fu PY, Li PD, Li ZN, Liu HY, Xin MG, Li W. (2014) Mechanisms of hepatic ischemia-reperfusion injury and protective effects of nitric oxide. *World J Gastrointest Surg*; 6:122e8.

12. Foley D.P, Fernandez L.A., Leverson G., Chin L.T., Krieger N., Cooper J.T., Shames BD, Becker YT, Odorico JS, Knechtle SJ, Sollinger HW, Kalayoglu M, D'Alessandro AM (2005). Donation after cardiac death: the University of Wisconsin experience with liver transplantation; *Ann Surg*, 242, pp. 724-731

13. Uemura, T., Randall, H. B., Sanchez, E. Q., Ikegami, T., Narasimhan, G., McKenna, G. J., Chinnakotla S., Levy M.F., Goldstein R.M.., Klintmalma, G. B. (2007). Liver retransplantation for primary nonfunction: analysis of a 20-year single-center experience. *Liver transplantation*, *13*(2), 227-233.

14. Briceno, J., Ciria, R. (2010). Early graft dysfunction after liver transplantation. In *Transplantation proceedings* (Vol. 42, No. 2, pp. 631-633).

15. Mourad, M. M., Algarni, A., Liossis, C., Bramhall, S. R. (2014). Aetiology and risk factors of ischaemic cholangiopathy after liver transplantation. *World Journal of Gastroenterology:*20(20), 6159.

16. Op den Dries, S., Sutton, M. E., Lisman, T., Porte, R. J. (2011). Protection of bile ducts in liver transplantation: looking beyond ischemia. *Transplantation*, *92*(4), 373-379.

17. O'Callaghan JM, Morgan RD, Knight SR, Morris PJ. (2014). The effect of preservation solutions for storage of liver allografts on transplant outcomes: a systematic review and metaanalysis. *Ann Surg*; 260: 46-55

18. Dondéro F, Paugam-Burtz C, Danjou F, Stocco J, Durand F, Belghiti J. (2010). A randomized study comparing IGL-1 to the University of Wisconsin preservation solution in liver transplantation. *Ann Transplant*; 15: 7-14

19. Nemes, B., Gámán, G., Polak, W. G., Gelley, F., Hara, T., Ono, S., Eguchi, S. (2016). Extended-criteria donors in liver transplantation Part II: reviewing the impact of extended-criteria donors on the complications and outcomes of liver transplantation. *Expert review of gastroenterology & hepatology, 10(7), 841-859.*

20. Carrel A, Lindbergh CA (1935). The culture of whole organs. *Science*; 81: 621.

21. Starzl TE, Kaupp Jr HA, Brock DR, Lazarus RE, Johnson RV. (1960) Reconstructive problems in canine liver homotransplantation with special reference to the postoperative role of hepatic venous flow. *Surg Gynecol Obstet*;111:733e43

22. Schlegel, A., Dutkowski, P. (2015). Role of hypothermic machine perfusion in liver transplantation. *Transplant International*, *28*(6), 677-689.

23. Dutkowski, P., De Rougemont, O., Clavien, P. A. (2008). Machine perfusion for 'marginal'liver grafts. *American Journal of Transplantation*, *8*(5), 917-924.

24. Brockmann, J., Reddy, S., Coussios, C., Pigott, D., Guirriero, D., Hughes, D., Morovat A., Roy D., Winter L., Friend, P. J. (2009). Normothermic perfusion: a new paradigm for organ preservation. *Annals of surgery*, *250*(1), 1-6.

25. Marecki, H., Bozorgzadeh, A., Porte, R. J., Leuvenink, H. G., Uygun, K., Martins, P. N. (2017). Liver ex situ machine perfusion preservation: A review of the methodology and results of large animal studies and clinical trials. *Liver Transplantation*, *23*(5), 679-695.

26. Op den Dries, S., Karimian, N., Sutton, M. E., Westerkamp, A. C., Nijsten, M. W. N., Gouw, A. S. H., Wiersema-Buist J., Lisman, T., Leuvenink H. G. D and Porte R. J. (2013). Ex vivo normothermic machine perfusion and viability testing of discarded human donor livers. American Journal of Transplantation, 13(5), 1327-1335.

27. Bruinsma BG, Berendsen TA, Izamis ML, Yarmush ML, Uygun K (2013). Determination and extension of the limits to static cold storage using subnormothermic machine perfusion. Int J Artif Organs; 36:775e80.

28. Berendsen TA, Bruinsma BG, Lee J, D'Andrea V, Liu Q, Izamis ML, Uygun K, Yarmush ML. (2012) A simplified subnormothermic machine perfusion system restores ischemically damaged liver grafts in a rat model of orthotopic liver transplantation. *Transplant Res*; 1: 6

29. Minor, T., Efferz, P., Fox, M., Wohlschlaeger, J., Lüer, B. (2013). Controlled oxygenated rewarming of cold stored liver grafts by thermally graduated machine perfusion prior to reperfusion. *American Journal of Transplantation*, *13*(6), 1450-1460.

30. Minor, T., von Horn, C., Paul, A. (2017). Role of temperature in reconditioning and evaluation of cold preserved kidney and liver grafts. *Current opinion in organ transplantation*, *22*(3), 267.

31. Tolboom, H., Pouw, R., Izamis, M. L., Milwid, J. M., Sharma, N., Soto-Gutierrez, Nahmias Y, Uygun K, Berthiaume F, Yarmush M.L. (2009). Recovery of warm ischemic rat liver grafts by normothermic extracorporeal perfusion. *Transplantation*, *87*(2), 170.

32. Schlegel, A., Kron, P., Graf, R., Dutkowski, P., Clavien, P. A. (2014). Warm vs. cold perfusion techniques to rescue rodent liver grafts. *Journal of hepatology*, *61*(6), 1267-1275.

33. Mergental, H., Perera, M. T. P. R., Laing, R. W., Muiesan, P., Isaac, J. R., Smith, A., Stephenson B. T. F., Cilliers H, Neil D. A. H., Hubscher S. G., Afford S. C., Mirza D.F. (2016). Transplantation of declined liver allografts following normothermic ex-situ evaluation. *American Journal of Transplantation*, *16*(11), 3235-3245.

34. Bral, M., Gala-Lopez, B., Bigam, D., Kneteman, N., Malcolm, A., Livingstone, S., Andres A., Emamaullee J., Russell L, Coussios C., West L. J., Friend P. J., Shapiro A. M. J. (2017).Preliminary single-center Canadian experience of human normothermic ex vivo liver perfusion: results of a clinical trial. American Journal of Transplantation, 17(4), 1071-1080.

35. Dar, W. A., Sullivan, E., Bynon, J. S., Eltzschig, H., Ju, C. (2019). Ischaemia reperfusion injury in liver transplantation: Cellular and molecular mechanisms. *Liver International*, *39*(5), 788-801.

36. Vardanian, A. J., Busuttil, R. W., Kupiec-Weglinski, J. W. (2008). Molecular mediators of liver ischemia and reperfusion injury: a brief review. *Molecular Medicine*, *14*(5-6), 337-345.

37. Kalogeris, T., Baines, C. P., Krenz, M., Korthuis, R. J. (2012). Cell biology of ischemia/reperfusion injury. In *International review of cell and molecular biology* Vol. 298, pp. 229-317.

38. Yellon DM, Hausenloy DJ. (2007). Myocardial reperfusion injury. *N. Engl. J. Med*. 357:1121–1135.

39. Datta, G., Fuller, B. J., Davidson, B. R. (2013). Molecular mechanisms of liver ischemia reperfusion injury: Insights from transgenic knockout models. *World Journal of Gastroenterology*, 19(11), 1683.

40. Abu-Amara, M., Yang, S. Y., Tapuria, N., Fuller, B., Davidson, B., Seifalian, A. (2010). Liver ischemia/reperfusion injury: Processes in inflammatory networks-A review. *Liver Transplantation*, 16(9), 1016–1032.

41. Granger, D. N., Kvietys, P. R. (2015). Reperfusion injury and reactive oxygen species: the evolution of a concept. *Redox biology*, *6*, 524-551.

42. Zhai Y, Qiao B, Gao F, Shen X, Vardanian A, Busuttil RW, Kupiec-Weglinski JW. (2008) Type I, but not type II, interferon is critical in liver injury induced after ischemia and reperfusion. *Hepatology* 47: 199-206

43. Tsung A, Klune JR, Zhang X Jeyabalan G, Cao Z, Peng X, Stolz DB, Geller DA, Rosengart MR, Billiar TR. (2007) HMGB1 release induced by liver ischemia involves Toll-like receptor 4 dependent reactive oxygen species production and calcium-mediated signalling. *J Exp Med*. 204:2913-2923.

44. Shen, J., Sakaida, I., Uchida, K., Terai, S., Okita, K. (2005). Leptin enhances TNF-α production via p38 and JNK MAPK in LPS-stimulated Kupffer cells. *Life Sciences*, 77(13), 1502–1515.

45. Zhai Y, Shen XD, Gao F, Zhao A, Freitas MC, Lassman C, Luster AD, Busuttil RW, Kupiec-Weglinski JW. (2008) CXCL10 regulates liver innate immune response against ischemia and reperfusion injury. *Hepatology*; 47: 207-214

46. Baggiolini M. (2001).Chemokines in pathology and medicine. *J Intern Med*. 250(2):91–104.

47. Kuboki, S., Shin, T., Huber, N., Eismann, T., Galloway, E., Schuster, R., Blanchard, J., Edwards, M.J., Lentsch, A. B. (2008). Hepatocyte signaling through CXC chemokine receptor-2 is detrimental to liver recovery after ischemia/reperfusion in mice. *Hepatology*, 48(4), 1213–1223.

48. Yang, W., Chen, J., Meng, Y., Chen, Z., Yang, J. (2018). Novel targets for treating ischemia-reperfusion injury in the liver. *International journal of molecular sciences*, 19(5), 1302.

49. Poisson J, Lemoinne S, Boulanger C, Durand F, Moreau R, Valla D, Rautou PE (2017); Liver sinusoidal endothelial cells: Physiology and role in liver diseases. *J Hepatol*. 66:212-227.

50. Gomez Perdiguero E, Klapproth K, Schulz C, Busch K, Azzoni E, Crozet L, Garner H, Trouillet C, de Bruijn MF, Geissmann F, Rodewald HR. (2015) Tissue-resident macrophages originate from yolk-sac-derived erythro-myeloid progenitors. *Nature*.;518:547-551.

51. Heymann F, Peusquens J, Ludwig-Portugall I, Kohlhepp M, Ergen C, Niemietz P, Martin C, van Rooijen N, Ochando JC, Randolph GJ, Luedde T, Ginhoux F, Kurts C, Trautwein C, Tacke F. (2015) Liver inflammation abrogates immunological tolerance induced by Kupffer cells. *Hepatology*. 62:279-291.

52. Perry BC, Soltys D, Toledo AH, Toledo-Pereyra LH. (2011) Tumor necrosis factor-alpha in liver ischemia/reperfusion injury. *J Invest Surg*. 24:178-188.

53. Andrukhiv, A., Costa, A. D., West, I. C., Garlid, K. D. (2006). Opening mitoK ATP increases superoxide generation from complex I of the electron transport chain. *American Journal of Physiology-Heart and Circulatory Physiology*, 291(5), H2067–H2074.

54. Caraceni P, Bianchi C, Domenicali M, Maria Pertosa A, Maiolini E, Parenti Castelli G, Nardo B, Trevisani F, Lenaz G, Bernardi M. (2004) Impairment of mitochondrial oxidative phosphorylation in rat fatty liver exposed to preservation-reperfusion injury. *J Hepatol*. 41:82-88.

55. Nardo B, Caraceni P, Pasini P, Domenicali M, Catena F, Cavallari G, Santoni B, Maiolini E, Grattagliano I, Vendemiale G, Trevisani F, Roda A, Bernardi M, Cavallari A (2001) Increased generation of reactive oxygen species in isolated rat fatty liver during postischemic reoxygenation. *Transplantation*. 71:1816-1820.

56. Friedman SL. (2000) Molecular regulation of hepatic fibrosis, an integrated cellular response to tissue injury. *J Biol Chem*. 275:2247-2250.

57. Cheng F, Li Y, Feng L, Li S. (2008) Hepatic stellate cell activation and hepatic fibrosis induced by ischemia/reperfusion injury. *Transplant Proc*. 40:2167-2170.

58. de Oliveira, T. H. C., Marques, P. E., Proost, P., Teixeira, M. M. M. (2018). Neutrophils: a cornerstone of liver ischemia and reperfusion injury. *Laboratory Investigation*, *98*(1), 51.

59. Konishi, T., Lentsch, A. B. (2017). Hepatic Ischemia/Reperfusion: Mechanisms of Tissue Injury, Repair, and Regeneration. *Gene Expression*, 17(4), 277–287.

60. Shen X, Wang Y, Gao F, Ren F, Busuttil RW, Kupiec-Weglinski JW, Zhai Y. (2009) CD4 T cells promote tissue inflammation via CD40 signaling without de novo activation in a murine model of liver ischemia/reperfusion injury. *Hepatology* 50(5):1537–46.

61. Pistritto, G., Trisciuoglio, D., Ceci, C., Garufi, A., D'Orazi, G. (2016). Apoptosis as anticancer mechanism: function and dysfunction of its modulators and targeted therapeutic strategies. *Aging (Albany NY)*, *8*(4), 603.

62. Ichim, G., Tait, S. W. (2016). A fate worse than death: apoptosis as an oncogenic process. *Nature Reviews Cancer*, *16*(8), 539.

63. Kroemer G, Galluzzi L, Vandenabeele P, Abrams J, Alnemri ES, Baehrecke EH, Blagosklonny MV, El-Deiry WS, Golstein P, Green DR, Hengartner M, Knight RA, Kumar S, Lipton SA, Malorni W, Nuñez G, Peter ME, Tschopp J, Yuan J, Piacentini M, Zhivotovsky B, Melino G. (2009) Classification of cell death: recommendations of the Nomenclature Committee on Cell Death 2009. *Cell Death Differ.* 16:3–11

64. Nikoletopoulou, V., Markaki, M., Palikaras, K., Tavernarakis, N. (2013). Crosstalk between apoptosis, necrosis and autophagy. *Biochimica et Biophysica Acta (BBA)-Molecular Cell Research*, *1833*(12), 3448-3459.

65. Linkermann, A., Bräsen, J. H., Darding, M., Jin, M. K., Sanz, A. B., Heller, J. O., De Zen F., Weinlich R., Ortiz A., Walczak H., Weinberg, J. M., Green D.R., Kunzerdorf U., Krautwald S. (2013). Two independent pathways of regulated necrosis mediate ischemia–reperfusion injury. *Proceedings of the National Academy of Sciences*, *110*(29), 12024-12029.

66. Sipieter, F., Ladik, M., Vandenabeele, P., Riquet, F. (2014). Shining light on cell death processes–a novel biosensor for necroptosis, a newly described cell death program. *Biotechnology journal*, *9*(2), 224-240.

67. Daar Abdallah S. and Greenwood Heather L. (2007). A proposed definition of regenerative medicine. Journal of Tissue Engineering and Regenerative Medicine, 1, 179–18

68. Dominici, M., Le Blanc, K., Mueller, I., Slaper-Cortenbach, I., Marini, F., Krause, D., Horwitz, E. (2006). Minimal criteria for defining multipotent mesenchymal stromal cells. The International Society for Cellular Therapy position statement. Cytotherapy, 8(4), 315–7.

69. McCulloch E.A., and Till J. E. (1960) The Radiation Sensitivity of Normal Mouse Bone Marrow Cells, Determined by Quantitative Marrow Transplantation into Irradiated Mice. Radiation Research: July 1960, 13(1), 115-125.

70. Friedenstein, A. J., Chailakhjan, R. K., Lalykina, K. (1970). The development of fibroblast colonies in monolayer cultures of guinea-pig bone marrow and spleen cells. *Cell Proliferation*, *3*(4), 393-403.

71. Pittenger, M. F., Mackay, A. M., Beck, S., Jaiswal, R. K., Douglas, R., Mosca, J. D., Marshak, D. (1999). Multilineage Potential of Adult Human Mesenchymal Stem Cells. *Science*, *284*(April), 143–147.

72. Kordes, Claus, and Dieter Häussinger. (2013) "Hepatic stem cell niches." *The Journal of clinical investigation*123.5: 1874-1880.

73. Pittenger, M. F., Martin, B. J. (2004). Mesenchymal stem cells and their potential as cardiac therapeutics. *Circulation Research*, *95*(1), 9–20.

74. Lv, F.-J., Tuan, R. S., Cheung, K. M. C., Leung, V. Y. L. (2014). Concise Review: The Surface Markers and Identity of Human Mesenchymal Stem Cells. *Stem Cells*, *32*(6), 1408–1419.

75. Herrera, M. B., Bruno, S., Buttiglieri, S., Tetta, C., Gatti, S., Deregibus, M. C., Bussolati, B. and Camussi, G. (2006), Isolation and Characterization of a Stem Cell Population from Adult Human Liver. STEM CELLS, 24: 2840–2850.

76. Mafi, R. (2011). Sources of Adult Mesenchymal Stem Cells Applicable for Musculoskeletal Applications - A Systematic Review of the Literature. *The Open Orthopaedics Journal*, *5*(1), 242–248.

77. Caplan, A. I., Correa, D. (2011). The MSC: An injury drugstore. *Cell Stem Cell*, 9(1), 11–15

78. Du, Z., Wei, C., Cheng, K., Han, B., Yan, J., Zhang, M., Liu, Y. (2013). Mesenchymal stem cell-conditioned medium reduces liver injury and enhances regeneration in reduced-size rat liver transplantation. *Journal of Surgical Research*, 183(2), 907–915.

79. Toma, C., Pittenger, M. F., Cahill, K. S., Byrne, B. J., Kessler, P. D., Toma, C., Kessler, P. D. (2002). Human Mesenchymal Stem Cells Differentiate to a Cardiomyocyte Phenotype in the Adult Murine Heart, *Circulation*, 93–99

80. Hoogduijn, M. J., Popp, F., Verbeek, R., Masoodi, M., Nicolaou, A., Baan, C., Dahlke, M. H. (2010). The immunomodulatory properties of mesenchymal stem cells and their use for immunotherapy. *International Immunopharmacology*, *10*(12), 1496–1500.

81. Alison, M. R., Vig, P., Russo, F., Bigger, B. W., Amofah, E., Themis, M., Forbes, S. (2004). Hepatic stem cells: from inside and outside the liver?. *Cell proliferation*, *37*(1), 1-21.

82. Farber E. (1956). Similarities of the sequence of the early histological changes induced in the liver of the rat by ethionine, 2-acetylaminofluorene, and 3-methyl-4-dimethylaminoazobenzene. *Cancer Res*; 16:142-148.

83. Akhurst, B., Croager, E. J., Farley-Roche, C. A., Ong, J. K., Dumble, M. L., Knight, B., Yeoh, G. C. (2001). A modified choline-deficient, ethionine-supplemented diet protocol effectively induces oval cells in mouse liver. *Hepatology*, *34*(3), 519-522.

84. Dabeva, M. D., Laconi, E., Oren, R., Petkov, P. M., Hurston, E., Shafritz, D. A. (1998). Liver regeneration and α-fetoprotein messenger RNA expression in the retrorsine model for hepatocyte transplantation. *Cancer research*, *58*(24), 5825-5834.

85. Rosenberg, D., Ilic, Z., Yin, L. I., Sell, S. (2000). Proliferation of hepatic lineage cells of normal C57BL and interleukin-6 knockout mice after cocaine-induced periportal injury. *Hepatology*, *31*(4), 948-955.

86. Yin, L., Lynch, D., Sell, S. (1999). Participation of different cell types in the restitutive response of the rat liver to periportal injury induced by allyl alcohol. *Journal of hepatology*, *31*(3), 497-507.

87. Lemire, J. M., Shiojiri, N., Fausto, N. (1991). Oval cell proliferation and the origin of small hepatocytes in liver injury induced by D-galactosamine. *The American journal of pathology*, *139*(3), 535.

88. Shafritz, D. A., Oertel, M., Menthena, A., Nierhoff, D., Dabeva, M. D. (2006). Liver stem cells and prospects for liver reconstitution by transplanted cells. *Hepatology*, *43*(S1).

89. Fausto, N. (2004). Liver regeneration and repair: hepatocytes, progenitor cells, and stem cells. *Hepatology*, *39*(6), 1477-1487.

90. Wang, X., Foster, M., Al-Dhalimy, M., Lagasse, E., Finegold, M., Grompe, M. (2003). The origin and liver repopulating capacity of murine oval cells. *Proceedings of the National Academy of Sciences*, *100*(suppl 1), 11881-11888.

91. Popper, H., Kent G., Stein R., (1957). Ductular cell reaction in the liver in hepatic injury.*J Mount Sinai Hosp* 24 (1957): 551-556.

92. Popper H. (1990). The relation of mesenchymal cell products to hepatic epithelial systems. Prog Liver Dis;9:27–38.

93. Haque, S., Haruna, Y., Saito, K., Nalesnik, M. A., Atillasoy, E., Thung, S. N., Gerber, M. A. (1996). Identification of bipotential progenitor cells in human liver regeneration. *Laboratory investigation; a journal of technical methods and pathology*, *75*(5), 699-705.

94. Roskams, T. A., Theise, N. D., Balabaud, C., Bhagat, G., Bhathal, P. S., Bioulac-Sage, P., Brunt, E. M., Crawford, J. M., Crosby, H. A., Desmet, V., Finegold, M. J., Geller, S. A., Gouw, A. S.H., Hytiroglou, P., Knisely, A.S., Kojiro, M., Lefkowitch, J. H., Nakanuma, Y., Olynyk, J. K., Nyun Park, Y., Portmann, B., Saxena, R., Scheuer, P. J., Strain, A. J., Thung, S. N., Wanless, I. R. and West, A. B. (2004), Nomenclature of the finer branches of the biliary tree: Canals, ductules, and ductular reactions in human livers. *Hepatology, 39*: 1739–1745.

95. Sangan, C. B., Tosh, D. (2010). Hepatic progenitor cells. *Cell and tissue research*, *342*(2), 131-137.

96. Bria, A., Marda, J., Zhou, J., Sun, X., Cao, Q., Petersen, B. E., Pi, L. (2017). Hepatic progenitor cell activation in liver repair. *Liver research*.

97. Li, J., Xin, J., Zhang, L., Wu, J., Jiang, L., Zhou, Q., Li J., Guo J., Cao H., Li, L. (2014). Human Hepatic Progenitor Cells Express Hematopoietic Cell Markers CD45 and CD109. *International Journal of Medical Sciences*, *11*(1), 65–79.

98. Lu, W. Y., Bird, T. G., Boulter, L., Tsuchiya, A., Cole, A. M., Hay, T., Guest R.V., Wojtacha D., Man T.Y., Mackinnon A., Ridgway R.A., Kendall T., Williams M.J., Jamieson T., Raven A., Hay D.C., Iredale J.P., Clarke A.R., Sansom O.J., Forbes S.J., (2015). Hepatic progenitor cells of biliary origin with liver repopulation capacity. *Nature cell biology*, *17*(8), 971.

99. Gho, Y. S. and Lee C. (2017)"Emergent properties of extracellular vesicles: a holistic approach to decode the complexity of intercellular communication networks." *Molecular BioSystems*13.7: 1291-1296.

100. Tetta, C., Ghigo, E., Silengo, L., Deregibus, M. C. and Camussi, G. (2013). Extracellular vesicles as an emerging mechanism of cell-to-cell communication. *Endocrine*, *44*(1), 11-19.

101. Théry, C., Witwer, K. W., Aikawa, E., Alcaraz, M. J., Anderson, J. D., Andriantsitohaina, R., [...] and Ayre, D. C. (2018). Minimal information for studies of extracellular vesicles 2018 (MISEV2018): a position statement of the International Society for Extracellular Vesicles and update of the MISEV2014 guidelines. *Journal of Extracellular Vesicles*, *7*(1), 1535750.

102. Schara K., Jansa V., Sustar V., Dolinar D., Pavlic J.I., Lokar M., Kralj-Iglic V., Veranic P., Iglic A., (2009). Mechanisms for the formation of membranous nanostructures in cell-to-cell communication. *Cell. Mol. Biol. Lett*. 14, 636–656.

103. Muralidharan-Chari V., Clancy J.W., Sedgwick A., D'Souza-Schorey C. (2010). Microvesicles: mediators of extracellular communication during cancer progression. *J. Cell Sci*. 123, 1603–1611

104. Cocucci E., Racchetti G., Meldolesi J., (2008). Shedding microvesicles: artefacts no more. *Trends Cell Biol.* 19, 43–51

105. Sarkar A., Mitra S., Mehta S., Raices R., Wewers M.D (2009). Monocyte derived microvesicles deliver a cell death message via encapsulated caspase-1. *PLoS ONE* 4, e7140.

106. Grange C., Tapparo M., Collino F., Vitillo L., Damasco C., Deregibus M.C., Tetta C., Bussolati B., Camussi G. (2011) Microvesicles released from human renal cancer stem cells stimulate angiogenesis and formation of lung premetastatic niche. *Cancer Res*. 71, 5346–5356.

107. Mittelbrunn, M., Gutiérrez-Vázquez, C., Villarroya-Beltri, C., González, S., Sánchez-Cabo, F., González, M. Á., Bernard, A., Sánchez-Madrid, F. (2011). Unidirectional transfer of microRNA-loaded exosomes from T cells to antigen-presenting cells. *Nature communications*, *2*, 282.

108. Ratajczak, J., Miekus, K., Kucia, M., Zhang, J., Reca, R., Dvorak, P., Ratajczak, M. Z. (2006). Embryonic stem cell-derived microvesicles reprogram hematopoietic progenitors: evidence for horizontal transfer of mRNA and protein delivery. *Leukemia*, *20*(5), 847.

109. Deregibus, M. C., Cantaluppi, V., Calogero, R., Iacono, M. L., Tetta, C., Biancone, L., Bruno, S., Bussolati, B., Camussi, G. (2007). Endothelial progenitor cell–derived microvesicles activate an angiogenic program in endothelial cells by a horizontal transfer of mRNA. *Blood*, *110*(7), 2440-2448.

110. Tamura, R., Uemoto, S., Tabata, Y. (2016). Immunosuppressive effect of mesenchymal stem cell-derived exosomes on a concanavalin A-induced liver injury model. *Inflammation and regeneration*, *36*(1), 26.

111. Haga H, Yan IK, Takahashi K, Matsuda A, Patel T. (2017) Extracellular vesicles from bone marrow-derived mesenchymal stem cells improve survival from lethal hepatic failure in mice. Stem Cells Transl Med.6:1262–72.

112. Haga H, Borrelli DA, Matsuda A, Parasramka M, Shukla N, Lee DD, Patel T. (2017) Extracellular vesicles from bone marrow-derived mesenchymal stem cells protect against murine hepatic ischemia/reperfusion injury. Liver Transpl. 23 (6):791–803.

113. Ohara, M., Ohnishi, S., Hosono, H., Yamamoto, K., Yuyama, K., Nakamura, H., Fu Q., Maehara O., Suda G., Sakamoto, N. (2018). Extracellular Vesicles from Amnion-Derived Mesenchymal Stem Cells Ameliorate Hepatic Inflammation and Fibrosis in Rats. *Stem cells international*, *2018*.

114. Li, T., Yan, Y., Wang, B., Qian, H., Zhang, X., Shen, L Wang M, Zhou Y, Zhu W, Li W, Xu, W. (2012). Exosomes derived from human umbilical cord mesenchymal stem cells alleviate liver fibrosis. *Stem cells and development*, *22*(6), 845-854.

115. Mardpour, S., Hassani, S. N., Mardpour, S., Sayahpour, F., Vosough, M., Ai, Jafar, Aghdami N., Hamidieh A. A., Baharvand, H. (2018). Extracellular vesicles derived from human embryonic stem cell-MSCs ameliorate cirrhosis in thioacetamide-induced chronic liver injury. *Journal of cellular physiology*, *233*(12), 9330-9344.

116. Tan CY, Lai RC, Wong W, Dan YY, Lim SK, Ho HK. (2014) Mesenchymal stem cell- derived exosomes promote hepatic regeneration in drug-induced liver injury models. Stem Cell Res Ther. 5(3):76

117. Herrera, M. B., Fonsato, V., Gatti, S., Deregibus, M. C., Sordi, A., Cantarella, D., Calogero, R., Bussolati, B., Tetta, C., Camussi, G. (2010). Human liver stem cell-derived microvesicles accelerate hepatic regeneration in hepatectomized rats. *Journal of cellular and molecular medicine*, *14*(6b), 1605-1618.

118. Herrera, M. B., Bruno, S., Grange, C., Tapparo, M., Cantaluppi, V., Tetta, C., Camussi, G. (2014). Human liver stem cells and derived extracellular vesicles improve recovery in a murine model of acute kidney injury. *Stem cell research & therapy*, *5*(6), 124.

119. Herrera Sanchez, M.B., Previdi, S., Bruno, S., Fonsato, V., Deregibus, M. C., Kholia, S., Petrillo, S., Tolosano, E., Critelli, R., Spada, M., Romagnoli, R., Salizzoni, M., Tetta, C., Camussi, G. (2017). Extracellular vesicles from human liver stem cells restore argininosuccinate synthase deficiency. *Stem cell research & therapy*, *8*(1), 176.

120. Kholia, S., Herrera Sanchez, M. B., Cedrino, M., Papadimitriou, E., Tapparo, M., Deregibus, M. C., Brizzi, M. F., Tetta, C., Camussi, G. (2018). human liver stem cell-Derived extracellular Vesicles Prevent aristolochic acid-induced Kidney Fibrosis. *Frontiers in immunology*, *9*, 1639.

121. Fonsato, V., De Lena, M., Tritta, S., Brossa, A., Calvetti, R., Tetta, C., Camussi, G., Bussolati, B. (2018). Human liver stem cell-derived extracellular vesicles enhance cancer stem cell sensitivity to tyrosine kinase inhibitors through Akt/mTOR/PTEN combined modulation. Oncotarget, 9(90), 36151.

122. Lopatina, T., Grange, C., Fonsato, V., Tapparo, M., Brossa, A., Fallo, S., Pitino, A., Herrera Sanchez MB, Kholia S, Camussi G., Bussolati, B. (2019). Extracellular vesicles from human liver stem cells inhibit tumor angiogenesis. International journal of cancer, 144(2), 322-333.

123. Monbaliu, D., Pirenne, J., Talbot, D. (2012). Liver transplantation using donation after cardiac death donors. *Journal of hepatology*, *56*(2), 474-485.

124. Gravante, G., Ong, S. L., Metcalfe, M. S., Sorge, R., Bikhchandani, J., Lloyd, D. M. and Dennison, A. R. (2010). Effects of hypoxia due to isovolemic hemodilution on an ex vivo normothermic perfused liver model. *Journal of Surgical Research*, *160*(1), 73-80.

125. Suzuki S, Toledo-Pereyra LH, Rodriguez FJ and Cejalvo D. (1993) Neutrophil infiltration as an important factor in liver ischemia and reperfusion injury. Modulating effects of FK506 and cyclosporine. Transplantation;55: 1265–1272.

126. Uygun K, Tolboom H, Izamis ML, Uygun B, Sharma N, Yagi H, Soto-Gutierrez A, Hertl M, Berthiaume F, Yarmush ML. (2010) Diluted blood reperfusion as a model for transplantation of ischemic rat livers: Alanine aminotransferase is a direct indicator of viability. *Transplant Proc*. 42(7):2463-2467.

127. Izamis, M. L., Calhoun, C., Uygun, B. E., Guzzardi, M. A., Price, G., Luitje, M., Saeidi N, Yarmush ML., Uygun, K. (2013). Simple machine perfusion significantly enhances hepatocyte yields of ischemic and fresh rat livers. *Cell medicine*, *4*(3), 109-123.

128. Op den Dries S, Karimian N, Westerkamp AC, Sutton ME, Kuipers M, Wiersema-Buist J, Ottens PJ, Kuipers J, Giepmans BN, Leuvenink HG, Lisman T, Porte RJ. (2016) Normothermic machine perfusion reduces bile duct injury and improves biliary epithelial function in rat donor livers. *Liver Transplant*. 22(7):994-1005.

129. Chung PY, Sitrin MD, Te HS. (2003) Serum phosphorus levels predict clinical outcome in fulminant hepatic failure. *Liver Transplant*.;9(3):248-253.

130. Verhoeven, C. J., Farid, W. R., de Jonge, J., Metselaar, H. J., Kazemier, G., van der Laan, L. J. (2014). Biomarkers to assess graft quality during conventional and machine preservation in liver transplantation. Journal of hepatology, 61(3), 672-684.

131. DeLeve, L. D., Maretti-Mira, A. C. (2017). Liver sinusoidal endothelial cell: an update. In *Seminars in liver disease* (Vol. 37, No. 04, pp. 377-387). Thieme Medical Publishers.

132. Lalor, P. F., Lai, W. K., Curbishley, S. M., Shetty, S., Adams, D. H. (2006). Human hepatic sinusoidal endothelial cells can be distinguished by expression of phenotypic markers related to their specialised functions in vivo. *World journal of gastroenterology: WJG*, *12*(34), 5429.

133. Grange C, Tapparo M, Bruno S, Chatterjee D, Quesenberry PJ, Tetta C, Camussi G (2014) et al. Biodistribution of mesenchymal stem cell-derived extracellular vesicles in a model of acute kidney injury monitored by optical imaging. Int J Mol Med.;33:1055–1063.

134. Dutkowski, P., Linecker, M., DeOliveira, M. L., Müllhaupt, B., Clavien, P. A. (2015). Challenges to liver transplantation and strategies to improve outcomes. *Gastroenterology*, *148*(2), 307-323.

135. Matton, A. P., Burlage, L. C., van Rijn, R., de Vries, Y., Karangwa, S. A., Nijsten, M. W., Gouw ASH, Wiersema-Buist J, Adelmeijer J, Westerkamp AC, Lisman T, Porte RJ. (2018). Normothermic machine perfusion of donor livers without the need for human blood products. *Liver Transplantation*, *24*(4), 528-538.

136. Tolboom, H., Izamis, M. L., Sharma, N., Milwid, J. M., Uygun, B., Berthiaume, F., Uygun K, Yarmush ML. (2012). Subnormothermic machine perfusion at both 20 C and 30 C recovers ischemic rat livers for successful transplantation. *Journal of Surgical Research*, *175*(1), 149-156.

137. Nasralla, D., Coussios, C. C., Mergental, H., Akhtar, M. Z., Butler, A. J., Ceresa, C. D., [...] Imber, C. (2018). A randomized trial of normothermic preservation in liver transplantation. *Nature*, *557*(7703), 50.

138. Gray, L. R., Tompkins, S. C., Taylor, E. B. (2014). Regulation of pyruvate metabolism and human disease. *Cellular and molecular life sciences*, *71*(14), 2577-2604.

139. Kotoh, K., Kato, M., Kohjima, M., Tanaka, M., Miyazaki, M., Nakamura, K., Enjoji M, Nakamuta M, Takayanagi R. (2011). Lactate dehydrogenase production in hepatocytes is increased at an early stage of acute liver failure. *ExpErimEntal and thErapEutic mEdicinE*, *2*(2), 195-199.

140. Manghat, P., Sodi, R., Swaminathan, R. (2014). Phosphate homeostasis and disorders. *Annals of clinical biochemistry*, *51*(6), 631-656.

141. Ravikumar R, Jassem W, Mergental H, Heaton N, Mirza D, Perera MT, Quaglia A, Holroyd D, Vogel T, Coussios CC, Friend PJ. (2016) Liver Transplantation After Ex Vivo Normothermic Machine Preservation: A Phase 1 (First-in-Man) Clinical Trial. *Am J Transplant*. 16(6):1779-1787.

142. Bhogal, R. H., Mergental, H., Mirza, D. F., Afford, S. C. (2018). The Emerging Importance of Liver Sinusoidal Endothelial Cells in Regulating Injury during Machine Perfusion of Deceased Liver Donors. In *Seminars in liver disease* (Vol. 38, No. 03, pp. 252-259). Thieme Medical Publishers.

143. Kato, H., Kuriyama, N., Duarte, S., Clavien, P. A., Busuttil, R. W., Coito, A. J. (2014). MMP-9 deficiency shelters endothelial PECAM-1 expression and enhances regeneration of steatotic livers after ischemia and reperfusion injury. *Journal of hepatology*, *60*(5), 1032-1039.

144. Ferrigno A, Di Pasqua LG, Bianchi A, Richelmi P, Vairetti M. (2015). Metabolic shift in liver: correlation between erfusion temperature and hypoxia inducible factor-1α. World J Gastroenterol. 21:1108–1116.

145. Roth KJ, Copple BL. (2015) Role of hypoxia-inducible factors in the development of liver fibrosis. Cell Mol Gastroenterol Hepatol. 1:589–597.

146. Rigo, F.; De Stefano, N.; Navarro-Tableros, V.; David, E.; Rizza, G.; Catalano, G.; Gilbo, N.; Maione, F.; Gonella, F.; Roggio, D.; Martini, S.; Patrono, D.; Salizzoni, M.; Camussi, G.; Romagnoli, R. (2018). Extracellular Vesicles from Human Liver Stem Cells Reduce Injury in an Ex Vivo Normothermic Hypoxic Rat Liver Perfusion Model. Transplantation, e205-e210.